Ocean Flux of Salt, Sulfate, and Organic Components to Atmospheric Aerosol

Lynn M. Russell[1], Richard H. Moore[2], Susannah M. Burrows[3], Patricia K. Quinn[4]
[1] Scripps Institution of Oceanography, University of California, San Diego, La Jolla, California, USA,
[2] NASA Langley Research Center, Hampton, Virginia, USA
[3] Pacific Northwest National Laboratory, Richland, Washington, USA
[4] Pacific Marine Environmental Laboratory, NOAA, Seattle, Washington, USA

Abstract
The oceans contribute to aerosol particles in the atmosphere through two different physical mechanisms: first by the production of sea spray aerosol (SSA), and second by emitting gases that condense to produce secondary marine aerosol (SMA). These aerosol emissions include three types of chemical compounds: salt particles account for >90% of the mass, most of which is >1 μm dry diameter; sulfate particles are mostly <0.5 μm, typically constituting most of the number and the largest impacts on clouds; organic components include the greatest variety of compounds and the most uncertain effects on clouds. Most SSA particles are expected to form from bubbles as film drops that are <1 μm dry diameter and form from flapping bursting bubbles, although >1 μm film drops can form by ligament fragmentation. SMA particles include contributions from marine biogenic gas emissions, including dimethylsulfide (DMS), isoprene, amines, and monoterpenes. The role of particles from the ocean in the atmosphere varies by region and by season, but since atmospheric concentrations of ocean-derived <1 μm particles are typically much smaller than the concentrations of their continental counterparts, they have the largest impacts on climate in regions where continental sources are limited. Most efforts to quantify global SSA and SMA emissions rely on global models, where representations of marine aerosol sources are constrained by a small number of field measurements. Satellite-based retrievals of coarse and marine aerosol optical depth provide near global coverage that has been linked to coincident wind speed, whitecaps, and biological productivity for >1 μm particles. The current best estimate of SSA flux of 5000 Tg/yr can be used to calculate SSA-related carbon flux as 35 TgC/yr, by approximating <1 μm SSA particles as 10% of SSA flux with 7% organic carbon and >1 μm particles as 90% of SSA flux with no organic carbon. SMA is estimated to contribute 0.6 TgC/yr as DMS, 0.6 TgC/yr as amines, and an additional trace amount from isoprene and monoterpenes for a total of <2 TgC/yr. Because of the limited availability of observations to constrain SSA and SMA global estimates, oceanic fluxes to aerosol and aerosol precursors could vary by over two orders of magnitude. Key open questions that require additional observational constraints include the variability in >1 μm SSA mass size distributions, the relative contributions of SSA and SMA to number concentrations of particles <0.5 μm, and the regional and seasonal factors that may control these <0.5 μm particle concentrations.

1. Introduction: Ocean Sources of Atmospheric Aerosol Particles

Oceans cover two-thirds of the Earth, and they produce two sources of aerosol particles – one directly as particles (primary) and the other as gases that later form particles (secondary). These naturally occurring sources are produced from most of the area covered by the world oceans, but quantifying the contributions of these sources is a complex challenge limited by instrument and simulation capabilities, as well as by logistical obstacles for open-ocean measurements. The direct or primary source of particles to the atmosphere is that of sea spray aerosol (SSA), the particles formed from the bursting of bubbles generated by wind-driven breaking waves (Gong, 2003; Monahan, 1968). The indirect source of particles is the emission of gases from the ocean that can condense to particles after they are in the atmosphere, which are considered "secondary" marine aerosol (SMA) (Gantt et al., 2010; Meskhidze et al., 2010; Shaw, 1987; S. L. Shaw et al., 2010). SSA consists largely of sea salts from the ocean but also includes a contribution of organic components that are produced by the metabolism of biological organisms in the ocean. These ocean ecosystems also produce and release organic gases that can form SMA.

This review provides an update on the understanding of SSA and SMA, building from prior reviews (de Leeuw et al., 2011; Gantt & Meskhidze, 2013; Lewis & Schwartz, 2004; O'Dowd & De Leeuw, 2007; Quinn et al., 2015; S. L. Shaw et al., 2010). The objective is to summarize the findings most relevant to the physical drivers of marine aerosol sources and impacts, focusing on the fluxes of SSA and SMA. We consider the regional and seasonal differences that may influence SSA and SMA, including the role of ocean biota, and compile estimates of their global fluxes. Finally, we discuss the most important open questions for which answers are needed to improve our understanding of the role of ocean fluxes of aerosol in contributing to Earth's climate.

2. SSA Fluxes

Aerosol particle fluxes from the ocean known as "sea spray aerosol" (SSA) are composed of inorganic sea salts, including mostly NaCl and trace amounts of other salts, and organic components (Gantt & Meskhidze, 2013; Russell et al., 2010). The flux of these particles has been characterized indirectly by measurements of particle concentrations in marine areas with minimal continental contributions, and have been shown to increase with wind speed (Monahan, 1968; Monahan et al., 1983). Laboratory measurements have quantified the links between bubbling of trapped air and particle production, showing that the flux may depend not only on the wind-speed-driven entrapment of air but also on the conditions of the sea surface and its composition (Blanchard, 1989; Martensson et al., 2003; Sellegri, O'Dowd, Yoon, Jennings, & de Leeuw, 2006). The understanding of the SSA number size distribution is well developed for particles >1 μm but quite limited for particles <0.5 μm, which has substantial implications for SSA contributions to CCN (O'Dowd, Lowe, & Smith, 1999; O'Dowd, Lowe, Smith, et al., 1999).

2.1 Modes of SSA Production

The modes of SSA have been associated with different processes involved in bubble bursting, with jet drops ejected from bubbles often attributed as the producers of

particles 1-10 μm dry diameter, film drops from bubble cap fragmentation as the producers of smaller particles <1 μm dry diameter (Woolf et al., 1987), and spume drops from wave tearing as producers of particles at 100 μm formation diameter (Anguelova et al., 1999; Fairall et al., 2009; Monahan et al., 2017; Veron, 2015; Wu, 1993). The formation processes for film and jet drops are illustrated in Figure 1, and the size ranges of film, jet, and spume particles are illustrated in Figure 2. The bubbles formed by wave-breaking in the ocean span a range of sizes from <50 μm radius to >10 mm radius (Figure 3), but there are few measurements characterizing bubble production in the open ocean (Deane & Stokes, 2002). Most of the quantitative relationships between bubble production and particle size distributions are based largely on laboratory rather than ocean conditions (Lewis & Schwartz, 2004). The scarcity of these measurements means that extrapolations to global and annual SSA are highly uncertain. This uncertainty means that current models use parameterizations rather than bottom-up calculations of sea spray particle production.

For this review as for most of the literature, bubble sizes are reported as observed geometric radius. Airborne particle sizes, in particular those related to chemical composition, typically are referenced to dry diameter to provide a more standard and reproducible metric for quantification. Aerosol particle diameter may be measured by mobility, aerodynamic, optical, or geometric properties, and here the diameter given is most often calculated as equivalent to geometric for spherical particles. Exceptions, as in Figure 2, are noted.

Bubbles larger than 1 mm radius have been observed to produce film drops with a maximum dry diameter given by the area and thickness of the bubble cap (Lhuissier & Villermaux, 2012) and apparent minimum diameters as small as 0.01 μm (Martensson et al., 2003). Photographic evidence indicated that ligaments form after the inertial destabilization of the rim enclosing the initial rupture in the bubble, and the elongation of those ligaments leads to the formation of droplets <10 μm wet diameter (Lhuissier & Villermaux, 2012; Spiel, 1998). Ligament-mediated (also called centripetal) fragmentation of the bubble film is thought to be relatively independent of bubble size (Lhuissier & Villermaux, 2012), producing a characteristic gamma distribution of drops (Spiel, 1998). The wet drops produced from bursting bubbles of radius 12 mm were measured from 5 to 500 μm (Lhuissier & Villermaux, 2012), which is approximately equivalent to dry diameters ranging from 1 to 100 μm (Figure 4). High speed photographic observations account for the formation of particles <0.1 μm by capturing the role of flapping bubble films for bubbles <2 mm (X. H. Jiang et al., 2022). The flapping of the film begins as the bubble film recedes from the initial hole at the foot of the bubble cap, resulting in film fragmentation and drop formation. The flapping motion of the bubble film results from the thinness of the films for small bubbles and has been proposed to control the size of particles produced, with particles as small as 0.04 μm from saltwater bubbles of radius 73 μm (Gañán-Calvo, 2022; X. Jiang et al., 2022; X. H. Jiang et al., 2022).

Film drops have been thought to represent the majority (60-80%) of the particles produced in wave breaking (Veron, 2015). Laboratory measurements with controlled

bubbling show production of many <1 μm particles from bubble bursting events (Martensson et al., 2003). Those laboratory experiments included a range of bubble sizes, precluding the use of these experiments to establish a quantitative relationship between particle production and bubble film fragmentation. Recent evidence shows that bubbles smaller than 10-20 μm radius produce particles with dry diameters 0.5-1 μm, suggesting that jet drops may also play a role in <1 μm particle production (Wang et al., 2017), even though there are not yet open-ocean photographic measurements of bubbles smaller than 50 μm radius (Deane & Stokes, 2002). Acoustic measurements of more complete bubble sizes have been captured in the open ocean, providing evidence of large numbers of particles as small as 10-20 μm radius (Medwin, 1977; Medwin & Breitz, 1989; Vagle & Farmer, 1998). Smaller bubbles have been measured in tanks with plunging water (Stokes et al., 2016; Stokes et al., 2013), with particles from jet drops with dry diameters 0.5-1 μm accounting for 20-40% of <1 μm particle number concentrations and the remainder being film drops with dry diameters 0.04-0.4 μm (Wang et al., 2017).

Unlike film drops, jet drops tend to form particles that are determined by the bubble size (Blanchard, 1989; Wang et al., 2017; Wu, 2002). The “10% rule” for jet drops predicts jet drop dry diameter to be 5% of the bubble radius, and observations typically find 1-3 jet drops are produced per bubble (Veron, 2015; Wang et al., 2017). Contamination from surfactants has been shown to change the distribution of surface bubbles, thereby changing the production of jet drops (Neel et al., 2022). Interestingly, the mean size for film drops has been shown to be a function of the bubble radius and the ratio of the density of the bubble film to the enclosed gas, making its size dependent on the surface water composition and temperature (X. H. Jiang et al., 2022). Interactions of multiple bubbles may also play a role in changing the production of particles, in ways not represented by single-bubble experiments (Bird et al., 2010). An upper limit on film drop size can be calculated from the bubble cap volume assuming one film drop per bubble, but larger production is expected and broad size distributions have been observed (Martensson et al., 2003). Consequently, there are a wide range of particle production functions (Figure 5) that may reflect the role of environmental conditions on bubble bursting. Several studies have reported a variety of dependences of SSA production on ocean and atmospheric parameters (Table 1). One notable similarity across laboratory-generated size distributions (Martensson et al., 2003), coastal observations of vertical differences in concentrations (Clarke et al., 2003; Clarke et al., 2006), and shipboard bubbling proxies (Keene et al., 2017) is the presence of a particle mode <0.1 μm dry diameter. There are not yet direct measurements of <0.1 μm SSA flux in open-ocean conditions because of the lack of instrumentation that are chemically specific for sea salt, quantitative for sea salt mass concentration, and sufficiently resolved for sizes <0.1 μm at time resolutions of hours or less. The impacts of ocean (or laboratory) conditions on the bubble bursting process likely explain the variability between proposed sea spray production functions, which have been derived from laboratory generation of SSA (Figure 5).

Spume drops are the largest and shortest-lived contributors to aerosol particles (Figure 2), with sizes extending from 30 to 4000 μm diameter (Erinin et al., 2022). Given dry

diameters >20 μm, their fall velocity often exceeds 0.1 m s^{-1} making it unlikely for them to persist in the atmosphere. In addition, most chemical and physical measurements of aerosol particles are limited to diameters <10 μm because of the high loss rates of larger particles in instrumentation, as discussed in Section 2.2.1. For these reasons, this review will focus on film and jet drops.

2.2 Approaches to Quantifying SSA Size Distributions

Direct measurements of SSA fluxes are generally not available for the <1 μm and >1 μm size distributions over most of the world oceans (Markuszewski et al., 2018; Norris et al., 2008), likely because of the combined challenges of designing instruments to measure sea salt components quantitatively at high time resolution and the low and dispersed ambient net flux rates. Instead, three complementary approaches have been used to identify the mass and number contributions of SSA particles to open-ocean and coastal aerosol. The first and most chemically specific is size-resolved measurements of Na and Cl composition of particles, which can then be scaled to estimate inorganic "sea salt" (Quinn et al., 2000; Russell & Singh, 2006). The second is to infer the sea salt concentration based on its characteristic contribution to the size distribution and correlation to wind speed (Dedrick et al., 2022; Modini et al., 2015; P. K. Quinn et al., 2017; Saliba et al., 2019). The third is to associate measured physical properties (such as volatility or hygroscopicity) of the size distribution with sea salt composition (Clarke et al., 2003; Clarke et al., 2006; Xu et al., 2022; Xu et al., 2021). The three methods vary in their uncertainty for different size ranges, their accuracy for number or mass, their time resolution, their labor intensiveness and consistency across groups, their reliance on assumptions that may be region-specific, and their ability to resolve non-salt contributions.

2.2.1 Chemical mass measurements

The most comprehensive and consistent set of size-resolved chemically-specific open-ocean sea salt measurements are available from a series of cruises by researchers at NOAA Pacific Marine Environmental Laboratory (PMEL) (https://saga.pmel.noaa.gov/data/). Size-resolved aerosol was collected and analyzed for Na^+ and Cl^- with analysis by ion chromatography on more than a dozen open-ocean cruises for typical sampling times of one day at heights of 10-20 m above sea level (Bates, 2009; Quinn & Bates, 2011; Quinn et al., 2019; Quinn et al., 2000). Compiling those concentrations from six different ocean cruises that had measurements quantifying the continental influence shows clear similarities for the marine air masses with peaks in mass concentrations between 2 and 6 μm, at ~3 μm aerodynamic dry diameter (Figure 6a). SSA mass concentrations have been shown to be correlated to wind speed in prior work (Lewis & Schwartz, 2004; Saliba et al., 2019) but the mass distributions illustrate the consistency in the peak of the >1 μm mass distribution and reflect a strong degree of similarity of SSA modes across seasons and regions.

These mass size distributions were dried and size-segregated during six open-ocean cruises that also measured *in situ* tracers to exclude continental influences, namely <1 μm absorption (at 530 nm from PSAP) less than 0.8 Mm^{-1} and radon concentration less than 540 mBq m^{-3}. In this simple summary of measurements, organic contributions are

excluded because they were not available for the seven stage impactor bins, and sea salt is scaled from measured Na^+ and Cl^- and ammonium bisulfate from measured non sea salt sulfate (SO_4^{2-}). The accuracy of the mass distributions is limited by the number and width of the impactor size bins, as well as by other sampling constraints, with an effective compromise afforded by sampling from a 7-stage Berner impactor (Quinn et al., 2000). The mass concentration distributions illustrate the large mass concentrations >1 μm, with <1 μm bins contributing 10% or less (Kleefeld et al., 2002; Murphy et al., 1998; Quinn et al., 1998; Zheng et al., 2018).

The open-ocean sea salt mass concentrations show a weak correlation ($0.12<R^2<0.2$) of the >1 μm mass concentrations (and the summed mass from all bins) to the local wind speed, but the correlations for the <1 μm bins have $R^2<0.15$. To quantify the size dependence on wind speed, the mass concentrations were normalized to wind speed and then the remaining variability was quantified as the ratio of the standard deviation to the mean. For >1 μm size bins, the standard deviations of the mass concentrations were near or below the means, making the ratio of standard deviation to mean approximately 1 or smaller (Figure 6d). For the <0.5 μm bins, the ratio of the standard deviations to the means of the mass concentration normalized to wind speed are all larger than 1. This high standard deviation relative to the mean of the wind speed normalized mass concentrations reflects an apparent weakness of the dependence of the <0.5 μm bin mass concentrations on wind speed. The low wind speed dependence for <0.5 μm particles is analogous to the higher correlations of sea spray particles to wind speed when <0.5 μm particles were excluded (Figure S17 of Saliba et al. (Saliba et al., 2019)). The <0.5 μm sea salt mass concentration may still be produced from breaking waves, but the processes that produce the smaller particles may have a greater dependence on other environmental conditions (such as surface composition, whitecaps, sea surface temperature (SST), and coastal effects) than on wind speed. Smaller particles could also experience more influence from confounding non-local sources contributing at longer lifetimes. Such variability in conditions could explain the wide range of reported parameterizations in this size range (Figure 5).

The measured mass concentrations for each size bin can also be used to estimate the number concentrations, assuming as a starting point that the two different types of particles are externally mixed, with one consisting of sea salt and the other of ammonium bisulfate (Quinn et al., 2000), and using an effective density of 2.0 for sea salt (Saliba et al., 2020) and 1.78 for ammonium bisulfate. The largest uncertainty in this calculation of number concentrations arises from the width of the measured bins (dlogD), which bounds the possible mean dry diameter of the particles within each bin. This sensitivity to the bin mean diameter is quantified here with three different estimates to bound the mean diameter: (1) an upper bound at the 50% cutoff diameter (D50) for the bin (Dhigh=D50), (2) a lower bound at approximately the 50% cutoff diameter of the next smaller bin (Dlow=D50-dlogD), and (3) a best estimate at the geometric mean of these two values (Dmid=D50-0.5dlogD). This range of mean diameter means that the mass per particle varies by a factor of 5-9 for the bins with D50 of 0.31, 0.55, 1.06, 2.02, 4.13, and by factors of 12 for the smallest bin (D50 of 0.18) and 16 for the largest bin (D50 of 10.3). The uncertainty in the smallest bin has the largest effect on the number

concentration, making the uncertainty in the number concentration a factor of 12 for the <0.18 μm bin. Since the number concentration in the <0.18 μm bin represents more than half of the summed 7-bin number concentration, the uncertainty in the sum is more than a factor of 12. This uncertainty is too large to use mass distributions to evaluate the absolute number flux, but since the error in bin mean diameter is likely to affect the sea salt and ammonium bisulfate number concentrations in the same way, the relative fractions of sea salt and ammonium bisulfate can be compared with less uncertainty. By normalizing the number per bin by the particles summed from all bins, for both sea salt and ammonium bisulfate particle types, the sensitivity to the mean diameter uncertainty is reduced (Figure 6c). The resulting number distributions show that ammonium bisulfate accounts for the majority of <0.5 μm particles in most projects (Figure 6c). In particular, the mean number concentration for the <0.18 μm bin range shows that sea salt accounts for 28% to 34% compared to 40% to 49% ammonium bisulfate particles (Figure 6c). If the assumption of two separate particle types is relaxed as is likely more realistic, then the <0.18 μm bin has particles with 44% sea salt and 56% ammonium bisulfate (neglecting organic and trace constituents). Such mixed particles could be classified either as SMA based on the majority of mass being ammonium bisulfate or as SSA based on the sea salt being the primary particles to which secondary mass was added.

2.2.2 Size distribution correlations

The size distribution correlation approach for estimating sea salt concentrations was developed to attribute modes fitted to merged submicron and supermicron size distributions to sea spray (Modini et al., 2015). The interpretation of particles as sea spray was supported by showing that the summed mass concentration increased with wind speed (Figure 7), from which a flux dependence on wind speed could be inferred (Saliba et al., 2019). By incorporating the high size resolution from differential mobility measurements along with >1 μm optical or aerodynamic size distributions, and using simultaneous <1 μm chemical composition measurements for corroboration, the contribution of SSA to smaller sizes has also been evaluated. This approach showed that a single SSA mode with median diameter ranging from 0.05 to 1.1 μm was correlated with <1.1 μm Na^+ and Cl^- concentrations as well as wind speed for a number of open-ocean campaigns (Modini et al., 2015; P. K. Quinn et al., 2017; Saliba et al., 2019). Smaller modes were also retrieved simultaneously from each distribution, but comparisons to chemical measurements and wind speed indicated their source was largely sulfate and organic components (Figure 8) without a wind speed dependence (Modini et al., 2015; Saliba et al., 2019).

Recent work has studied the accuracy of this approach in the absence of >1 μm size distribution measurements (Dedrick et al., 2022; Sanchez et al., 2020), showing that reasonable SSA number concentrations are retrieved with only <1 μm size distributions but that SSA mass concentrations are improved by constraining to coarse-mode scattering measurements (Dedrick et al., 2022). The range of retrieved sea spray modes does vary in not only number but also size and width (Table 2). The range of the reported parameters from each study does not appear to depend on the relative humidity of the measurements, suggesting the variability is greater than the

dependence on hygroscopicity. The advantage of the size distribution-based approach is that it measures particle number concentrations directly with 10 bins or more per decade of diameter at high time resolution (<10 min), even though chemical composition is inferred. The correlation of retrieved SSA mode mass to measured <1.1 μm Na^+ and Cl^- composition provides indirect support for the chemical identification, although this approach is not expected to be sufficiently sensitive to identify particles <0.1 μm. The small and variable mass concentrations for particles <0.1 μm noted above may obscure any relationship between chemical composition and modes in this size range, which makes it difficult to rule out SSA <0.1 μm but also provides no support for the contribution of SSA in that size range.

2.2.3 Physical property proxies

The physical property proxy approach has used the low volatility or the high hygroscopicity of sea salt particles to identify particles with those properties as sea salt. The volatility approach separates the particles in optical or mobility size distributions by heating sufficient to evaporate sulfate and some organic components and identifying the remaining particles as nonvolatile SSA (Blot et al., 2013; Clarke et al., 1987; Clarke & Kapustin, 2003; Odowd & Smith, 1993). Measurements at three levels of a coastal tower were used to identify the SSA contribution by the amount the >0.04 μm concentrations at 360ºC sampled at 5m above sea level (ASL) exceeded the 20m ASL concentrations, where the near-surface concentration exceedances at 5 m were interpreted as recent emissions of SSA in the coastal zone that had not yet mixed up to the 20m level (Clarke et al., 2003; Clarke & Kapustin, 2003; Clarke et al., 2006). The measurements showed a heated peak in the number size distribution at 0.03 μm, which could result from evaporation of semi-volatile material from ~0.1 μm. These particles could be consistent with a mixture of the sea salt and sulfate mass concentration in the <0.18 μm bin measured by Quinn and colleagues (Figure 6c). Mass spectrometry and combined thermal/electron microscopy measurements also support the presence of sea salts in particles as small as 0.13 μm over the Southern Ocean (Murphy et al., 1998) and at Macquarrie Island (Kreidenweis et al., 1998). To rule out the confounding effects of nonvolatile organic components that may be associated with quantifying the contribution from SSA, chemical measurements were used to show that SSA represented a small contribution by excluding measurements with significant organic or black carbon from open-ocean cruises (Blot et al., 2013). A disadvantage is that the heated size distributions measure particles at diameters reduced from their size at ambient temperature, making it necessary to back-calculate the ambient particle size distribution from the lower concentrations in the heated distribution.

Hygroscopicity has also been used as an indirect way to identify sea salt particles at a coastal site in the northeastern North Atlantic, showing that 2% of the measurements collected during a 5 year period have a large number contribution to hygroscopic particle concentrations <0.2 μm dry diameter (Xu et al., 2022; Xu et al., 2021). This method relies on a cutoff value of κ=0.67 for the size-selected hygroscopic tandem differential mobility analyzer measurements, which is interpreted as a mixture of organic components contributing less than half of the volume (assuming κ<0.1 for organic components) and sea salt contributing the majority (with a 20% uncertainty from the

uncertainty in its hygroscopicity for κ=1.0-1.2) (Zieger et al., 2017). The interpretation of particles with κ>0.67 as SSA assumes no contribution from ammonium bisulfate (κ=0.8 for ammonium bisulfate), even though the ammonium bisulfate is typically measured in particles <0.18 μm in marine environments (Quinn et al., 2000). (Note that the hygroscopicity of ammonium bisulfate was estimated from Köhler theory, with the molality-dependent osmotic coefficient using an ion-interaction approach with tabulated parameters (Pilinis & Seinfeld, 1987; Pitzer & Mayorga, 1973)). This interpretation of particles with κ>0.67 as sea salt results in a much higher SSA number concentration and contradicts the open-ocean results for the measured mass distributions (Figure 6a) and for the size distribution correlation approach (Figure 8). The high SSA concentration implies that there are no sulfate or organic particles contributing to CCN during the 2% of measurements selected. Certainly, this is possible for the 940 hr of measurements during a 5-yr period (with unspecified selection criteria), but the absence of supporting chemical correlations for the hygroscopicity identification suggest the results should be considered with caution. The sparse sampling of the extended data set suggests also that the apparent contradiction between this finding for a coastal location and those for the open-ocean studies, and the lack of correlation to wind speed, may indicate that regional and seasonal variability, as well as coastal differences from open-ocean wave-breaking, are important factors.

2.3 Composition of SSA

Seawater includes a mixture of dissolved inorganic salts, with Na^+ and Cl^- typically accounting for 86% of the inorganic mass and the remainder constituted primarily by Mg^{2+}, Ca^{2+}, K^+, SO_4^{2-} (sulfate), HCO_3^-, Br^-, B^{3+}, and F^- (Holland, 1978). Together the mass contribution of these sea salts can be estimated as from the relation Na^++1.47*Cl^- (Quinn et al., 2000). The contribution of trace salts to seawater means that the particle hygroscopicity is slightly lower than that of pure NaCl (de Leeuw et al., 2011; Ming & Russell, 2001; Tang et al., 1997; Zieger et al., 2017). The inorganic components of sea spray are expected to be generally refractory, which is the term used in aerosol mass spectrometry to indicate that they are largely nonvolatile when heated to 600°C. The presence of SO_4^{2-} as nearly 8% of the dissolved inorganic salts means that measurements of sulfate in marine aerosol will include both sulfate from seawater and sulfate from SMA and other secondary sources. To distinguish between these types of sulfate, the amount of sulfate associated with sea salt is calculated from the seawater composition and the remainder is designated as “non sea salt” sulfate. Analogous “non sea salt” quantities can also be defined for Br^- and K^+, in order to calculate the amount of these constituents that may be associated with wildfires, and for Ca^{2+}, in order to identify the amount that may be associated with dust (Bottenus et al., 2018; Gilardoni et al., 2009; Gilardoni et al., 2016; Song et al., 2021).

The presence of Na^+ and Cl^- in the <0.18 μm bin of the open-ocean ion chromatography measurements (Figure 6) is important because the presence of nonvolatile components can only be explained by the direct production of droplets during bubble bursting, namely there is no secondary source of Na^+ and Cl^-. Reports of SSA particles <0.03 μm dry diameter in coastal and lab measurements are consistent with a tail of larger modes, although separate modes of particles <0.1 μm dry diameter have been reported (Clarke

et al., 2003; Martensson et al., 2003; Xu et al., 2022). There are no direct chemical measurements in this size range, but hygroscopicity values less than that of salt and mass loss during volatility measurements indicate the measured modes are partially sea salt with the remainder including less hygroscopic and more volatile sulfate and organic components.

The ocean contains both dissolved (DOC) and particulate (POC) forms of organic carbon, which are usually defined operationally as the quantities that do (dissolved) and do not (particulate) pass through a submicron-sized pore filter when suspended in seawater (Carlson & Hansell, 2015). Several techniques have been used to identify organic components of SSA (Table 3). Both DOC and POC mix with sea salts when film and jet drops are formed (Gong, 2003; Walls & Bird, 2017), although the contributions of 20% on average (but up to 60%) organic components for 0.1-1 μm fraction are likely associated primarily with film drops (Bates et al., 2020; Keene et al., 2017). In contrast, the >1 μm sizes have negligible organic contributions, with 100% of mass produced by bubbling proxies having a negligible organic volume fraction according to open-ocean bubbling experiments (Keene et al., 2017) and open-ocean ambient measurements (Quinn et al., 1998). The qualitative explanation for the size dependence of the organic contribution is that the thinner the bubble film (and the smaller the bubble), the larger the contribution of the organic surface constituents to the film composition (Figure 9)(Frossard, Russell, Burrows, et al., 2014; X. H. Jiang et al., 2022).

Many experiments using realistic physical simulations of the sea spray aerosol production process have shown that organic components can be measured in primary submicron SSA immediately or very shortly after emission, suggesting that at least some organic components enter the aerosol together with salt rather than through secondary formation from condensation of volatile gases (Alpert et al., 2017; Ault et al., 2013b; Bates, Quinn, Frossard, Russell, Hakala, Petaja, et al., 2012; Maria Cristina Facchini et al., 2008; Frossard, Russell, Burrows, et al., 2014; Gao et al., 2012; W. C. Keene et al., 2007; Kieber et al., 2016; Long et al., 2014; Quinn et al., 2014; Schmitt-Kopplin, Liger-Belair, Koch, Flerus, Kattner, Harir, Kanawati, Lucio, Tziotis, Hertkorn, & Gebefugi, 2012). The primary sea spray origin of marine organic components is also supported by laboratory studies and field experiments using a variety of analytical methods (including Proton Nuclear Magnetic Resonance (H-NMR), Fourier Transform Infrared Spectroscopy (FTIR), Fourier Transform Ion Cyclotron Resonance (FT-ICR), Gas Chromatography Mass Spectrometry (GCMS), High Resolution Time-of-Flight Aerosol Mass Spectrometry (HR-ToF-AMS), Evolved Gas Analysis (EGA), Ion Chromatography (IC), High Performance Liquid Chromatography (HPLC), liquid-phase Total Organic Carbon (TOC), Raman microspectroscopy, and Atomic Force Microscopy (AFM)) (Ault et al., 2013b; Bondy et al., 2017; Frossard, Russell, Massoli, et al., 2014). Because inorganic sea salts are generally refractory, measurements of organic contributions to sea salt by non-refractory methods have been shown to miss the organic components on particles with sea salt (Frossard, Russell, Massoli, et al., 2014).

The organic components of seawater are expected to be produced as the metabolic byproducts of phytoplankton and other ocean biota, which also serve as nutrients for a

variety of ocean organisms (Aluwihare et al., 1997; Burrows et al., 2014; Gantt et al., 2011). Some of the organic components are expected to track with the populations of these biota for which chlorophyll has been used as a proxy, however the variety of organisms and their differing (or nonexistent) amounts of chlorophyll make it problematic as a general tracer for all organic-producing organisms. The composition of the organic components of seawater is likely to include thousands of molecules that range from carbohydrates to amino sugars to lipids, many of which are macromolecules that are difficult to isolate or to characterize fully as molecular structures (Aluwihare et al., 1997; Aluwihare et al., 2005; Repeta et al., 2002). Individual molecules have been speciated by GCMS and other techniques, accounting for a few percent of the seawater composition (Maria Cristina Facchini et al., 2008; M. C. Facchini et al., 2008; Gagosian, 1983; Lawler et al., 2020). Indirect characterization of the organic carbon in <1 μm marine aerosols has accounted for a larger proportion of organic components using functional group characterization (Russell et al., 2010). Subsequent work has shown consistently a majority of quantified organic mass can be characterized by alcohol groups with minor contributions from amine and alkane groups (Figure 10) (Frossard, Russell, Burrows, et al., 2014). This composition is consistent with amino sugars and more generally carbohydrates, although the uncertainties do not preclude contributions from lipids.

Primary contributions of amine groups are evident in <1 μm samples collected from proxies of bubble bursting and ambient particles (Berta et al., 2022 in review; Frossard, Russell, Burrows, et al., 2014). Measurements of the organic functional groups of marine aerosol particles <0.5 μm show some similarities to the <1 μm composition (Lewis et al., 2021). The higher variability and stronger contribution from secondary amine and acid groups <0.5 μm likely indicates a combination of primary and secondary marine sources to the aerosol (Berta et al., 2022 in review).

2.4 SSA Contribution to Scattering, CCN, and INP

SSA particles contribute to light scattering in the atmosphere, cloud condensation nuclei (CCN), and ice nucleating particles (INP). To quantify SSA impacts, a combination of laboratory measurements and clean marine observations have been incorporated in global transport and climate models using parameterizations that predict particle mass as functions of wind speed for a specified size distribution (Anguelova & Webster, 2006; Brumer et al., 2017; Gong, 2003). More sophisticated parameterizations have also incorporated dependence on white caps and SST. Verification of these parameterizations with observations has been promising but limited in scope due to the mismatch of time scales between available observations and global models (Figure 11) (Jaegle et al., 2011). Recent advances in satellite retrievals may improve these comparisons with new products for coarse and fine marine-related particle mass concentrations (Dasarathy et al., 2021; Dror et al., 2018), although chemical composition cannot be retrieved directly by satellite.

SSA is important in the atmosphere because of its direct contributions to albedo, as well as its indirect impacts on clouds and precipitation. The direct contribution is from the scattering of light, and this effect is controlled by the mass concentration of salt particles

and their humidity-dependent hydration. Almost all of the particle mass (>90%) comes from particles >1 μm dry diameter (Figure 6a). The indirect effect on albedo is the result of the provision of CCN to clouds, which often scales with the number concentration of particles and provides the nucleation sites on which droplets form. Clouds respond to increases in CCN number immediately by an increase in cloud droplet number, resulting in brighter clouds (Twomey, 1977). A variety of "knock-on" effects and more subtle aerosol-cloud impacts also occur that can change the extent, depth, and optical thickness of clouds (Fan et al., 2016). These so-called "cloud adjustments" typically enhance the sensitivity of Earth's climate to aerosol emissions (Sherwood et al., 2015). Supermicron salt particles can also act as "giant" CCN and affect precipitation (Dziekan et al., 2021; Feingold et al., 1999; Jensen & Lee, 2008; Jung et al., 2015; Reiche & Lasher-Trapp, 2010).

In addition, the glaciation of supercooled cloud droplets can be affected by particles that act as ice nucleating particles (INP), potentially impacting cloud evolution, precipitation, Earth's radiative budget, and cloud feedback, especially when emissions occur in remote regions such as the Arctic and Southern Ocean, where cloud phase feedbacks are important (Burrows, McCluskey, et al., 2022; Gettelman & Sherwood, 2016; Tan et al., 2022; Tan & Storelvmo, 2016; Tan et al., 2016; Vergara-Temprado et al., 2018).

The impacts of SSA on CCN, INP, and scattering depend strongly on SSA size distributions. CCN are primarily sensitive to number concentrations; the majority of sea spray particle number concentration is <1 μm dry diameter (Figure 6c). In contrast, marine INP are more sensitive to larger SSA; supermicron SSA particles contribute more effectively to INP populations but quantifying the impact of these larger SSA in the atmosphere remains challenging (Mitts et al., 2021; Steinke et al., 2022). Supermicron SSA also play an important role in scattering, although this effect is driven by mass rather than number concentration (Figure 6a). The different size dependences of these effects make it important to identify the size distribution of sea spray particles and their relative contribution to the atmosphere in open-ocean regions.

2.4.1 SSA Contribution to Light Scattering

Sea salt particles >1 μm have been shown to have a large role in scattering light in clean marine conditions, indicating a large role for wind-driven particles in scattering light over the ocean (Chamaillard et al., 2006; Covert et al., 1972; Kleefeld et al., 2000; O'Dowd et al., 2010; Quinn et al., 1998; Quinn et al., 2004). Satellite and surface-based aerosol optical depth (AOD) measurements in clear sky conditions have shown a dependence on local wind speed that is consistent with parameterizations based on *in situ* observations (Mulcahy et al., 2008; O'Dowd et al., 2010; Smirnov et al., 2012), suggesting that the satellite retrievals provide reasonable proxies for sea spray particle mass concentrations. Early retrievals based on Moderate Resolution Imaging Spectroradiometer (MODIS) Collection 5 may have overestimated AOD at wind speeds >6 m/s, due to wind-speed dependent changes in open-ocean surface roughness and white cap foam fraction that affected the assumed surface albedos (Kleidman et al., 2012). MODIS Collection 6 resolved this systematic bias by employing a wind speed look-up table (Kleidman et al., 2012; Levy et al., 2013). This revision produced a more

modest dependence of AOD on wind speed over the open ocean (Merkulova et al., 2018). The remaining wind speed dependence, when combined with the observations of >1 μm particles accounting for 90% or more of sea spray mass (Section 3.2.1, Figure 6), indicates that satellite clear-sky retrievals of aerosol optical depth include signatures for wind-driven sea spray aerosol in marine regions.

Column retrievals of coarse-mode aerosol optical depth (AODc) from MODIS are limited by cloud coverage and lack of vertical resolution (Ichoku et al., 2004), but recent approaches to marine aerosol optical depth (MAOD) have used the NASA Cloud-Aerosol Lidar and Infrared Pathfinder Satellite Observation (CALIPSO) spaceborne lidar to retrieve vertical profiles of layer-specific AOD (including the marine boundary layer) (Dasarathy et al., 2021; Kim et al., 2018). The lidar technique can measure under conditions that would challenge passive remote sensors, such as partial cloud cover and low sun angles. Recent work based on AODc and MAOD retrievals has investigated a seasonal biological contribution in the tropics and in the Antarctic, which show that the dependence on wind speed may be reduced or enhanced by biologically-produced surfactants in the summer (Dasarathy et al., 2022 in review; Dror et al., 2018). Comparisons with surface-based column optical depth measurements from AERONET have shown good correspondence between with satellite and *in situ* measurements (Asmi et al., 2018; Heslin-Rees et al., 2020; Holben et al., 2001; Kaufman et al., 2001; Porter et al., 2003; Smirnov et al., 2011; Virkkula et al., 2022).

2.4.2 SSA as CCN

The most direct measurements of SSA are chemical mass distributions, but CCN concentrations require the accurate size resolution afforded by number distributions. Calculating the contribution of SSA to CCN based on the chemical mass approach is uncertain, since the largest number of particles resides in the smallest bin. The estimated mean diameter of 0.12 μm for the <0.18 μm bin is below the critical diameter of 0.13 μm for sea salt particles for a supersaturation of 0.1% (Figure 12) (Sanchez et al., 2018), meaning that the high uncertainty in the <0.18 μm bin may not be relevant for low marine stratocumulus. However, for higher supersaturations the uncertainty in estimating number from mass reduces the utility of using size-resolved mass concentrations to estimate chemically specific number concentrations.

Using the size distribution correlation approach to evaluate the contribution of SSA to CCN has shown that SSA contributes a third or less of CCN in open-ocean clean marine conditions (Figure 13) (P. K. Quinn et al., 2017). This contribution is similar to the results suggested by the mass distribution-based calculation of number distribution in Figure 6c, which indicates <1 μm particles have an SSA contribution of 38% compared to 62% from SMA (ammonium bisulfate) for the Dmid mean diameters including the smallest bin with Dmid=0.12 μm. SMA is discussed in detail in Section 3, and the role of SMA in contributing to CCN is summarized in Section 3.3. If only particles larger than the SSA critical diameter of 0.13 μm at 0.1% supersaturation are included, that would give contributions of 30% SSA and 70% SMA. The similarity of the open-ocean results from size-distribution correlations approach (Figure 13) and chemical mass measurements approach (based on the number distributions in Figure

6c) shows broad agreement across the first two approaches for open-ocean measurements from six cruises. The physical property approach with volatility found that SSA accounted for 20%-40% of CCN over the southeastern Pacific (Blot et al., 2013), consistent with the first two approaches described above. More larger particles, implying more CCN, were also attributed to entrainment of free tropospheric aerosol than to <1 μm SSA particles at Christmas Island (Clarke et al., 1996). A model-based estimate of CCN for the Southern Ocean was also consistent with this result, concluding that the seasonal variations in sulfate aerosol were primarily attributable to SMA rather than SSA (McCoy et al., 2015).

The physical property approach with hygroscopicity has identified a much higher contribution of SSA to CCN, estimated as 2 or 3 times more than the size distribution correlation approach (Xu et al., 2022). There is occasional evidence for this higher CCN contribution in estimated number concentrations from the open-ocean mass mode <0.18 μm (Figure 6c) for a few times in each project, possibly representing 2% or more of the sampling time. Such similar conditions could explain the Mace Head observations (Xu et al., 2022), although the high number contributions they reported do not seem sufficiently representative to use as the basis for a global mean parameterization for marine areas since the majority of time the number concentrations are generally lower for sea salt than for ammonium bisulfate.

While satellite-derived AOD has retrieved reasonable estimates of the SSA mass concentration, the large contribution of relatively few >1 μm SSA to the light scattering limits its ability to quantify the more numerous and CCN-relevant <1 μm SMA and SSA particles. Recent advances in relating AOD to fine particle mass concentration in urban environments using high-spectral resolution lidar (Sawamura et al., 2017) are not effective in the presence of the coarse mode aerosol found in marine environments. However, combining satellite retrievals of cloud drop number concentrations (Painemal et al., 2020; Painemal et al., 2021) with AOD retrievals may provide an approach to quantifying CCN number concentrations.

2.4.3 SSA as Ice Nuclei

Although SSA is largely composed of inorganic salts that tend to suppress ice formation, SSA can provide a source of ice-nucleating particles (INP). In particular, the inclusion of organic and biological components appears to play a critical role in enabling SSA to act as INP, thereby enhancing the immersion-mode nucleation of supercooled droplets to ice (DeMott et al., 2016). The ice-nucleating entities that contribute to the INP activity of SSA may be associated with the sea surface microlayer (Wilson et al., 2015), and the presence of marine INP in the ambient atmosphere may correlate to ocean biological indicators (Trueblood et al., 2021).

Marine INP are typically less effective and more scarce than dust or terrestrial biological particles (DeMott et al., 2016; Ickes et al., 2020; Irish et al., 2017; Irish et al., 2019; McCluskey, Hill, et al., 2018; Twohy et al., 2021; Wex et al., 2019). Specifically, results from a wave tank experiment showed that SSA particles have <1% of the ice nucleation effectiveness (nucleating sites per particle area) compared to continental particles

(DeMott et al., 2016). In addition, INP concentrations in clean marine regions such as the Southern Ocean are two or more orders of magnitude smaller than INP concentrations in continental air (McCluskey, Hill, et al., 2018). However, both models and observations have shown that SSA particles can serve as INP in the absence of better nuclei such as dust (Chen et al., 2021; DeMott et al., 2016; McCluskey, Hill, et al., 2018; Vergara-Temprado et al., 2017; T. W. Wilson et al., 2015). Observations have identified episodes in which marine INP provide the main INP source along the coastlines of the North Atlantic and Pacific Oceans (Cornwell et al., 2019; McCluskey, Ovadnevaite, et al., 2018).

In addition to acting as INP when immersed in supercooled cloud droplets, some constituents of SSA have been shown to be capable of contributing to ice formation by serving as nuclei for the deposition of water vapor, a mode of ice nucleation that can be important in the upper troposphere (Knopf et al., 2011; Patnaude et al., 2021; Wolf et al., 2019). However, observations of this ice nucleation mode for ambient SSA are limited, and it is unclear how to extrapolate from the observed ice nucleation behavior of individual constituents to complex ambient SSA particles. Few direct observations are available of particle chemical composition and INP in the upper troposphere. Consequently, constraining the impacts of SSA on deposition-mode ice nucleation remains difficult.

Global models have been used as a tool to estimate climate impacts of INP, but such models are not yet capable of representing all of the processes important in controlling the climate response to INP at the necessary scales. Given the limited role of SSA as INP when better INP such as dust are present, it is not yet possible to quantify the overall role of SSA as INP globally. More research is needed to better quantify SSA contributions to INP in order to assess which areas of the Earth would be most sensitive to SSA contributions to INP (Burrows, McCluskey, et al., 2022).

3. SMA Fluxes

The contributions of gases to the aerosol are considered “secondary” because they are emitted in the vapor phase and only form liquid or solid particles after atmospheric processing, which typically includes oxidation to convert the emissions into less volatile compounds. Several approaches have been used to distinguish secondary contributions of SMA from the primary contributions of SSA (Table 4). Chemically-specific contributors are methanesulfonate (MSA) and non-sea-salt sulfate, which are known to form as secondary aerosol from DMS (Quinn & Bates, 2011; Sanchez et al., 2018). A variety of organic compounds also contribute to SMA.

3.1 Marine Gas Emissions

DMS, which is produced from dimethylsulfoniopropionate (DMSP) (Hatton & Wilson, 2007; Stefels et al., 2007), is the sole source of MSA and the marine source of sulfate in the atmosphere. DMS emissions are poorly quantified at the global scale, and climatologies of their emissions are heavily dependent on sparse observations (Bock et al., 2021; Lana et al., 2011). A recently proposed satellite-based parameterization uses Chlorophyll-a, ocean mixed-layer depth, photosynthetically available radiation, and SST

as inputs to an algorithm that predicts ocean DMS concentrations (Gali et al., 2018). DMS emissions have been increasing at high latitudes as Arctic sea ice recedes, which could mean that additional sulfate aerosol serving as CCN would have a disproportionate impact on global climate by slowing the loss of Arctic ice (Gali et al., 2019; Levasseur, 2013). Prediction of future DMS is complicated by shifts in phytoplankton community composition (Wang et al., 2018).

Other ocean-emitted gases that may contribute to SMA include isoprene, monoterpenes, iodine, and amines (Maria Cristina Facchini et al., 2008; Gantt et al., 2010; O'Dowd et al., 2002; Shaw, 1987), but there are very limited observations of the magnitude of their contributions. The limited observations that are available suggest that the contributions of these gases to SMA production are minor in comparison to the contributions from DMS. For example, Kim et al. (2017) conducted ship-board eddy covariance measurements of the vertical flux of isoprene, monoterpenes, and DMS over the North Atlantic during fall, and calculated the SMA production rates from DMS to be ten times greater than production from either isoprene or monoterpenes. Other ocean-emitted gases, such as acetone, acetaldyhyde, and alkyl nitrates, do not contribute significantly to SMA, but have important impacts on OH, HOx, and NOx chemical reactions (Novak & Bertram, 2020). More details on the ocean production of volatile organic compounds (VOCs) are provided by Halsey (this issue). After production, gases in the ocean are transferred to the atmosphere by wind-driven, bubble-mediated sea-to-air transfer processes, which have been reviewed elsewhere (Blomquist et al., 2017; Blomquist et al., 2014; Brumer et al., 2017; Garbe et al., 2014; Liss & Slater, 1974; Liss et al., 1993; Yu, 2019; Zavarsky & Marandino, 2019).

3.2 Secondary Marine Aerosol Composition

The organic components of SMA are typically formed from the oxidation and condensation of volatile precursor gases emitted from the ocean that contribute to observed sulfate and organic mass in marine aerosol (Ceburnis et al., 2008b; Maria Cristina Facchini et al., 2008; Facchini, Decesari, et al., 2010; M. C. Facchini et al., 2008; P. Fu et al., 2013; Meskhidze & Nenes, 2006; C. D. O'Dowd et al., 2004; M. Rinaldi et al., 2010; S. L. Shaw et al., 2010; Turekian et al., 2003). The Quinn and colleagues measurements support these observations over a broad range of clean marine conditions (Figure 6b) (Quinn et al., 2000; P. K. Quinn et al., 2017), with non-sea salt sulfate providing the largest contribution to <1 μm inorganic mass concentration, consistent with studies in a variety of ocean conditions (Sanchez et al., 2018; Sanchez et al., 2016; Twohy et al., 2021). Some organic mass contributions for <1 μm particles have also been identified as SMA based on their carboxylic acid group composition, their non-refractory molecular fragments, and their increases with shortwave radiation (Frossard, Russell, Burrows, et al., 2014; Lewis et al., 2021; Saliba et al., 2020). Isoprene oxidation products include molecules with carboxylic acid groups (Claflin et al., 2021; Ziemann & Atkinson, 2012) and may be consistent with an ocean source, although field observations may also have contributions from continental sources. Amines have been shown to have both primary and secondary contributions to marine aerosol (Maria Cristina Facchini et al., 2008).

There is recent evidence suggesting that secondary products have larger relative contributions to particle fractions <0.5 μm than to <1 μm (Sanchez et al., 2018), which is consistent with expected contributions for condensational growth (Maria et al., 2004; Seinfeld & Pandis, 2016). Volatile gases can also be produced by photosensitized heterogeneous reactions at the air-water interface, potentially leading to formation of SMA (Bernard et al., 2016; Tinel et al., 2016). Detailed chemical analyses of marine aerosol at coastal sites have shown organic and sulfate as SMA contributions, including a study at Amsterdam Island that showed that water-soluble organic matter (WSOM) accounted for 2.8% of fine aerosol mass and was predominantly from MSA. Additional WSOM was attributed to oxidation of fatty acid residues from SSA (Claeys et al., 2010).

Open-ocean measurements in the North Atlantic in four seasons showed SMA in remote marine aerosol during late spring and summer months (Lewis et al., 2021; Saliba et al., 2020; Sanchez et al., 2018), despite relatively low measured rates of local production of dimethyl sulfide and isoprene (among other VOCs) (Davie-Martin et al., 2020). The apparent inconsistency of low DMS with substantial submicron sulfate may be attributed to lofting to the free troposphere, where colder conditions with lower particle concentrations enhance gas-to-particle transfer (Clarke et al., 1999; Clarke et al., 2013; Raes, 1995; Sanchez et al., 2018). The SMA signature of carboxylic acid groups by FTIR was clearly present in May-June and September, but almost entirely absent in November and March (Lewis et al., 2021). This seasonal dependence is generally consistent with the chlorophyll and sunlight-based emission parameterization used in global models (Myriokefalitakis et al., 2010). Observed carboxylic acid group mass of 10% of marine organic mass implies a larger vapor-phase precursor concentration than was explained by measured DMS or isoprene (Saliba et al., 2020). Carboxylic acid groups are a common component of SMA from isoprene and monoterpenes (Claflin et al., 2021; Lewis et al., 2021), but the lack of simultaneous precursor measurements precludes a specific source attribution.

3.3 Secondary Marine Aerosol as CCN

SMA can add new CCN either by growing particles from sizes too small to be CCN (generally <0.1 μm for 0.1% supersaturation) to sizes large enough to be CCN or by adding new particles through homogeneous nucleation. For example, SMA could provide crucial increases in particle size that allow SSA and other particles emitted at sizes <0.1 μm dry diameter to grow to sizes large enough to serve as CCN at supersaturations of <0.2% (Robert J. Charlson et al., 1987; Sanchez et al., 2018). While there is little evidence for new particle formation occurring in the marine boundary layer given the competing sink of aerosol surface area (Quinn & Bates, 2011), exchange between the free troposphere and the boundary layer may provide transported or nucleated particles that can be grown into CCN by SMA (Zheng et al., 2018; Zheng et al., 2021). The magnitude of this contribution to CCN varies with the condensable gases, ambient temperature and relative humidity, and the availability of other sinks. For example, in the North Atlantic, the seasonal difference in the role of SMA as CCN varies from sulfate contributing 34% of CCN at 0.1% supersaturation in windy fall compared to 64% in the sunny late spring, both to wind-driven differences in the SSA produced and differences in the DMS emitted and oxidized (Sanchez et al., 2018). For cloud

supersaturations >0.1%, the contribution of SMA to CCN number concentration would be expected to increase given the typically high concentrations of particles <1 μm.

4. Regional Ocean Differences and other Controlling Factors

Parameterizations of SSA rely on empirical measurements rather than a theoretical formulation, since even idealized bubble bursting process simulations at micrometer scales have not quantified particle production (Bird et al., 2010; Lhuissier & Villermaux, 2012; Veron et al., 2012). Ocean conditions include diverse processes at many scales that interact with small scale processes. In addition, ocean ecosystems differ across ocean regions (Burrows et al., 2018; Burrows, Easter, et al., 2022; Burrows et al., 2014), with different organic components of sea spray contributing compounds from different ecosystem populations (Figure 14). There is considerable evidence that SSA and SMA have some similar properties globally, including the general similarity of the mass size distributions of sea salt and non-sea salt sulfate in regions as diverse as the North Atlantic and the Southern Ocean (Figure 6a). However, in the absence of *a priori* (bottom up) predictions of either SSA or SMA, it is reasonable to consider that differences in regions, seasons, and other environmental conditions influence both the concentrations of aerosol sources and their sizes.

Future climate may also bring significant changes in SSA associated with changes in surface wind speeds. SSA emissions will change as surface wind speeds are either increased or decreased by a warming climate and a recovering ozone layer (Gettelman et al., 2016; Korhonen et al., 2010). In addition, the retreat of sea ice and ice shelves leaves more ocean surface exposed and increases the emissions of SSA, although the net climate effects of such an increase in emissions are uncertain (Browse et al., 2014; Struthers et al., 2011).

4.1 Open-Ocean, Coastal, and Polar Regions of Marine Aerosol

Marine regions include three distinct types of ocean areas, namely open-ocean, coastal, and polar regions. Open-ocean areas are expected to be characterized by large and relatively homogeneous expanses of wave breaking, with consistent near-surface wind speeds and temperatures. Coastal regions are generally expected to be influenced by open-ocean conditions upwind, with only recent production of SSA and SMA affected by shore-influenced wave breaking (Clarke et al., 2003). Polar regions may have a mix of breaking waves as well as processes associated with sea ice and open-lead formation, below-ice ecosystems, and resuspension of deposited SSA and SMA as blowing snow or frost flowers (Abbatt et al., 2019; Chang et al., 2011; Frey et al., 2020).

Open-ocean measurements are very limited given the deployment costs, but such measurements are most likely to represent sea spray emissions over the largest fraction of the area of global oceans. No direct flux measurements are available for the open ocean, although proxies from bubbled seawater have been collected underway on the open ocean to determine fluxes (Keene et al., 2017). The chemical composition measurements of Quinn and colleagues (Figure 6) provide a consistent >1 μm SSA size distribution signature across many regions, with a mass concentration peak at ~3 μm dry diameter. Their measurements have also characterized the role of SMA in the open

ocean, typically showing an NH_4^+/SO_4^{2-} molar ratio of 1, consistent with ammonium bisulfate.

Substantial differences between open-ocean SSA (interpreted as aerosol measured at 20 m during onshore winds) and near-shore SSA (measured as the difference between 5 m and 20 m ASL) were observed at Hawaii. Their observations showed a majority of particles at 5 m ASL were smaller than 0.1 μm dry diameter (Clarke et al., 2003), similar to the inferred fluxes at a North Atlantic coastal site at Mace Head (Xu et al., 2022). There is some support for a small particle mode similar to that observed in coastal studies in open-ocean observations (<0.18 μm bin, Figure 6a) and laboratory studies, but this SSA mode could also be generated by coastal dynamics since open-ocean studies do not show a clear wind speed dependence (Figure 6d).

SSA in polar regions has a strong seasonal variation with sea ice coverage, because sea ice reduces the area of breaking waves in winter when the wind speeds are expected to be highest (Liu et al., 2018; P. M. Shaw et al., 2010). Polar regions are very different between the north and the south, with Antarctic measurements lacking the springtime haze events that confound measurements of SSA and SMA in the Arctic (Lubin et al., 2020). The unique biogeochemistry associated with seasonal sea ice could also result in differences in SSA and SMA to a greater extent than at the milder lower latitudes.

4.2 Temperature Dependence

Wave breaking and the subsequent bursting of bubbles is controlled by the fluid motion of seawater at the ocean surface (Veron, 2015). The sea surface temperature changes the density, viscosity, and surface tension of the fluid, of which the viscosity is likely the most sensitive parameter for the film rupture process (Lhuissier & Villermaux, 2012). Laboratory experiments demonstrated the role that temperature played in changing the size distribution of bubble-generated particles, showing a significant increase in flux with temperature (Martensson et al., 2003). Incorporating this effect in a global model showed that this increase improved the model correspondence to open-ocean SSA measurements (Jaegle et al., 2011). Further evidence of the effect of SST on SSA is provided by four seasons of open-ocean measurements in the North Atlantic, where the mean size of the SSA mode varied with SST (Liu et al., 2021; Saliba et al., 2019).

4.3 Whitecap Dependence

Persistent bubbles on the ocean surface appear as “whitecaps” that can affect the persistence and bursting of bubbles (Andreas & Monahan, 2000; Monahan et al., 1983). Whitecaps are difficult to replicate in laboratory measurements, although foam persistence has been noted to change SSA production (Keene et al., 2017; Stokes et al., 2016; Stokes et al., 2013). Open-ocean observations of whitecaps have also been carried out (Callaghan et al., 2008), but correlations to SSA are difficult because of the mismatch in the spatial scale of the observed whitecaps and the fetch of the SSA produced (Hoppel et al., 2002). Retrievals of whitecaps from satellite may improve parameterizations for SSA (Albert et al., 2016; Anguelova & Webster, 2006; Salisbury et al., 2013).

4.4 Sea Surface Microlayer

Rudimentary separation of a lighter, more surface-active layer in the top millimeter of the ocean from the seawater below has been accomplished with rotating drums and simple mesh screens (Miller et al., 2015). These methods are not able to quantify the thickness of the layer collected, but the composition and properties of the material have been shown to be substantially different from the seawater below (Aller et al., 2017; Crocker et al., 2022; Ickes et al., 2020; Irish et al., 2017; Lewis et al., 2022; Mungall et al., 2017; Theodore W. Wilson et al., 2015). The location of this layer at the sea surface means that it is expected to affect the bubble formation and bursting processes, unless sufficiently disturbed by wave-breaking processes. Modeling of bubble drainage shows an important role for contamination of the seawater surface (Poulain et al., 2018). Laboratory experiments have included proxies for this layer, from simple surfactants to complex biological mixtures (Modini et al., 2013; K. A. Prather et al., 2013).

Comparison of the organic functional group signature in the FTIR alcohol group absorbance of the sea surface microlayer reveals a heterogeneity from day to day that is consistent with other microlayer measurements and with the atmospheric aerosol composition measured in clean conditions (Lewis et al., 2022). Similarities in composition of <1 μm marine aerosol and the sea surface microlayer have included the presence of TEP and similar moieties from biological sources (Maria Cristina Facchini et al., 2008). The variability in the shape and peak locations of the alcohol group absorbance in the microlayer and aerosol particles supports a role for the microlayer in SSA formation, although the quantitative ratios of alcohol to alkane and amine group mass concentrations are also generally consistent with the subsurface water composition (Lewis et al., 2022). Combined these results indicate that both subsurface seawater and sea surface microlayers contribute to SSA formation, consistent with general expectations.

4.5 Biological Diversity

Since ocean ecosystems produce organic compounds that contribute to subsurface and sea surface composition, SSA and SMA will be affected by regional and seasonal differences in those ecosystems. Ocean ecosystems in the “polar”, “westerlies” (mid-latitude), ”trades” (equatorial) and “coastal” biomes are controlled by different processes and exhibit different seasonality (Longhurst, 1995). The dominant phytoplankton functional groups and their seasonal cycles also vary between ocean biomes (Figure 15)(Alvain et al., 2008). In particular, the Phaeocystis group, which is a dominant group only at high latitudes, has long been recognized as an important contributor to atmospheric DMS emissions (Belviso et al., 2004; Liss et al., 1994).

Several studies have supported the connection between ecosystems and marine aerosol by showing correlations between SSA and Chlorophyll (Colin D. O'Dowd et al., 2004), but limited observations from open-ocean studies have shown no dependence on daily time scales and only a weak dependence on seasonal time scales (Bates et al., 2020; Saliba et al., 2020). A metric more specific to overall biological productivity is net primary productivity (NPP), which has also been shown to explain some of the variability

in SSA (Lewis et al., 2022; Saliba et al., 2019). Observation-based efforts to link SMA to either Chl or NPP have not been successful, perhaps due to the time lag and complexity of those processes (K. J. Sanchez et al., 2021). However, bottom-up modeling of ocean ecosystems has shown that the seasonal cycle in the North Atlantic for ocean biological effects on sea spray may have a narrow maximum that occurs in July (Figure 16) rather than during the peak in chlorophyll intensity that was sampled in May (Burrows, Easter, et al., 2022) (Burrows et al.,2022). More complete sampling of the seasonal dependence, as well as the latitude dependence, of open-ocean measurements of SSA would be required to observe the seasonal cycles predicted by models and observed at coastal sites (Rinaldi et al., 2013; Sciare et al., 2009).

5. SSA and SMA Carbon Budget

The best model-based estimates for the global emissions of primary marine organic mass (OM) span the range of 6.9 – 76 Tg/yr for <1 μm emissions and 7.5—58 Tg/yr for >1 μm emissions (using an organic mass to organic carbon ratio of 3 to convert where appropriate) (Gantt et al., 2011; Ito & Kawamiya, 2010; Long et al., 2011; Myriokefalitakis et al., 2010; Spracklen et al., 2008; Vignati et al., 2010; Westervelt et al., 2012), with earlier estimates reviewed previously (Tsigaridis et al., 2013). These studies used both different emissions parameterizations and different model systems, which may impact the simulated atmospheric residence time of SSA and SMA. As a simple comparison, we can use the open-ocean measurements from Quinn and colleagues (Figure 6) to see that >90% of <10 μm sea salt mass concentration is coarse (>1 μm), with the remaining <1 μm contribution ranging from 3% to 10%. The average ambient organic fraction of SSA <1 μm is 20% OM or 7% OC. Using the global SSA estimate of 5000 Tg/yr, organic components account for 7% of <1 μm SSA at 105 Tg/yr (35 TgC/yr), which is within the range from the models noted above for the combined <1 μm and >1 μm emissions of 134 Tg/yr. If >1 μm organic carbon measurements have shown negligible contributions to SSA mass as has been typically reported (Keene et al., 2017), then the <1 μm organic mass flux estimated here is within the model-estimated range.

Secondary aerosol formed from DMS oxidation products is an important aerosol source in remote marine regions (Ayers & Gras, 1991; Charlson et al., 1992). The recent multi-model estimate of contemporary global ocean DMS emissions is 16–24 TgS/yr, even though the observation-derived range is 16--28 TgS/yr. Global sources of SOA from oceanic precursor gases are thought to be substantially smaller than primary organic. This is especially true of sources other than DMS and its oxidation products, which are already included in models. According to one set of estimates, marine volatile organic carbon emissions contribute less than 2 TgC/yr to organic SMA globally, with DMS oxidation contributing about 0.6 TgC/yr (Quinn et al., 2015). Combined amine compounds contribute approximately 0.6 TgC/yr and isoprene and monoterpenes up to 1 TgC/yr (Quinn et al., 2015).

Oxidation products of marine isoprene may contribute a substantial fraction (over 30%) of organic aerosol mass over oceans in the tropics, where the SSA source is small due to low wind speeds (Gantt et al., 2009). The SMA contribution to marine organic carbon

at mid- and high latitudes, and globally, was minor, <0.2% of global marine organic aerosol mass (Gantt et al., 2009). SMA from marine hydrocarbon precursors was found to be negligible compared to the estimated marine <1 μm organic SMA source of about 5 Tg/yr, but this flux consisted primarily of DMS oxidation products (78%), with most of the remaining mass originating from dialkyl amine salts (21%) (Myriokefalitakis et al., 2010).

These fluxes of 35 TgC/yr as SSA and 1.5 TgC/yr as SMA to the atmosphere are expected to have a lifetime of 5-7 days in the marine boundary layer, after which time they will generally be deposited to the surface with a small fraction transported upwards to the free troposphere. A general estimate based on the ocean-covered area of the Earth would be that more than 70% would be deposited back to the ocean and the remaining fraction would be deposited to land. The resulting flux from ocean to land may be about 30% of 37 TgC/yr, or 11 TgC/yr.

6. Open Questions

SSA plays an important role in light scattering in Earth's atmosphere, contributing approximately 5000 Tg/yr of mostly >1 μm particle mass. *In situ* measurements and satellite retrievals show a clear wind speed dependence of these particles, providing reasonable constraints for global models. The uncertainties in satellite retrievals of SSA-specific AOD prevents global inventories from including accurate size distributions, so *in situ* measurements of SSA provide important constraints. Consequently whether the SSA coarse mode is correctly represented by satellite AOD retrievals and wind speed parameterizations merits additional evaluation (Schutgens et al., 2021), and observationally-constrained global modeling simulations could reduce the uncertainty associated with this question. Additional measurements of >1 μm mass and number size distributions would be essential for improving constraints on SSA direct and indirect radiative effects.

Open-ocean measurements of SSA and SMA are limited in availability and in specificity of either number concentration or chemical composition, especially for particles <0.5 μm and <0.1 μm dry diameter. These open-ocean reports include sea salt particle modes <0.5 μm (Figure 6b) similar to coastal and laboratory reports. However, the open-ocean observations of SSA <0.5 μm do not show a clear dependence on wind speed and vary substantially with region and time (Figure 6d). These limitations and the contrasting observations from open-ocean studies mean that there remain several open questions about the magnitude and contribution of <0.5 μm and <0.1 μm particles, as well as very little information on the extent to which wind speed or other factors control their production. Specifically, there are no direct measurements of how many CCN are SSA or SMA, so it is an open question whether they contribute 10%-30% of CCN or much higher numbers globally. Open-ocean observations with simultaneous measurements of size-resolved composition and hygroscopic and volatility properties could help to close the gap on these questions. More complete sampling of the open-ocean seasonal cycle could also address the extent to which ocean biology impacts SSA composition. Combining satellite retrievals of cloud drop number concentrations (Painemal et al., 2020; Painemal et al., 2021) with AOD-based fine particle mass concentrations

(Sawamura et al., 2017) may also make it possible to continuously retrieve marine CCN, or possibly even SMA and SSA, number concentrations from remote regions with continued global coverage.

While the mechanism and size dependence for producing most SSA >1 μm particles is expected to be jet drops at 10% of the bubble radius, particles smaller than 0.5 μm are produced from film drops that extend over a wide range of sizes for a given bubble size. This process is also likely affected by regional and seasonal conditions, with an important open question relating to the mechanistic role of the sea surface microlayer. Further work on theoretical approaches and numerical simulations is needed to understand these processes, with supporting observations from atmospheric and ocean conditions.

7. Acknowledgements

This work was funded by NASA grant NNX15AE66G and by the U.S. Department of Energy under Contract DE-SC0021045. The authors thank two anonymous reviewers and Sonia Kreidenweis for helpful comments. SB was supported by the U.S. Department of Energy (DOE), Office of Science, Office of Biological and Environmental Research through the Early Career Research Program and the Energy Exascale Earth System Model (E3SM) project. This review is PMEL contribution 5403.

8. Data Availability

Data shown in Figure 6 are available at https://saga.pmel.noaa.gov/data/.

FIGURE CAPTIONS

Figure 1. The multiscale approach discussed in this review to model mass exchange due to breaking waves, drops, and bubbles. At moderate to high wind speeds, breaking waves form whitecaps on the ocean surface. (a) The breaking statistics can be described by the length distribution $\Lambda(c)$. (c) of breaking crests moving at speed c, typically from 1 to 10 m s^{-1}. (b) Each breaker's dynamics is assumed to be self-similar and is described by its speed c, leading to scaling models for the associated energy dissipation, air entrainment, and bubble statistics. At the smallest scales, bubbles with sizes ranging from ~1 μm to ~10 mm (c,d) burst at the surface to produce liquid sea sprays via (c) film and (d) jet drops, with sizes ranging from ~0.1 μm to ~1 mm, and (e) exchange gas in the turbulent upper ocean. Reproduced from (Deike, 2022).

Figure 2. Terminal fall velocity of a water droplet in quiescent air at ambient temperature and pressure. The gray line shows the Stokes solution. Additional axes shown are the particle Reynolds number, Re_p, and drag coefficient, C_{Dp} , as well as the particle inertial relaxation time. R_0 is the radius at formation and R_{80} is the radius at 80% relative humidity. Also shown is the size range for the film, jet, and spume drops. Reproduced from (Veron, 2015).

Figure 3. The average bubble size spectrum estimated from 14 breaking events during their acoustic phase. Two camera magnifications were used and the results superimposed to obtain the slightly greater than two decades of bubble radii observed. The vertical scale is number of bubbles per m^3 in a bin radius 1 μm wide. Vertical bars show +/- one standard deviation. The size distribution shows a marked change in slope at a radius that we are identifying as the Hinze scale. Bubbles larger and smaller than this scale respectively vary as $(\text{radius})^{-10/3}$ and $(\text{radius})^{-3/2}$ denoted by β and α. Inset, the bubble size distribution at the beginning of the quiescent phase (crosses) and 1.5 s into the quiescent phase (open circles). Both slopes of the bubble spectrum have increased noticeably during this time interval. This rapid evolution becomes important when interpreting size distributions collected during the plume quiescent phase. Reproduced from (Deane & Stokes, 2002).

Figure 4. Summary of relationships identified between bubble radius, jet drop dry diameter, and film drop dry diameter, with selected references included (Blanchard, 1989; X. H. Jiang et al., 2022; Lhuissier & Villermaux, 2012; Spiel, 1998; Veron, 2015; Wang et al., 2017; Wu, 2002). Connecting lines are approximate representations of the size ranges from the references cited. For film drops, the different size regimes for flapping bursting and ligament fragmentation (centripetal) processes are noted (X. H. Jiang et al., 2022). Spume drop production is not included. The size ranges indicated are on different scales to show relevant ranges.

Figure 5. Parameterizations of size-dependent SSA production flux, evaluated for wind speed U_{10} = 8 m s^{-1} (or U_{22} = 8 m s^{-1} for Geever et al.(Geever et al., 2005)). Also

shown are central values (curves) and associated uncertainty ranges (bands) from review of Lewis and Schwartz (Lewis & Schwartz, 2004), which denote subjective estimates by those investigators based on the statistical wet deposition method (green), the steady state deposition method (blue), and taking into account all available methods (gray); no estimate was provided for r_{80} < 0.1 μm. Lower axis denotes radius at 80% relative humidity, r_{80}, except for formulations of Nilsson et al. (Nilsson et al., 2001), Mårtensson et al. (Martensson et al., 2003), and Clarke et al. (Clarke et al., 2006), which are in terms of dry particle diameter, d_p, approximately equal to r_{80} and those of Geever et al. (Geever et al., 2005), Petelski and Piskozub (Petelski & Piskozub, 2006) (dry deposition method), and Norris et al. (Norris et al., 2008) which are in terms of ambient radius, r_{amb}. Formulation of Petelski and Piskozub (Petelski & Piskozub, 2006) by the dry deposition method. Formulations of Tyree et al. (Tyree et al., 2007) are for artificial seawater of salinity 33 at the two specified bubble volume fluxes. Formulations of Nilsson et al. (Nilsson et al., 2001) and Geever et al. (Geever et al., 2005) of particle number production flux without size resolution are plotted arbitrarily as if the flux is independent of r_{amb} over the size ranges indicated to yield the measured number flux as an integral over that range. Note that the different diameters indicated on the horizontal axis represent different measurement conditions that limit direct comparisons of some measurements. Reproduced from (de Leeuw et al., 2011).

Figure 6. Mass size distributions (a,b) collected from six open-ocean cruises that also measured *in situ* tracers to exclude continental influences, namely <1 μm absorption (at 530 nm from PSAP) less than 0.8 Mm^{-1} and radon concentration less than 540 mBq m^{-3} (Quinn et al., 2000). Panel b has the same information as panel a, but with the axes zoomed in to show the submicron concentrations. The six cruises with appropriate measurements were the First Aerosol Characterization Experiment (ACE1) in 1995, the International Chemistry Experiment in the Arctic Lower Troposphere (ICEALOT) in 2008, the Western Atlantic Climate Study (WACS) in 2014, and the North Atlantic Aerosol and Marine Ecosystem Study (NAAMES) campaigns in Winter 2015 (NAAMES1), Late Spring 2016 (NAAMES2), and Autumn 2017 (NAAMES3). Organic contributions are excluded because they were not available. Sea salt is scaled from measured Na^+ and Cl^-; ammonium bisulfate is based on measured non sea salt sulfate (SO_4^{2-}). Relative number size distributions (c) averaged over all six cruises in (a) are calculated using effective sea salt density of 2.0 (Saliba et al., 2020) and 1.78 for ammonium bisulfate. This sensitivity to the mean diameter is quantified here with three different estimates to bound the mean diameter: (1) an upper bound at the 50% cutoff diameter for the bin (Dhigh=D50), (2) a lower bound at approximately the 50% cutoff diameter of the next smaller bin (Dlow=D50-dlogD), and (3) a best estimate at the geometric mean of these two values (Dmid=D50-0.5dlogD). The ratio of the standard deviation to the mean of the mass distributions normalized to the wind speed (d) are also shown for the six cruises.

Figure 7. SSA mode diameter (d_m) versus (A) wind speed (U_{18}), (B) seawater particle attenuation at 660 nm ($c_{p,660}$), (C) and SST. SSA number concentrations (N_{SSA}) versus (D) wind speed, (E) $c_{p,660}$, and (F) SST. The measurements are colored by campaign for Winter 2015 (NAAMES1), Late Spring 2016 (NAAMES2), Autumn 2017 (NAAMES3), and Early Spring 2018 (NAAMES4). Lines of best fit for all four NAAMES campaigns are plotted as solid black lines if |R|> 0.3. Published parameterizations are plotted as dotted colored lines. The dotted blue curve in C is the mean diameter of the flux size distribution from Mårtensson et al. (Martensson et al., 2003) (first right y axis) and the dotted yellow curve in C is the mean diameter of the particle size distribution from Salter et al. (Salter et al., 2015) (second right y axis). The O'Dowd et al. (Odowd et al., 1997) SSA parameterization versus wind speed is shown in (D) as a dotted blue line. SSA flux production versus SST from Jaeglé et al. (Jaegle et al., 2011) at a wind speed of 8 m s−1 (green dotted line right y axis) and SSA flux production from Mårtensson et al. (Martensson et al., 2003) (blue dotted line, right y axis) versus SST are shown in F. Parameterization for dm versus SST is shown in bold in C. The correlation between dm and SST (R = 0.61) decreased when excluding NAAMES 4 measurements sampled at latitudes south of 30°N (R = 0.46). Reproduced from (Saliba et al., 2019).

Figure 8. (Top row) AMS-based organic + sulfate (Org + SO_4^{2-}) submicron mass concentrations and accumulation mode mass concentration (M_{acc}, calculated by integrating the marine number size distribution between 0.08 μm and 0.32 μm and assuming spherical particles and a density of 1.0 g/cm^3) for NAAMES. (Bottom row) AMS submicron chloride mass concentrations versus Macc. Solid black lines are lines of best fit obtained. AMS-based concentrations are calculated assuming a collection efficiency of unity, so the numerical values the slopes shown are not quantitative. Reproduced from (Saliba et al., 2019)

Figure 9. Average functional group composition of OM in (top) particles generated with Sea Sweep (a floating bubble generator) and Bubbler (a continuous-feed, on-board bubble generator), (middle) surface seawater, and (bottom) deep seawater at 27.4 m and 2500 m measured in (left column) productive and (right column) nonproductive seawater during WACS. The term "productive" is used to mean seawater with high chlorophyll relative to the campaign average. The colors in the pies represent the organic functional group fractions for hydroxyl (pink), alkane (blue), and amine (orange). The bubbles show the bubble draining process in both seawater types, with more surfactant in the productive seawater. The OM is shown as hydrophobic (blue squares), hydrophyllic (pink circles), and polysaccharides (red circles). Reproduced from (Frossard, Russell, Burrows, et al., 2014).

Figure 10. Comparison of the selected normalized organic FTIR spectra and average functional group composition measured at (a) the California Nexus study (CalNex), (b) WACS Station 1, and (c) WACS Station 2 in the gPMA generated with (top) the Bubbler, (middle) the Sea Sweep, and (bottom) the corresponding composition of OM in surface seawater. Pies represent the organic functional group composition as hydroxyl (pink), alkane (blue), and amine (orange). The dashed vertical lines indicate hydroxyl functional group peak absorption at 3369 cm^{-1} (pink) and amine functional group peak absorption

at 1630 cm^{-1} (orange). The range of alkane functional group absorption from 2980 to 2780 cm^{-1} (blue dashed lines) is also shown. The higher wave number peak absorption of the hydroxyl functional groups is evident in the seawater panel. The functional group compositions and spectra are from the subset of collocated samples. Reproduced from (Frossard, Russell, Burrows, et al., 2014).

Figure 11. Time series of coarse mode sea spray mass concentration during the Radiatively-Important Trace Species 1993 (RITS-93), ACE1, and ICEALOT PMEL cruises. For each cruise, observations of sea salt concentrations are shown with black circles. The horizontal bar corresponds to the instrumental averaging period. The three lines are the three different models: standard model (MODEL-STD, red), model using Eq. (3) (MODELU2, blue), model using Eq. (4) (MODEL-SST, green). The bottom panel shows the timeseries of observed 10m wind speed (black dots) compared to the modeled windspeed (red line) as well as the observed SST (blue). Reproduced from (Jaegle et al., 2011).

Figure 12. Particle type size distributions for examples from NAAMES1 and NAAMES2. Black arrows identify the 0.1% supersaturation activation diameters for the Estimated Salt (at 0.13 μm), New Sulfate, and Added Sulfate types. Reproduced from (Sanchez et al., 2018).

Figure 13. Calculated CCN modal number fraction as a function of supersaturation and latitude. a–f, Data are based on combined, latitudinally binned data from RITS-93, RITS-94, ACE-1 Legs 1 and 2, ICEALOT, the second Western Atlantic Climate Study (WACS-2), and NAAMES-1 for the SSA mode with a composition of sea salt and OM (a), Aitken mode for a composition of nss SO_4^{2-} (as NH_4HSO_4) and OM (b), accumulation mode for a composition of nss SO_4^{2-} (as NH_4HSO_4) and OM (c),SSA mode as pure SSA (d), Aitken mode as pure nss SO_4^{2-} (as NH_4HSO_4) (e) and accumulation mode as pure nss SO_4^{2-} (as NH_4HSO_4) (f). Reproduced from (P. K. Quinn et al., 2017).

Figure 14. Submicron SSA dry mass fraction from each compound class for February from the Organic Compounds from Ecosystems to Aerosols: Natural Films and Interfaces via Langmuir Molecular Surfactants (OCEANFILMS) model BASE case. Fractions of processed and humic classes (not shown) are negligible. Reproduced from (Burrows et al., 2014).

Figure 15. Monthly climatology (January and June, 1998–2006) of the dominant phytoplankton group as retrieved by the spectral-based method for identifying phytoplankton from anomalies in satellite retrievals of ocean color known as PHYSAT. The colors indicate diatoms in red, nanoeucaryotes in blue, Synechococcus in yellow, Prochlorococcus in green, and phaeocystis-like in light blue. Reproduced from (Alvain et al., 2008).

Figure 16. OCEANFILMS-predicted seasonal cycle of biological enhancement in the emission flux (a; ratio of predicted marine organic aerosol plus sea salt flux to flux of

pure sea salt) and the organic mass fraction (b) of sea spray particles with diameter <1 μm, for the region of the NAAMES field campaign. The NAAMES campaign consisted of four cruises in different seasons, with most scientific sampling occurring close to 40ºW and between approximately 40ºN and 50ºN (Behrenfeld et al., 2019)(Behrenfeld et al., 2019). All model results are monthly mean output at 40ºW and at the latitudes indicated in the legend. Vertical lines indicate the months during which each variable was measured by NAAMES. Reproduced from (Burrows, Easter, et al., 2022).

TABLES

Table 1. Publications relevant to SSA production. Modified from Saliba et al. (2019).

Reference	Type	Findings
(Grythe et al., 2014)	Review	Positive dependence of SSA production on SST
(Lewis & Schwartz, 2004)	Review	SSA flux dependence on wind speed based on multiple laboratory and field studies
(Meskhidze et al., 2013)	Review	CCN fluxes and optical properties are still poorly constrained
(Forestieri & Moore, 2018; Forestieri et al., 2018)	Laboratory	Positive dependence of SSA concentration on SST using artificial seawater, but no correlation when using filtered but not autoclaved seawater
(Fuentes et al., 2010)	Laboratory	Complex response of SSA number and mean diameter to dissolved organic amount for water collected off the West African coast
(Martensson et al., 2003))	Laboratory	Complex dependence of SSA concentrations on SST using artificial seawater
(Modini et al., 2013)	Laboratory	Decreased SSA production efficiency and increased mean diameter of largest SSA mode (~0.2μm) with decreased surface tension
(Sellegri, O'Dowd, Yoon, Jennings, & DeLeeuw, 2006)	Laboratory	Enhancement of largest SSA mode (0.3μm - 0.5μm) with increased surfactants and wind stress (1m/s)
(J. Zabori et al., 2012)	Laboratory	SSA flux dependence on wind speed based on multiple laboratory and field studies
(Salter et al., 2015)	Laboratory and model	Increased SSA mean diameter with increased water temperature for laboratory experiments using artificial sea water and a temperature-controlled chamber
(Jaegle et al., 2011)	Model	Positive dependence of SSA production on SST using field measurements and satellite observations
(Burrows et al., 2016)	Model	Represented organic emissions in sea-spray using the OCEANFILMS partitioning model
(Kasparian et al., 2017)	Observational	Aerosol number concentrations in the North Atlantic for 1.0 - 2.5 μm were consistent with Jaeglé et al. (2011)
(Lehahn et al., 2014)	Observational	Positive correlation with wind speed and negative correlation with SST and chlorophyll for SSA number concentrations with diameter larger than 0.5μm
(Middlebrook et al., 1998)	Observational	Most particles larger than 0.16μm contained organic compounds near Cape Grim in the Southern Ocean
(Modini et al., 2015)	Observational	Fitted the tail of the marine size distribution to a lognormal function and argued that this mode was the salt mode using measurements from the Eastern Pacific
(Murphy et al., 1998)	Observational	Large fraction of particles larger than 0.16μm sampled at Cape Grim in Southern Ocean contained sea salt
(Odowd et al., 1997)	Observational	Positive correlation of SSA concentrations on wind speed for the Northeast Atlantic
(C. D. O'Dowd et al., 2004)	Observational	Organics components contributed a substantial part of the submicron aerosol mass, especially during plankton blooms
(Ovadnevaite et al., 2012)	Observational	Gong (2003), Mårtensson et al. (2003), and Fuentes et al. (2010) SSA parameterizations with wind speed were higher than measured NaCl mass in the Eastern Atlantic

(Quinn et al., 2000)	Observational	SSA concentrations and size depend on location, with submicron particles dominating SSA in the Northeastern Atlantic and Southern Ocean.
(P. K. Quinn et al., 2017)	Observational	Sea salt number concentrations contributed up to 30% of CCN in clean marine conditions and correlated positively with wind speed, using the Modini et al. (Modini et al., 2015) method
(Russell et al., 2010)	Observational	Organic compounds (similar to saccharides) contribute less than 50% of submicron particle mass and correlated positively with wind speed and Na^+ mass
(Gong, 2003)	Observational + model	Modified the Monahan et al. (1986) parameterization of sea spray on wind speed to best fit concentrations from O'Dowd et al. (1997)
(Dror et al., 2018)	Satellite observations	Positive correlation between wind speed and AOD on daily and yearly timescales but not on seasonal timescales and negative correlation between AOD and chlorophyll concentrations on seasonal timescales

Table 2. Literature reported values of sea spray modal parameters. Number mean diameters ($D_{g,number}$) were converted to mass mean diameters ($D_{g,mass}$) using Eq. (7), integrating over particle sizes 0.01 – 10 μm, and averaging over a total particle concentration range of 1 – 100 cm^{-3}. Values are averages unless noted as an upper or lower bound. Modified from Dedrick et al. (2022).

			Parameter		
Reference	**Experiment type**	**Ocean basin**	**$D_{g,number}$ (μm)**	**$D_{g,mass}$ (μm)**	**σ_g**
(Lewis & Schwartz, 2004), (Sellegri, O'Dowd, Yoon, Jennings, & de Leeuw, 2006),	field measurements (RH: 80%)		0.3	1.3	3
(W. Keene et al., 2007), (Fuentes et al., 2010), (Modini et al., 2010), (Bates, Quinn, Frossard, Russell, Hakala, Petaja, et al., 2012), (J Zabori et al., 2012)	laboratory-based bubble bursting (RH: ambient)		0.05 (lower bound) 0.1 (upper bound)	0.25 (lower bound) 0.48 (upper bound)	2.8
(K. Prather et al., 2013)	laboratory-based breaking wave flume (RH: 10 ± 15%)	N.E. Pacific	0.16	0.88	3
(Modini et al., 2015)	field measurements (RH: < 40%)	N.E. Pacific	0.14 (lower bound) 0.26 (upper bound)	0.5 (lower bound) 1.3 (upper bound)	2.5 (lower bound) 3 (upper bound)
(P. Quinn et al., 2017)	field measurements (RH: variable, mostly < 50%)	Pacific, Southern, Arctic, and Atlantic	0.3	1.08	2.5
(Saliba et al., 2019)	field measurements (RH: < 40%)	N. Atlantic	0.5	1.6	2.3
(K. Sanchez et al., 2021)	field measurements (RH: ambient)	Southern Ocean	0.6	0.71	1.4
(Dedrick et al., 2022)	field measurements (RH = 55 ± 10%)	S. Atlantic	0.4 (UHSAS-only) 0.5 (UHSAS-NEPH)	0.68 (UHSAS-only) 1.47 (UHSAS-NEPH)	1.8 (UHSAS-only) 2.4 (UHSAS-NEPH)

Table 3. Selected references investigating the organic composition and concentration of SSA, generated SSA, SMA, and general Marine Aerosol measured in different ocean regions (from Frossard et al., 2014).

Reference	Ocean Region[a]	OM Composition	Particle Size (OM, $\mu g\ m^{-3}$)
SSA			
(P. Q. Fu et al., 2013)	Arctic	Saccharides	Bulk
(Leck et al., 2013)	Arctic	Heteropolysaccharides	0.035 – 10 μm
(Russell et al., 2010)	Arctic and N Atlantic	Polysaccharides	Submicron
(Hawkins & Russell, 2010)	Arctic and SE Pacific	Polysaccharides, proteins, and phytoplankton fragments	Submicron and Supermicron
(C. D. O'Dowd et al., 2004)	NE Atlantic (Ireland)	Enriched in WIOC with high molecular weight	Submicron
(Ceburnis et al., 2008a)	NE Atlantic (Ireland)	WIOC	Submicron
(M. C. Facchini et al., 2008)	NE Atlantic (Ireland)	WIOM	Submicron
(Bigg & Leck, 2008)	NE Atlantic (Ireland)	Exopolymers	Submicron, < 200 nm
(Ovadnevaite et al., 2011)	NE Atlantic (Ireland)	Hydrocarbon	Submicron
(Mochida et al., 2002)	N Pacific	LMW saturated fatty acids	Bulk
(Sciare et al., 2009)	Austral Ocean	WIOC	Bulk
Generated SSA			
(Gao et al., 2012)	Arctic	Polysaccharides	Bulk
(M. C. Facchini et al., 2008)	NE Atlantic (Ireland)	WIOM: colloids	Submicron
(Facchini, Rinaldi, et al., 2010)	NE Atlantic (Ireland)	WIOM: lipo-polysaccharides	Submicron
(W. C. Keene et al., 2007)	NW Atlantic (Sargasso Sea)	WSOC	Submicron and Supermicron
(Schmitt-Kopplin, Liger-Belair, Koch, Flerus, Kattner, Harir, Kanawati, Lucio, Tziotis, Hertkorn, & Gebefuegi, 2012)	SE Atlantic	Biomolecules with high aliphaticity	< 10 μm
(Bates, Quinn, Frossard, Russell, Hakala, Petäjä, et al., 2012)	NE Pacific (Coastal)	Polysaccharide-like, Alkyl-like, pattern of CH-fragments	Submicron
(Ault et al., 2013a)	NE Pacific (Coastal)	Aliphatic hydrocarbons	0.15-10 μm
(Quinn et al., 2014)	NE Pacific (Coastal) and NW Atlantic	Saccharide-like	Submicron
SMA			
(P. Q. Fu et al., 2013)	Arctic	Isoprene product	Bulk

(C. D. O'Dowd et al., 2004)	NE Atlantic (Ireland)	Enriched in WSOC (partly oxidized species with extended aliphatic moieties)	Submicron
(Ceburnis et al., 2008a)	NE Atlantic (Ireland)	WSOC	Submicron
(M. C. Facchini et al., 2008)	NE Atlantic (Ireland)	WSOM	Submicron
(Maria Cristina Facchini et al., 2008)	NE Atlantic	WSOC – dimethyl and diethyl ammonium salts	Submicron
(Facchini, Rinaldi, et al., 2010)	NE Atlantic (Ireland)	Diethyl and dimethyl amine salts	Submicron
(Matteo Rinaldi et al., 2010)	NE Atlantic (Ireland)	WSOC: MSA, alkylammonium salts, dicarboxylic acids	Submicron
(Meskhidze & Nenes, 2006)	Southern Ocean	Isoprene product	Bulk
(Turekian et al., 2003)	NW Atlantic (Sargasso Sea)	Oxalate	Submicron and Supermicron
Marine Aerosol[b]			
(Cavalli et al., 2004)	NE Atlantic (Ireland)	WIOC; aliphatic and partially oxidized humic-like substances	Submicron OC (0.66); Supermicron OC (0.26)
(Cavalli et al., 2004)	NE Atlantic (Ireland)	WSOC	Submicron 0.25
(C. D. O'Dowd et al., 2004)	NE Atlantic (Ireland)	WIOC and WSOC	Total OC (0.07, LBA; 0.62, HBA)
(Yoon et al., 2007)	NE Atlantic (Ireland)		Total OC (1.2, spring; 0.1, winter) Submicron OC (0.2, spring; 0.05, winter)
(Ovadnevaite et al., 2011)	NE Atlantic (Ireland)		Submicron (3.8)
(Decesari et al., 2011)	NE Atlantic	WIOC similar to lipids; WSOC containing fatty acids, alkanoic acids, aliphatic acids, sulfate esters	Submicron
(Schmitt-Kopplin, Liger-Belair, Koch, Flerus, Kattner, Harir, Kanawati, Lucio, Tziotis, Hertkorn, & Gebefuegi, 2012)	SE Atlantic	Biomolecules with high aliphaticity	< 10 μm
(Crahan et al., 2004)	Tropical Mid-Pacific	Dicarboxylic acids, carbohydrates	< 3.5 μm
(Kawamura & Gagosian, 1987)	N Pacific	Oxo-, mono-, and di-carboxylic acids	Bulk
(Matsumoto & Uematsu, 2005)	N Pacific	Free amino acids in WSOC	< 2.5 μm
(Bigg, 2007)	SW Pacific (Tasmania)	WIOC aggregates; exopolymeric gels	Submicron, < 200 nm

(Shank et al., 2012)	SE Pacific	N/A	Submicron (0.01)
(Kuznetsova et al., 2005)	NW Mediterranean	Proteins, amino acids, and polysaccharides in gels	Bulk
(Fu et al., 2011)	N Pacific, N Atlantic, Indian, South China	LMW fatty acids, fatty alcohols, and sterols	Bulk

[a]The specific stationary sampling locations are in parentheses.

[b]The OM in the studies in this category were not identified as SSA or SMA and are thus included as general atmospheric marine aerosol particles (aMA).

Table 4. Selected references on DMS as an SMA source (from Sanchez et al., 2018).

Relevant Findings	Ref.	Location	Observations or Model
Relationship between DMS and CCN			
DMS-derived sulfate aerosol account for most of the CCN in the remote marine boundary layer.	(R. J. Charlson et al., 1987)	Global	Model plus Observations
MSA and CCN vary seasonally and have a non-linear relationship.	(Ayers & Gras, 1991)	Cape Grim	Observations
DMS and CCN in boundary layer are strongly (non-linearly) correlated.	(Hegg et al., 1991)	NE Pacific	Observations
CCN and DMS are correlated but relationship can be nonlinear because of SO_2 sinks.	(Russell et al., 1994)	N/A	Model
CN correlates strongly with atmospheric DMS and DMS flux but weakly with CCN.	(Andreae et al., 1995)	S. Atlantic	Observations
Modeled CN and CCN correlate with DMS flux; free tropospheric entrainment affects CN and CCN concentration in the marine boundary layer.	(Raes, 1995)	N/A	Model
New Particle Formation from DMS Products			
The number of particles formed by homogeneous nucleation depends on the preexisting aerosol concentration.	(Warren & Seinfeld, 1985)	N/A	Model
Particle number concentration increases rapidly after a decrease in particle surface area and increase in SO_2 concentration.	(Covert et al., 1992)	NE Pacific	Observations
After precipitation, marine boundary layer aerosol particles can be replenished from new particles formed by nucleation if DMS concentrations are high.	(Pirjola et al., 2000)	N/A	Model
Evidence of New Particle Formation in the Free Troposphere			
Vertical profiles of Aitken mode aerosol concentrations showed maximum values just above cloud tops.	(Hegg et al., 1990)	NW and NE Pacific	Observations
Aerosol nucleation is observed above cloud top and downwind of cloud outflows.	(Perry & Hobbs, 1994)	N. Pacific	Observations
CN and CCN were replenished on time scales of 2-4 days with transported nuclei from the free troposphere after precipitation scavenging.	(Clarke et al., 1996)	Christmas Island	Observations
Variability in marine boundary layer aerosol concentration is closely linked to changes in vertical transport.	(Raes et al., 1997)	NE Atlantic	Observations
Nucleation is observed in the free troposphere but not the marine boundary layer, and it is observed more frequently for particle surface area less than 5-10 μm^2 cm^{-3}.	(Clarke et al., 1998)	Southern Ocean	Observations
CN concentration in the marine boundary layer is controlled by the rate of entrainment from the free troposphere in most conditions.	(Katoshevski et al., 1999)	N/A	Model

Observed growth rates of new particles in the free troposphere cannot be explained by SO_2 products and water vapor so other components must contribute to condensation.	(Reus et al., 2000)	NE Atlantic	Model/Observations
New sulfate particles do not form in the marine boundary layer but instead in the free troposphere and then are entrained downward.	(Kazil et al., 2006)	Global	Model
Entrainment of nucleated sulfate particles from the free troposphere account for 43-65% of CCN, but only 7-20% in the winter; long range transport of marine CCN results in a time lag between CCN and DMS concentrations.	(Korhonen et al., 2008)	Southern Ocean	Model
45% of marine boundary layer CCN (at 0.2%) are from nucleation that occurred in the free troposphere.	(Merikanto et al., 2009)	Global	Model
Sulfate particles from DMS mixed up to the free troposphere are a source of marine boundary layer CCN.	(Clarke et al., 2013)	Tropical Pacific	Observations

FIGURE 1

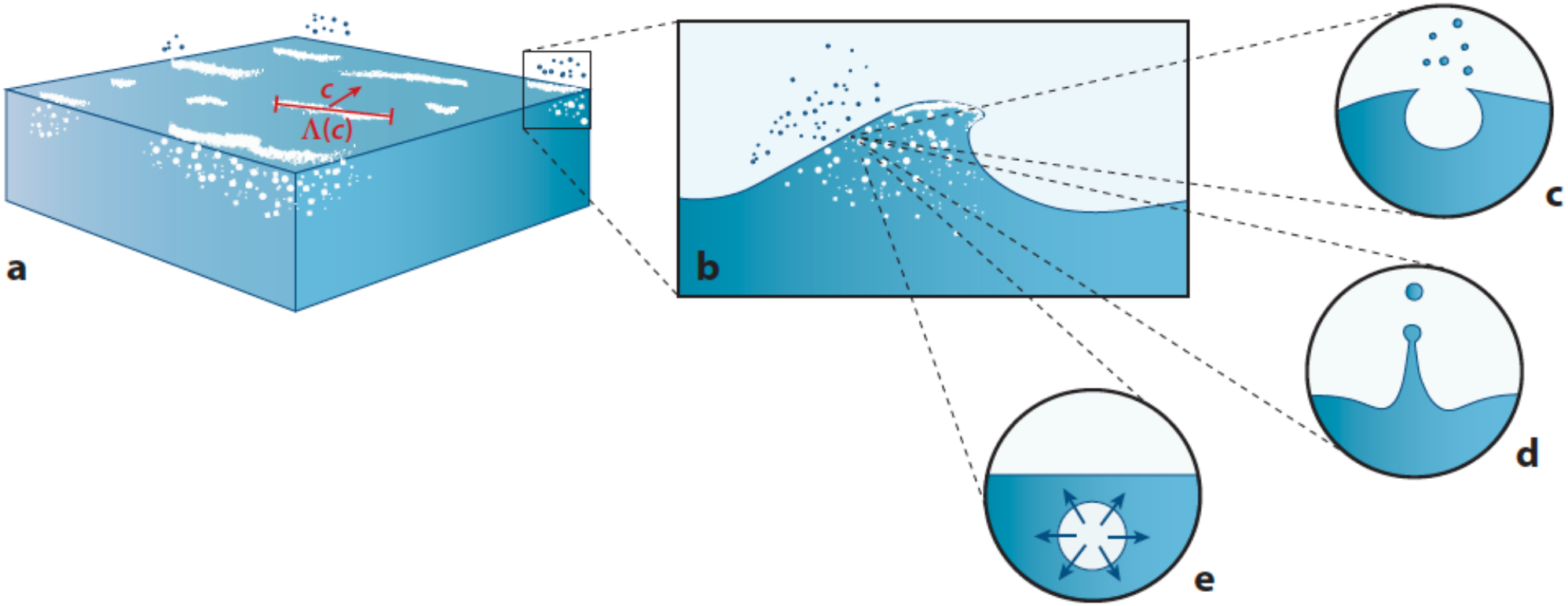

FIGURE 2

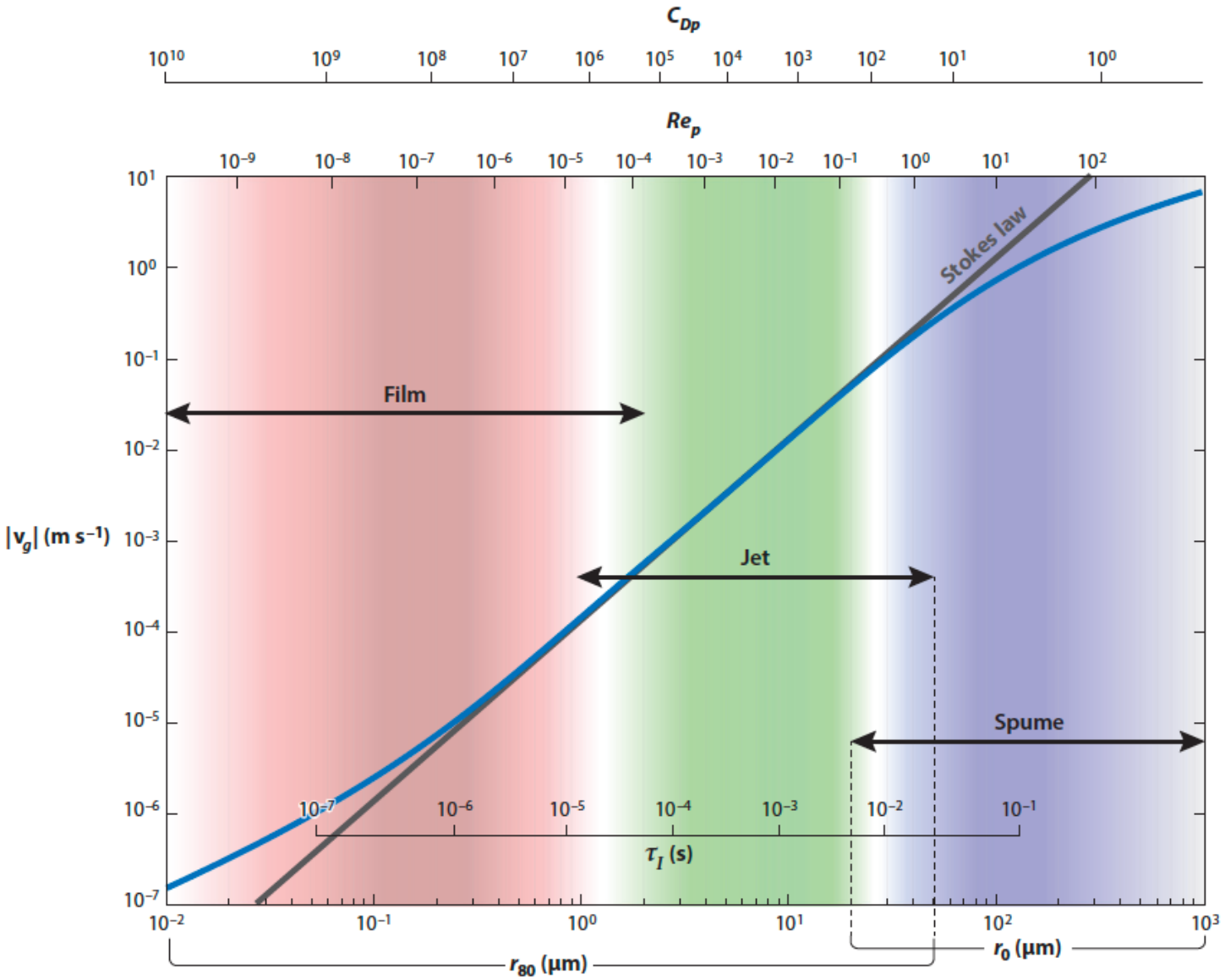
C_{Dp}
10^{10} 10^{9} 10^{8} 10^{7} 10^{6} 10^{5} 10^{4} 10^{3} 10^{2} 10^{1} 10^{0}
Re_p
10^{-9} 10^{-8} 10^{-7} 10^{-6} 10^{-5} 10^{-4} 10^{-3} 10^{-2} 10^{-1} 10^{0} 10^{1} 10^{2}
$|v_g|$ (m s^{-1})
10^{1} 10^{0} 10^{-1} 10^{-2} 10^{-3} 10^{-4} 10^{-5} 10^{-6} 10^{-7}
Stokes law
Film
Jet
Spume
10^{-7} 10^{-6} 10^{-5} 10^{-4} 10^{-3} 10^{-2} 10^{-1}
τ_I (s)
10^{-2} 10^{-1} 10^{0} 10^{1} 10^{2} 10^{3}
r_{80} (μm)
r_0 (μm)

FIGURE 3

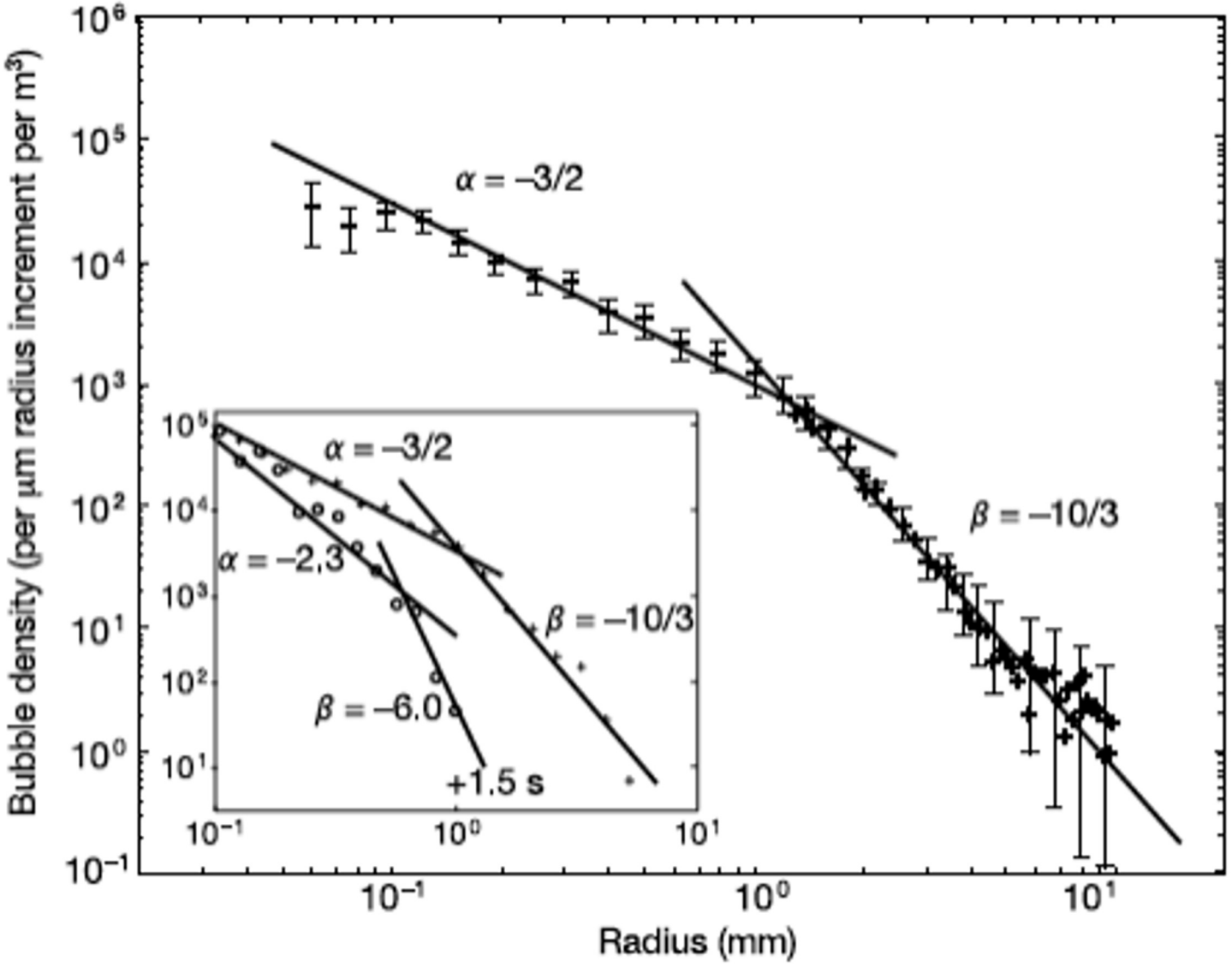
Bubble density (per µm radius increment per m³)
Radius (mm)
α = –3/2
β = –10/3
α = –3/2
α = –2.3
β = –10/3
β = –6.0
+1.5 s

FIGURE 4

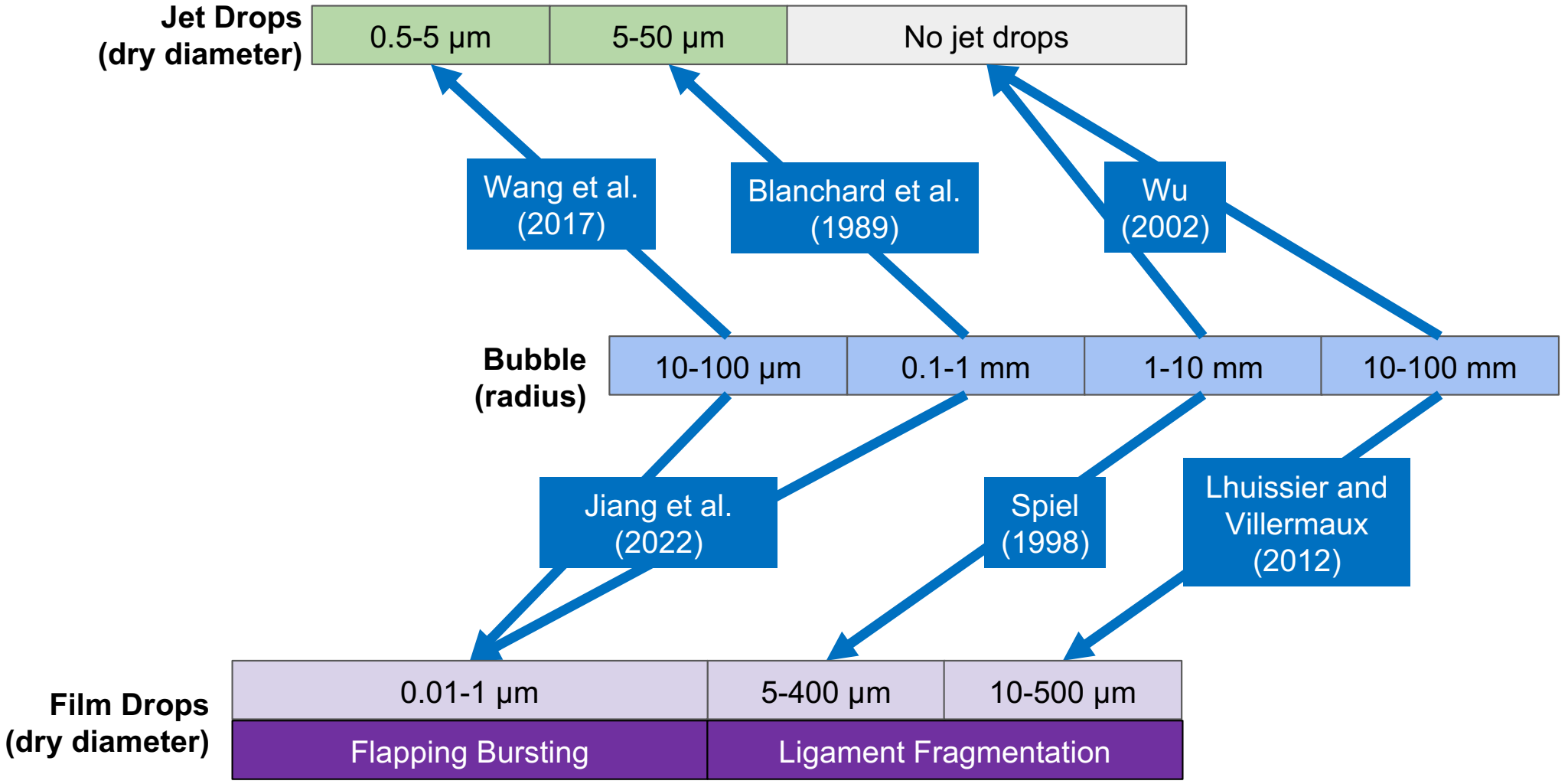
Jet Drops
(dry diameter)
0.5-5 µm
5-50 µm
No jet drops
Wang et al.
(2017)
Blanchard et al.
(1989)
Wu
(2002)
Bubble
(radius)
10-100 µm
0.1-1 mm
1-10 mm
10-100 mm
Jiang et al.
(2022)
Spiel
(1998)
Lhuissier and
Villermaux
(2012)
Film Drops
(dry diameter)
0.01-1 µm
5-400 µm
10-500 µm
Flapping Bursting
Ligament Fragmentation

FIGURE 5

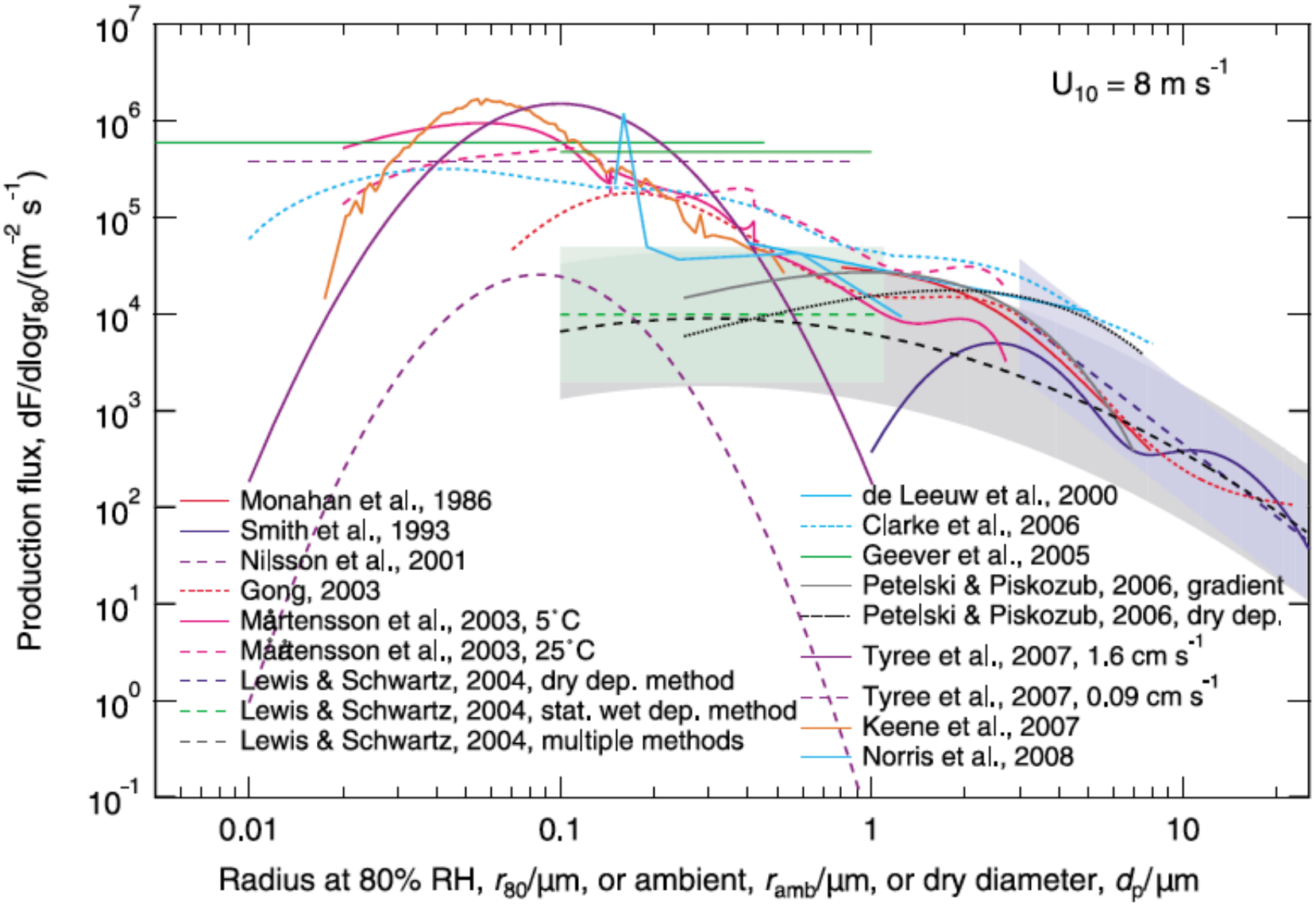
U_{10} = 8 m s^{-1}
Production flux, dF/dlogr$_{80}$/(m^{-2} s^{-1})
Radius at 80% RH, r_{80}/µm, or ambient, r_{amb}/µm, or dry diameter, d_p/µm
Monahan et al., 1986
Smith et al., 1993
Nilsson et al., 2001
Gong, 2003
Mårtensson et al., 2003, 5˚C
Mårtensson et al., 2003, 25˚C
Lewis & Schwartz, 2004, dry dep. method
Lewis & Schwartz, 2004, stat. wet dep. method
Lewis & Schwartz, 2004, multiple methods
de Leeuw et al., 2000
Clarke et al., 2006
Geever et al., 2005
Petelski & Piskozub, 2006, gradient
Petelski & Piskozub, 2006, dry dep.
Tyree et al., 2007, 1.6 cm s^{-1}
Tyree et al., 2007, 0.09 cm s^{-1}
Keene et al., 2007
Norris et al., 2008

FIGURE 6

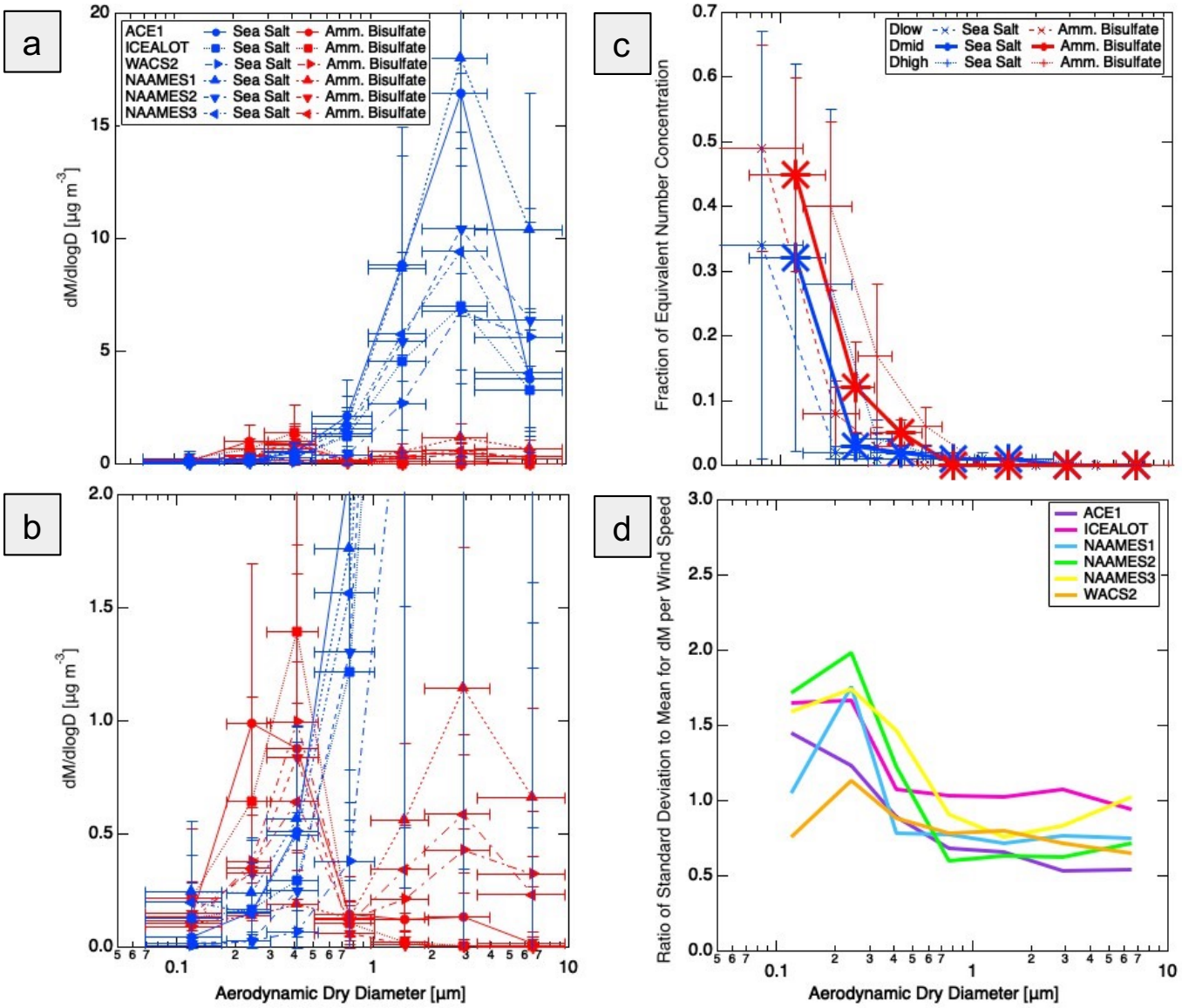
a
ACE1 Sea Salt Amm. Bisulfate
ICEALOT Sea Salt Amm. Bisulfate
WACS2 Sea Salt Amm. Bisulfate
NAAMES1 Sea Salt Amm. Bisulfate
NAAMES2 Sea Salt Amm. Bisulfate
NAAMES3 Sea Salt Amm. Bisulfate
dM/dlogD [µg m-3]
b
dM/dlogD [µg m-3]
Aerodynamic Dry Diameter [µm]
c
Dlow Sea Salt Amm. Bisulfate
Dmid Sea Salt Amm. Bisulfate
Dhigh Sea Salt Amm. Bisulfate
Fraction of Equivalent Number Concentration
d
ACE1
ICEALOT
NAAMES1
NAAMES2
NAAMES3
WACS2
Ratio of Standard Deviation to Mean for dM per Wind Speed
Aerodynamic Dry Diameter [µm]

FIGURE 7

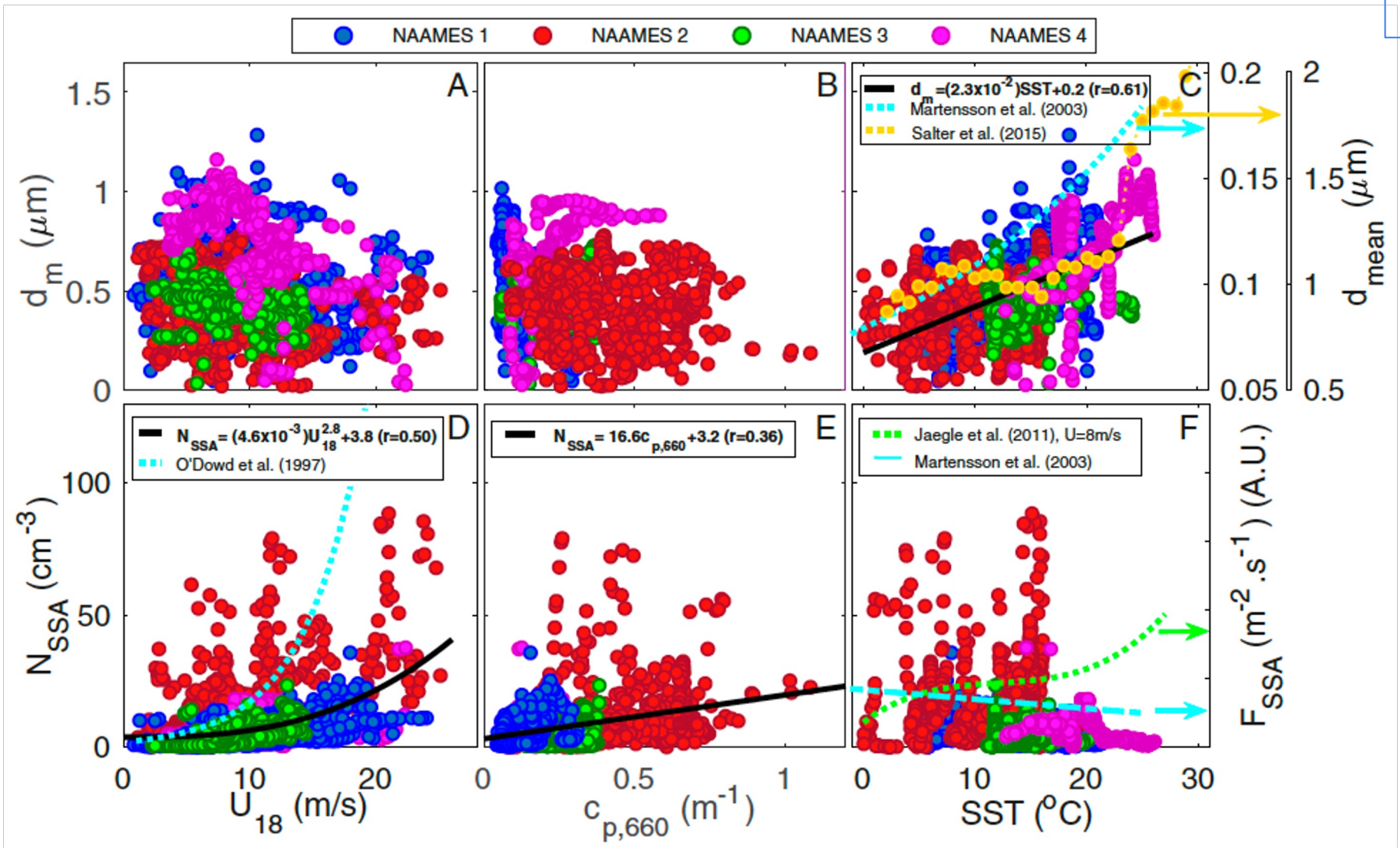
NAAMES 1
NAAMES 2
NAAMES 3
NAAMES 4
A
B
C
D
E
F
d_m (μm)
d_m=(2.3x10^{-2})SST+0.2 (r=0.61)
Martensson et al. (2003)
Salter et al. (2015)
d_{mean} (μm)
N_{SSA}= (4.6x10^{-3})$U_{18}^{2.8}$+3.8 (r=0.50)
O'Dowd et al. (1997)
N_{SSA} (cm^{-3})
N_{SSA}= 16.6$c_{p,660}$+3.2 (r=0.36)
Jaegle et al. (2011), U=8m/s
Martensson et al. (2003)
F_{SSA} (m^{-2}.s^{-1}) (A.U.)
U_{18} (m/s)
$c_{p,660}$ (m^{-1})
SST (^{o}C)

FIGURE 8

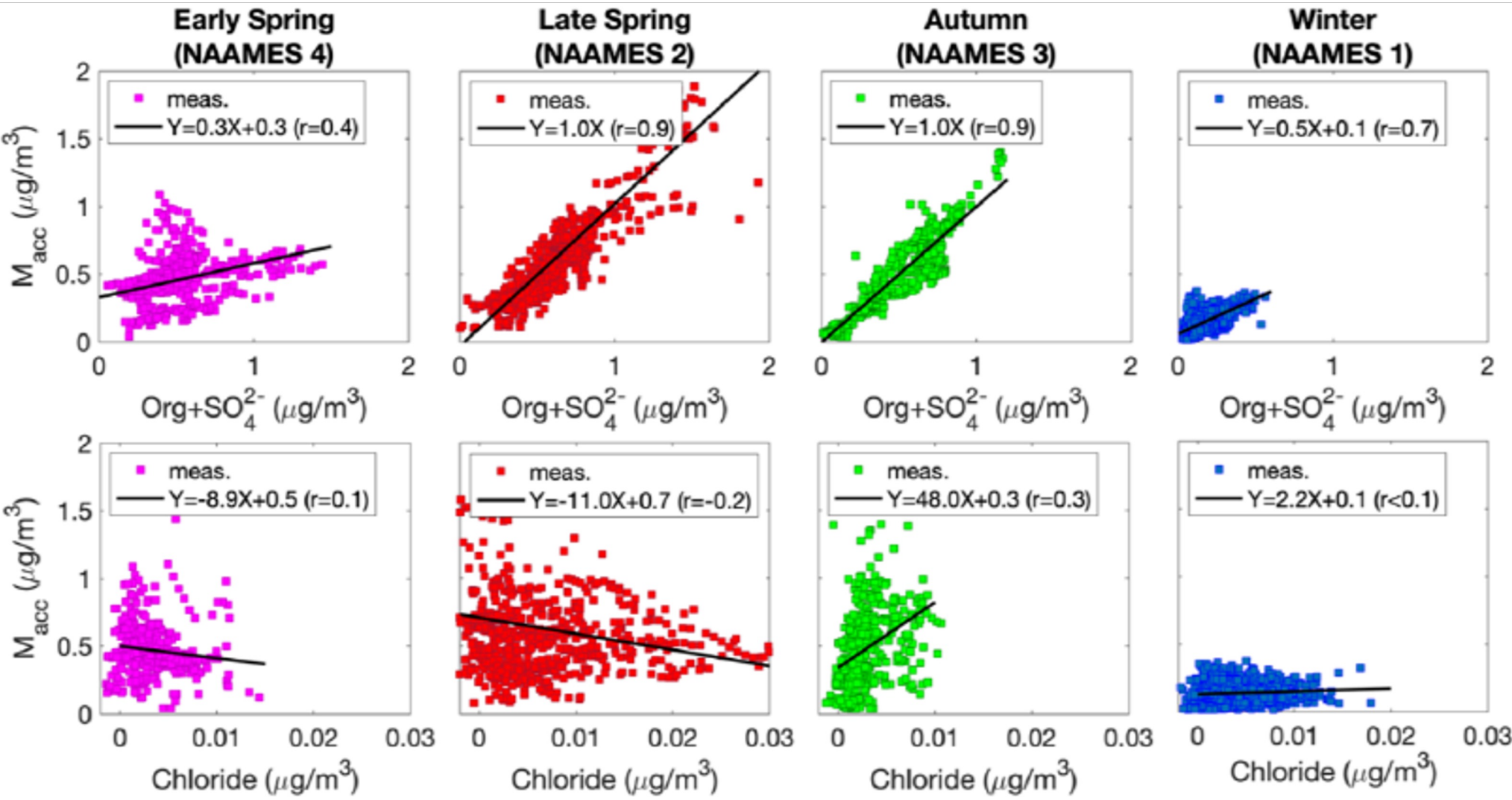
Early Spring
(NAAMES 4)
Late Spring
(NAAMES 2)
Autumn
(NAAMES 3)
Winter
(NAAMES 1)
meas.
Y=0.3X+0.3 (r=0.4)
Y=1.0X (r=0.9)
Y=1.0X (r=0.9)
Y=0.5X+0.1 (r=0.7)
Y=-8.9X+0.5 (r=0.1)
Y=-11.0X+0.7 (r=-0.2)
Y=48.0X+0.3 (r=0.3)
Y=2.2X+0.1 (r<0.1)
M_acc (μg/m^3)
Org+SO4^2- (μg/m^3)
Chloride (μg/m^3)

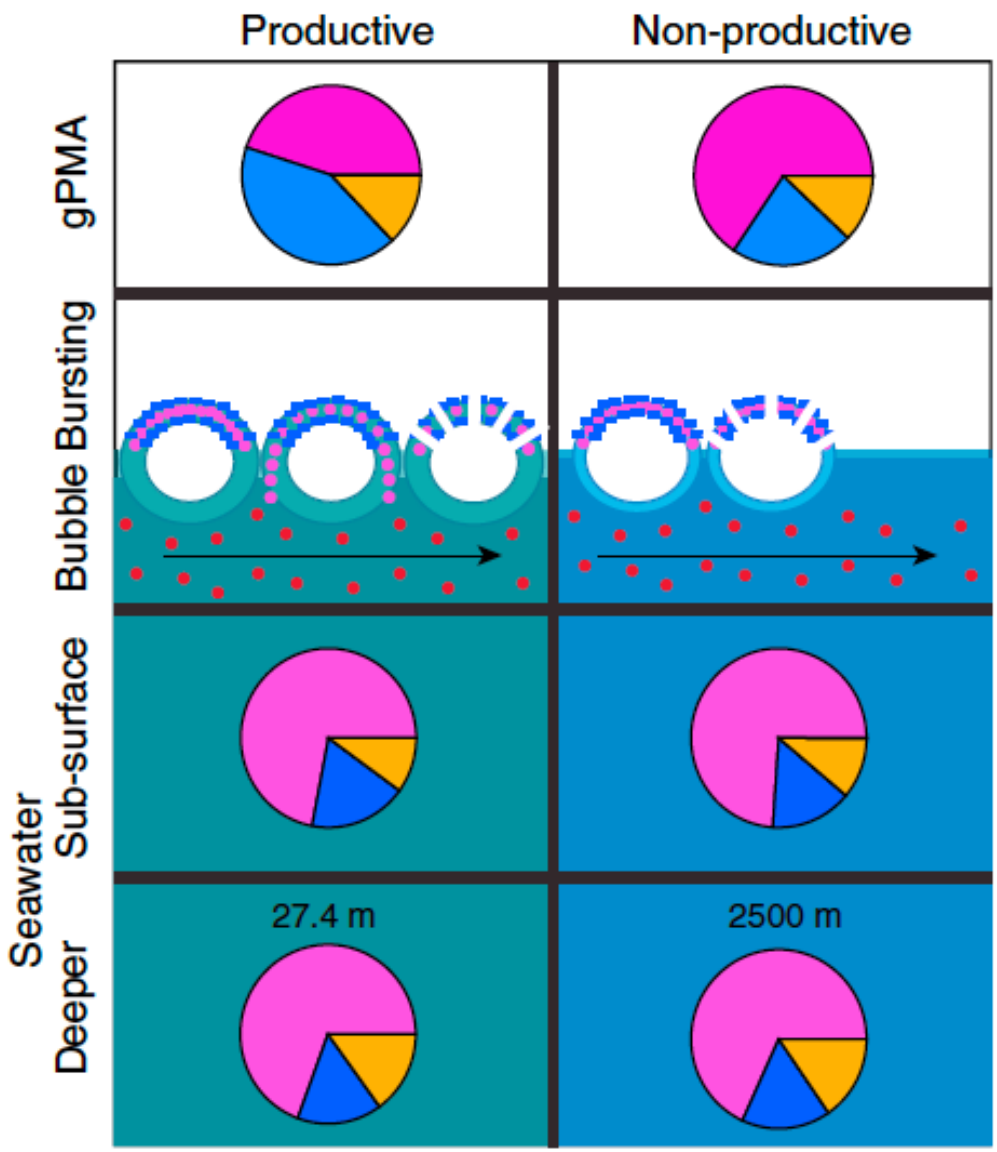
Productive
Non-productive
gPMA
Bubble Bursting
Seawater
Sub-surface
Deeper
27.4 m
2500 m

FIGURE 9

FIGURE 10

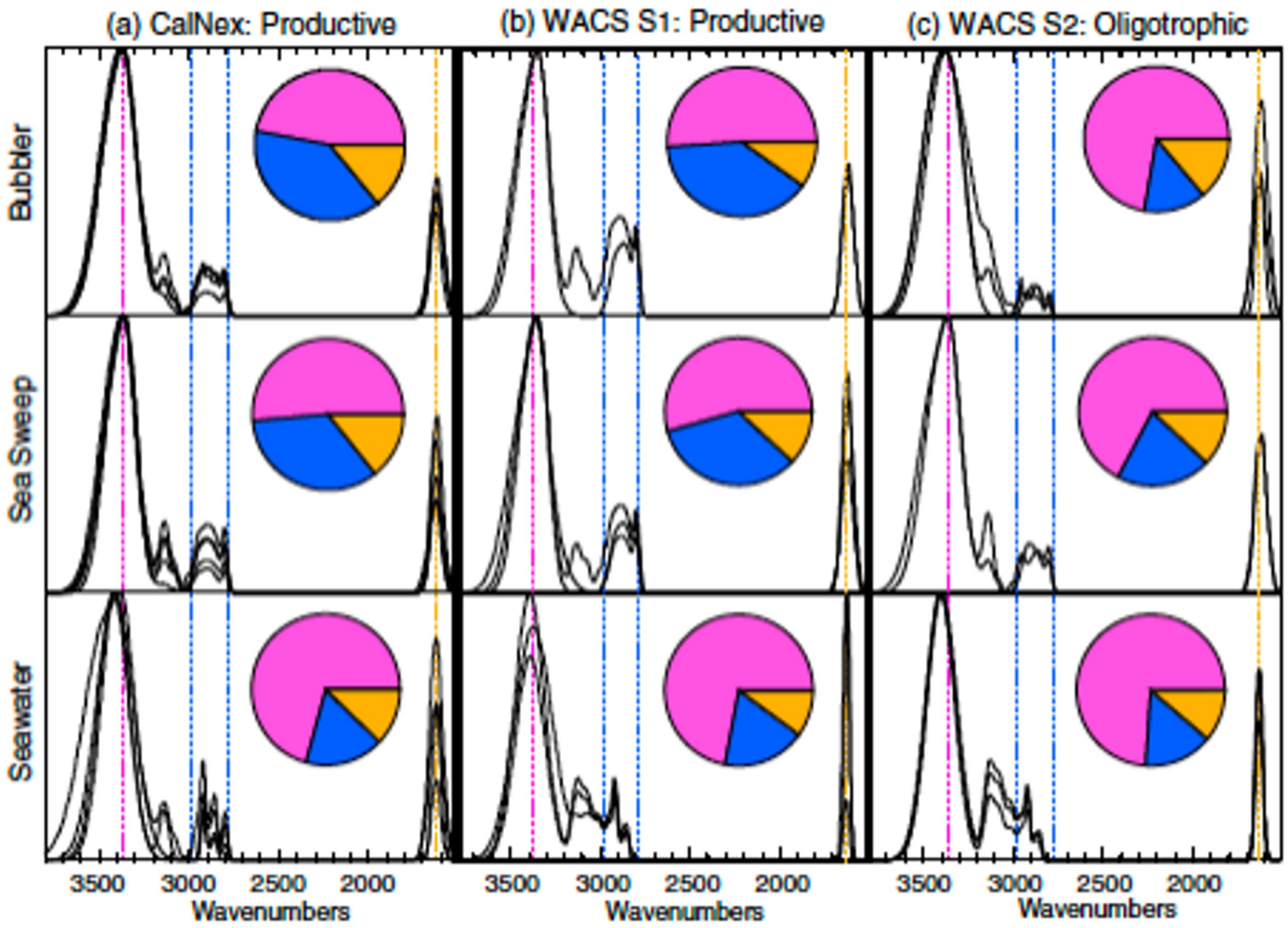
(a) CalNex: Productive
(b) WACS S1: Productive
(c) WACS S2: Oligotrophic
Bubbler
Sea Sweep
Seawater
3500
3000
2500
2000
Wavenumbers

FIGURE 11

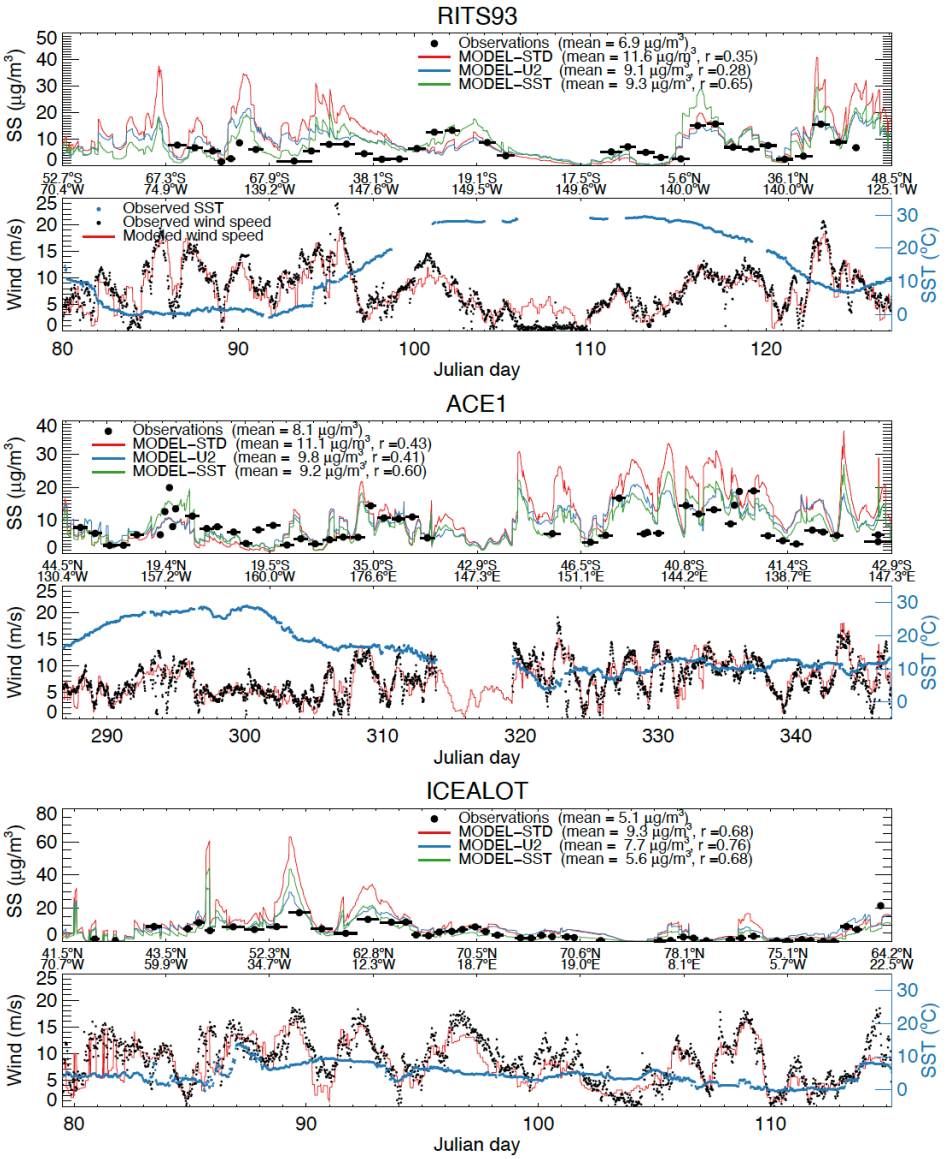
RITS93
Observations (mean = 6.9 µg/m³)
MODEL–STD (mean = 11.6 µg/m³, r =0.35)
MODEL–U2 (mean = 9.1 µg/m³, r =0.28)
MODEL–SST (mean = 9.3 µg/m³, r =0.65)
SS (µg/m³)
52.7°S 70.4°W
67.3°S 74.9°W
67.9°S 139.2°W
38.1°S 147.6°W
19.1°S 149.5°W
17.5°S 149.6°W
5.6°N 140.0°W
36.1°N 140.0°W
48.5°N 125.1°W
Observed SST
Observed wind speed
Modeled wind speed
Wind (m/s)
SST (°C)
Julian day
ACE1
Observations (mean = 8.1 µg/m³)
MODEL–STD (mean = 11.1 µg/m³, r =0.43)
MODEL–U2 (mean = 9.8 µg/m³, r =0.41)
MODEL–SST (mean = 9.2 µg/m³, r =0.60)
SS (µg/m³)
44.5°N 130.4°W
19.4°N 157.2°W
19.5°S 160.0°W
35.0°S 176.6°E
42.9°S 147.3°E
46.5°S 151.1°E
40.8°S 144.2°E
41.4°S 138.7°E
42.9°S 147.3°E
Wind (m/s)
SST (°C)
Julian day
ICEALOT
Observations (mean = 5.1 µg/m³)
MODEL–STD (mean = 9.3 µg/m³, r =0.68)
MODEL–U2 (mean = 7.7 µg/m³, r =0.76)
MODEL–SST (mean = 5.6 µg/m³, r =0.68)
SS (µg/m³)
41.5°N 70.7°W
43.5°N 59.9°W
52.3°N 34.7°W
62.8°N 12.3°W
70.5°N 18.7°E
70.6°N 19.0°E
78.1°N 8.1°E
75.1°N 5.7°W
64.2°N 22.5°W
Wind (m/s)
SST (°C)
Julian day

FIGURE 12

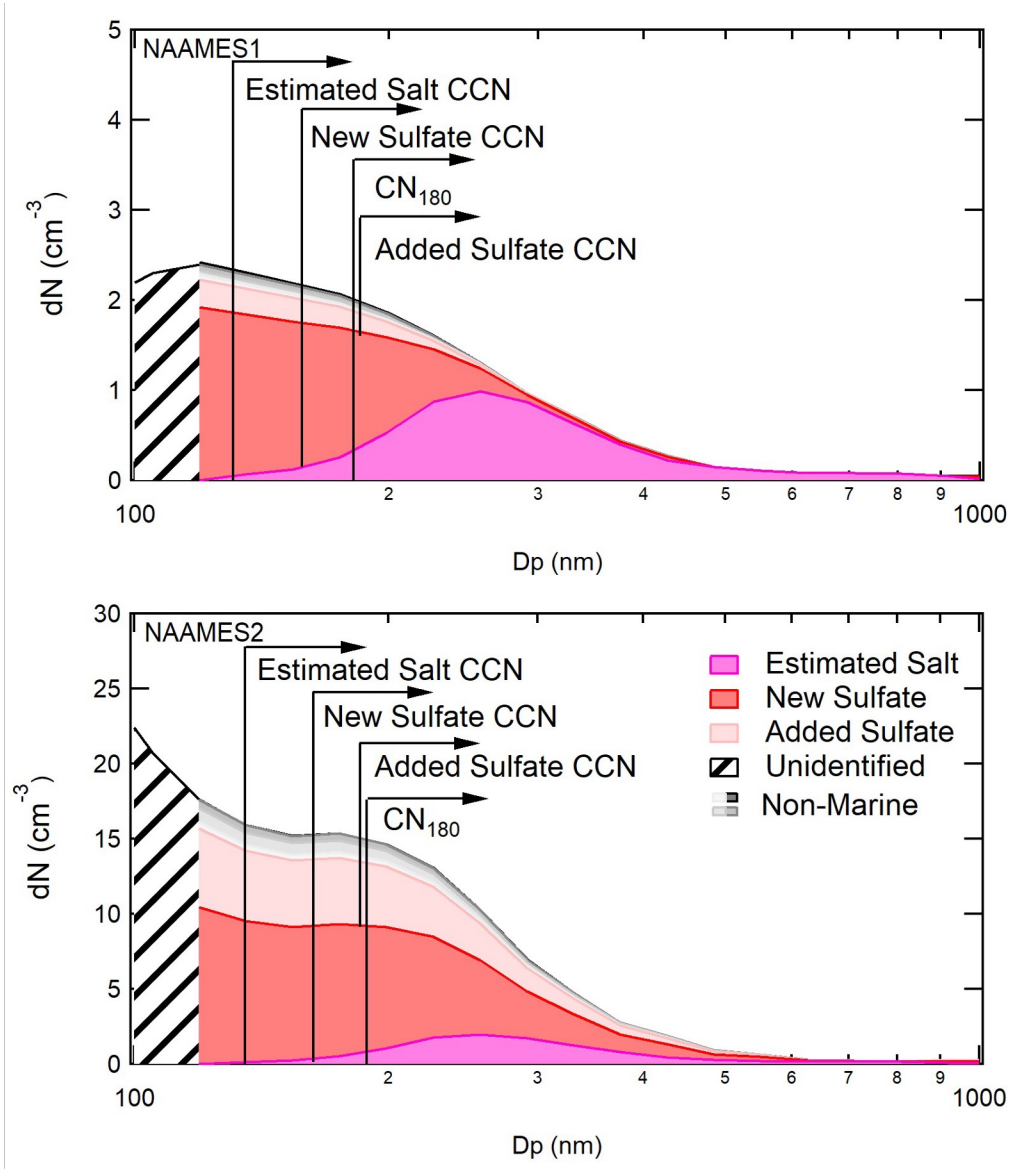
NAAMES1
Estimated Salt CCN
New Sulfate CCN
CN180
Added Sulfate CCN
dN (cm-3)
Dp (nm)
NAAMES2
Estimated Salt CCN
New Sulfate CCN
Added Sulfate CCN
CN180
Estimated Salt
New Sulfate
Added Sulfate
Unidentified
Non-Marine
dN (cm-3)
Dp (nm)

FIGURE 13

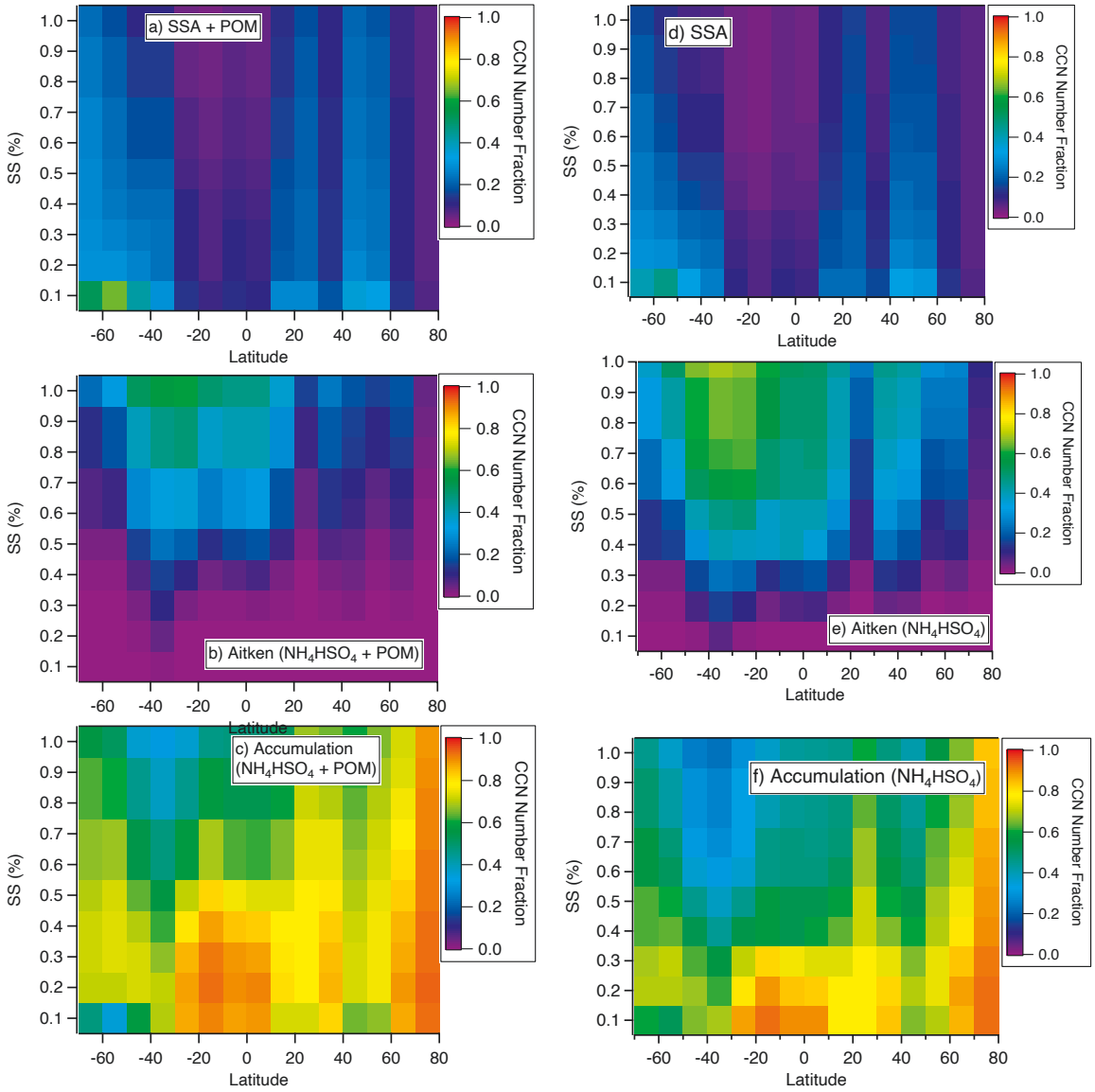
a) SSA + POM
b) Aitken (NH_4HSO_4 + POM)
c) Accumulation (NH_4HSO_4 + POM)
d) SSA
e) Aitken (NH_4HSO_4)
f) Accumulation (NH_4HSO_4)
SS (%)
Latitude
CCN Number Fraction

FIGURE 14

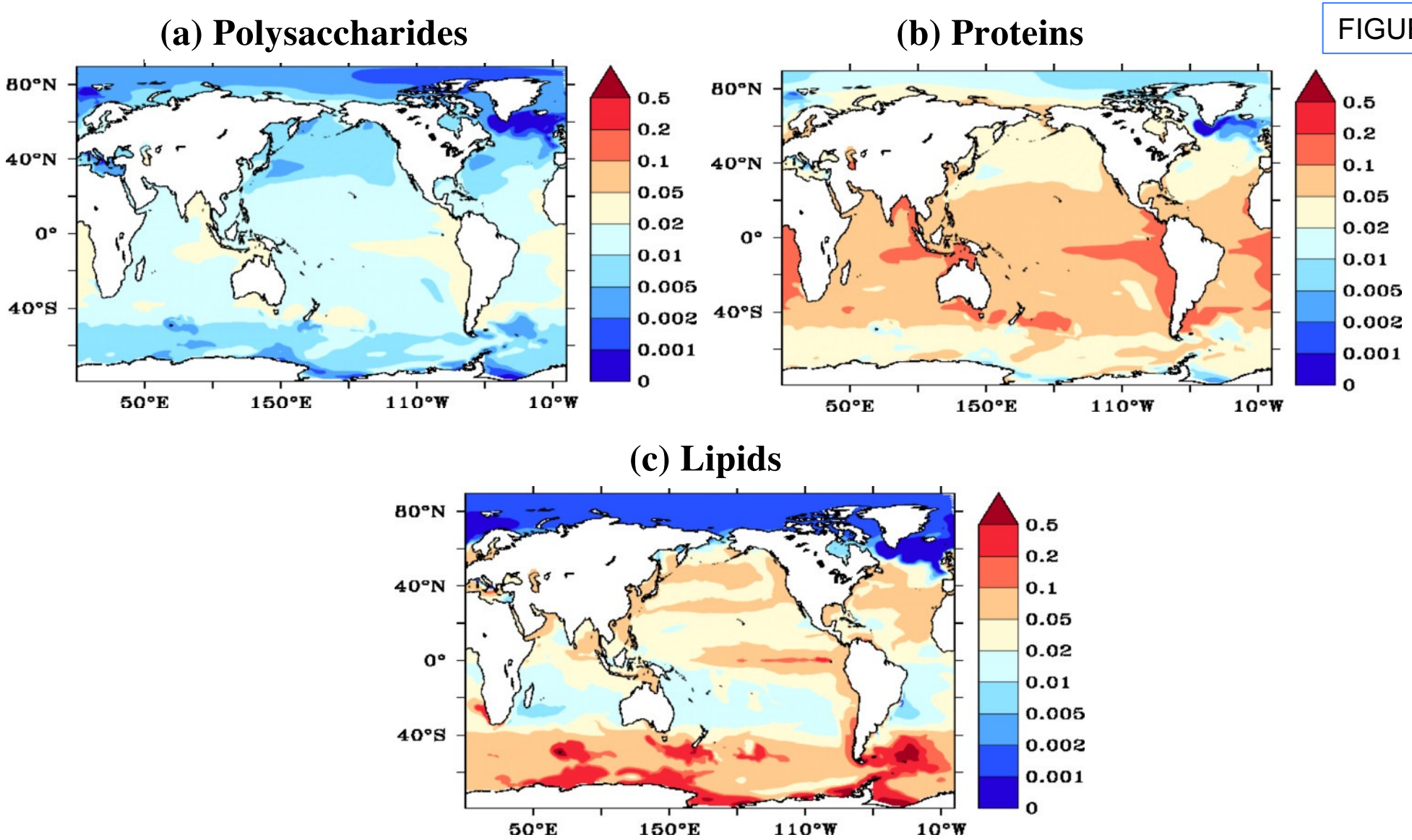
(a) Polysaccharides
(b) Proteins
(c) Lipids
80°N
40°N
0°
40°S
50°E
150°E
110°W
10°W
0.5
0.2
0.1
0.05
0.02
0.01
0.005
0.002
0.001
0

FIGURE 15

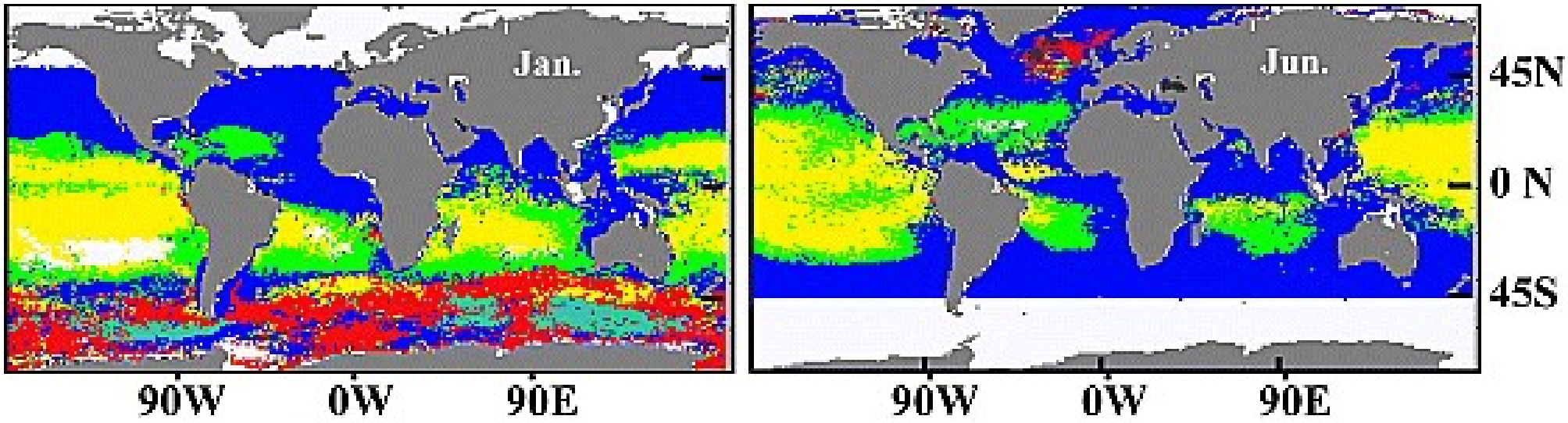

FIGURE 16

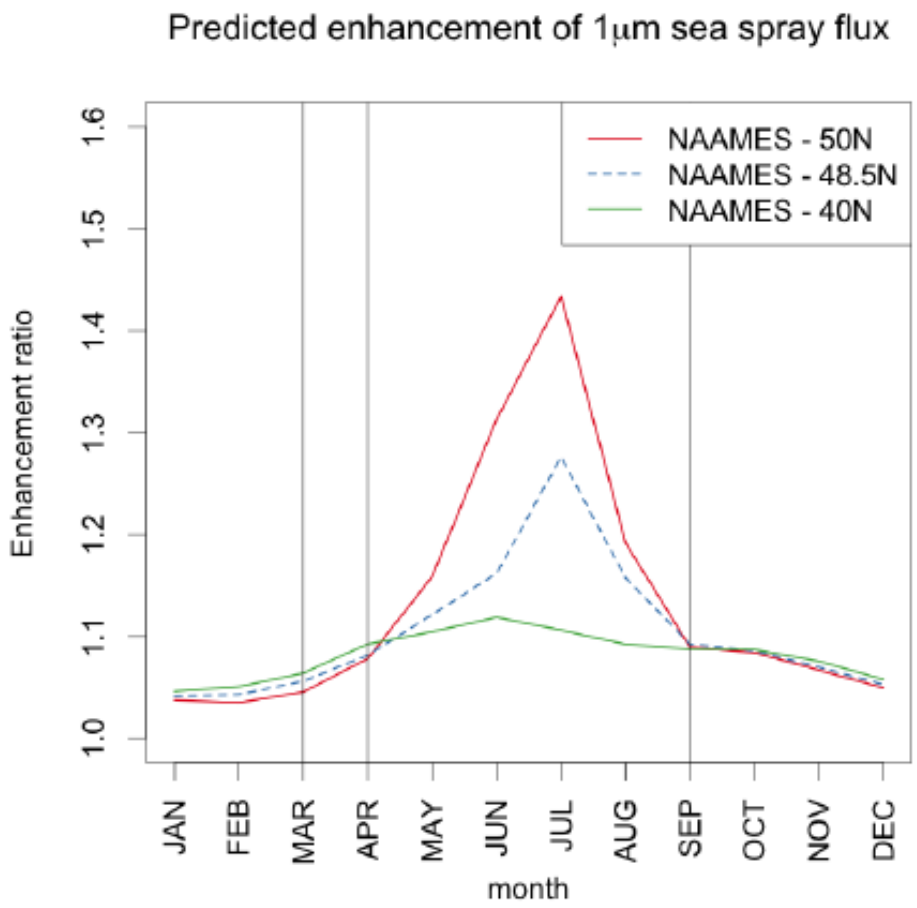
Predicted enhancement of 1μm sea spray flux
Enhancement ratio
1.0
1.1
1.2
1.3
1.4
1.5
1.6
NAAMES - 50N
NAAMES - 48.5N
NAAMES - 40N
JAN
FEB
MAR
APR
MAY
JUN
JUL
AUG
SEP
OCT
NOV
DEC
month

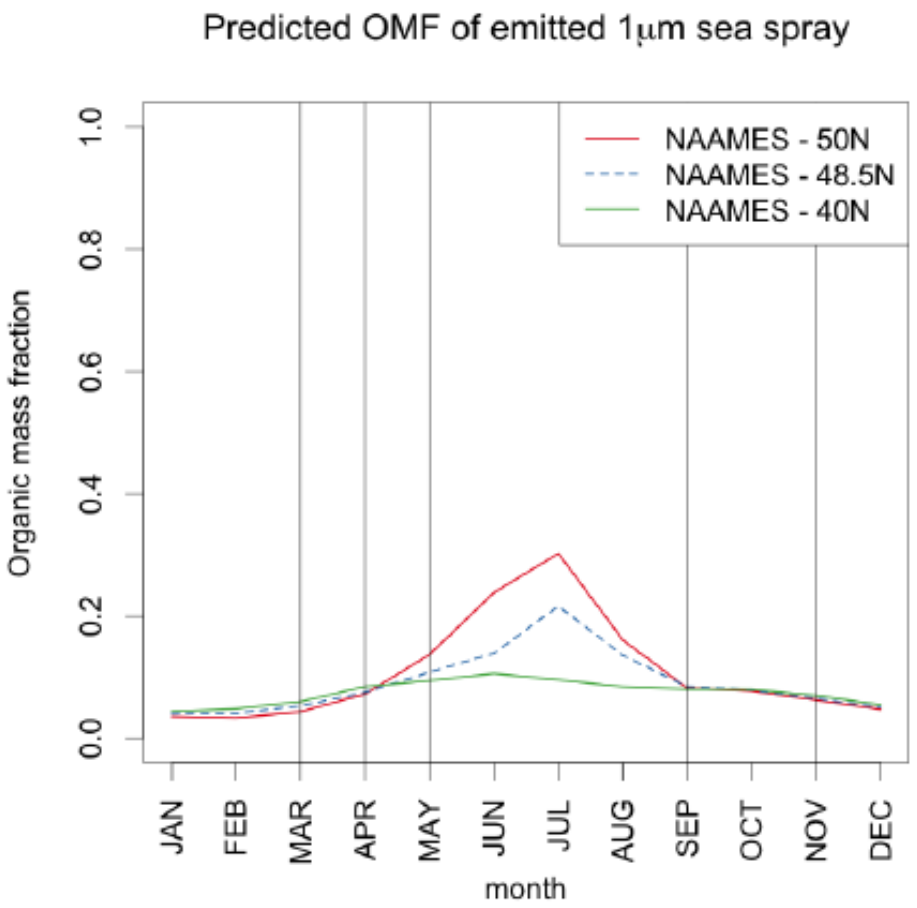
Predicted OMF of emitted 1μm sea spray
Organic mass fraction
0.0
0.2
0.4
0.6
0.8
1.0
NAAMES - 50N
NAAMES - 48.5N
NAAMES - 40N
JAN
FEB
MAR
APR
MAY
JUN
JUL
AUG
SEP
OCT
NOV
DEC
month

REFERENCES CITED

Abbatt, J. P. D., Leaitch, W. R., Aliabadi, A. A., Bertram, A. K., Blanchet, J. P., Boivin-Rioux, A., . . . Yakobi-Hancock, J. D. (2019). Overview paper: New insights into aerosol and climate in the Arctic. *Atmospheric Chemistry and Physics*, *19*(4), 2527-2560. https://doi.org/10.5194/acp-19-2527-2019

Albert, M., Anguelova, M. D., Manders, A. M. M., Schaap, M., & de Leeuw, G. (2016). Parameterization of oceanic whitecap fraction based on satellite observations. *Atmospheric Chemistry and Physics*, *16*(21), 13725-13751. https://doi.org/10.5194/acp-16-13725-2016

Aller, J. Y., Radway, J. C., Kilthau, W. P., Bothe, D. W., Wilson, T. W., Vaillancourt, R. D., . . . Knopf, D. A. (2017). Size-resolved characterization of the polysaccharidic and proteinaceous components of sea spray aerosol. *Atmospheric Environment*, *154*, 331-347. https://doi.org/10.1016/j.atmosenv.2017.01.053

Alpert, P. A., Ciuraru, R., Rossignol, S., Passananti, M., Tinel, L., Perrier, S., . . . George, C. (2017). Fatty Acid Surfactant Photochemistry Results in New Particle Formation. *Scientific Reports*, *7*, Article 12693. https://doi.org/10.1038/s41598-017-12601-2

Aluwihare, L. I., Repeta, D. J., & Chen, R. F. (1997). A major biopolymeric component to dissolved organic carbon in surface sea water. *Nature*, *387*(6629), 166-169. https://doi.org/10.1038/387166a0

Aluwihare, L. I., Repeta, D. J., Pantoja, S., & Johnson, C. G. (2005). Two chemically distinct pools of organic nitrogen accumulate in the ocean. *Science*, *308*(5724), 1007-1010. https://doi.org/10.1126/science.1108925

Alvain, S., Moulin, C., Dandonneau, Y., & Loisel, H. (2008). Seasonal distribution and succession of dominant phytoplankton groups in the global ocean: A satellite view. *Global Biogeochemical Cycles*, *22*(3), Article Gb3001. https://doi.org/10.1029/2007gb003154

Andreae, M. O., Elbert, W., & Demora, S. J. (1995). BIOGENIC SULFUR EMISSIONS AND AEROSOLS OVER THE TROPICAL SOUTH-ATLANTIC .3. ATMOSPHERIC DIMETHYLSULFIDE, AEROSOLS AND CLOUD CONDENSATION NUCLEI. *Journal of Geophysical Research-Atmospheres*, *100*(D6), 11335-11356. https://doi.org/10.1029/94jd02828

Andreas, E. L., & Monahan, E. C. (2000). The role of whitecap bubbles in air-sea heat and moisture exchange. *Journal of Physical Oceanography*, *30*(2), 433-442. https://doi.org/10.1175/1520-0485(2000)030<0433:trowbi>2.0.co;2

Anguelova, M., Barber, R. P., & Wu, J. (1999). Spume drops produced by the wind tearing of wave crests. *Journal of Physical Oceanography*, *29*(6), 1156-1165. https://doi.org/10.1175/1520-0485(1999)029<1156:sdpbtw>2.0.co;2

Anguelova, M. D., & Webster, F. (2006). Whitecap coverage from satellite measurements: A first step toward modeling the variability of oceanic whitecaps. *Journal of Geophysical Research-Oceans*, *111*(C3), Article C03017. https://doi.org/10.1029/2005jc003158

Asmi, E., Neitola, K., Teinila, K., Rodriguez, E., Virkkula, A., Backman, J., . . . Sanchez, R. (2018). Primary sources control the variability of aerosol optical properties in the Antarctic Peninsula. *Tellus Series B-Chemical and Physical Meteorology*, *70*, Article 1414571. https://doi.org/10.1080/16000889.2017.1414571

Ault, A. P., Zhao, D. F., Ebben, C. J., Tauber, M. J., Geiger, F. M., Prather, K. A., & Grassian, V. H. (2013a). Raman microscpectroscopy and vibrational sum frequency generation spectroscopy as probles of the bulk and surface compositions of size-resolved sea spray particles. *Physical Chemistry - Chemical Physics*, *15*(17), 6206-6214.

Ault, A. P., Zhao, D. F., Ebben, C. J., Tauber, M. J., Geiger, F. M., Prather, K. A., & Grassian, V. H. (2013b). Raman microspectroscopy and vibrational sum frequency generation

spectroscopy as probes of the bulk and surface compositions of size-resolved sea spray aerosol particles. *Physical Chemistry Chemical Physics*, *15*(17), 6206-6214. https://doi.org/10.1039/c3cp43899f

Ayers, G. P., & Gras, J. L. (1991). SEASONAL RELATIONSHIP BETWEEN CLOUD CONDENSATION NUCLEI AND AEROSOL METHANESULFONATE IN MARINE AIR. *Nature*, *353*(6347), 834-835. https://doi.org/10.1038/353834a0

Bates, T. S., P.K. Quinn, D. Coffman, D. Covert, L.M. Russell, and J. Burkhart. (2009). Aerosol chemical, physical, and optical properties over the ice-free region of the Arctic during the International Chemistry Experiment in the Arctic Lower Troposphere (ICEALOT).

Bates, T. S., Quinn, P. K., Coffman, D. J., Johnson, J. E., Upchurch, L., Saliba, G., . . . Behrenfeld, M. J. (2020). Variability in Marine Plankton Ecosystems Are Not Observed in Freshly Emitted Sea Spray Aerosol Over the North Atlantic Ocean. *Geophysical Research Letters*, *47*(1), Article e2019GL085938. https://doi.org/10.1029/2019gl085938

Bates, T. S., Quinn, P. K., Frossard, A. A., Russell, L. M., Hakala, J., Petaja, T., . . . Keene, W. C. (2012). Measurements of ocean derived aerosol off the coast of California. *Journal of Geophysical Research-Atmospheres*, *117*. https://doi.org/10.1029/2012jd017588

Bates, T. S., Quinn, P. K., Frossard, A. A., Russell, L. M., Hakala, J., Petäjä, T., . . . Keene, W. C. (2012). Measurements of Ocean Derived Aerosol off the Coast of California. *Journal of Geophysical Research - Atmospheres*, *117*(D00V15). https://doi.org/10.1029/2012JD017588

Behrenfeld, M. J., Moore, R. H., Hostetler, C. A., Graff, J., Gaube, P., Russell, L. M., . . . Ziemba, L. (2019). The North Atlantic Aerosol and Marine Ecosystem Study (NAAMES): Science Motive and Mission Overview. *Frontiers in Marine Science*, *6*(122). https://doi.org/10.3389/fmars.2019.00122

Belviso, S., Moulin, C., Bopp, L., & Stefels, J. (2004). Assessment of a global climatology of oceanic dimethylsulfide (DMS) concentrations based on SeaWiFS imagery (1998-2001). *Canadian Journal of Fisheries and Aquatic Sciences*, *61*(5), 804-816. https://doi.org/10.1139/f04-001

Bernard, F., Ciuraru, R., Boreave, A., & George, C. (2016). Photosensitized Formation of Secondary Organic Aerosols above the Air/Water Interface. *Environmental Science & Technology*, *50*(16), 8678-8686. https://doi.org/10.1021/acs.est.6b03520

Berta, V., Russell, L. M., Price, D. J., Chen, C. L., Lee, A., Quinn, P. K., . . . Behrenfeld, M. (2022 in review). Comparison of non-volatile marine and and non-refractory continental sources of particle-phase amine during the North Atlantic Aerosols and Marine Ecosystems Study (NAAMES). https://doi.org/https://doi.org/10.5194/acp-2022-601

Bigg, E. K. (2007). Sources, nature and influence on climate of marine airborne particles. *Environmental Chemistry*, *4*(3), 155-161. https://doi.org/10.1071/en07001

Bigg, E. K., & Leck, C. (2008). The composition of fragments of bubbles bursting at the ocean surface. *Journal of Geophysical Research-Atmospheres*, *113*(D11). https://doi.org/10.1029/2007jd009078

Bird, J. C., de Ruiter, R., Courbin, L., & Stone, H. A. (2010). Daughter bubble cascades produced by folding of ruptured thin films. *Nature*, *465*(7299), 759-762. https://doi.org/10.1038/nature09069

Blanchard, D. C. (1989). THE SIZE AND HEIGHT TO WHICH JET DROPS ARE EJECTED FROM BURSTING BUBBLES IN SEAWATER. *Journal of Geophysical Research-Oceans*, *94*(C8), 10999-11002. https://doi.org/10.1029/JC094iC08p10999

Blomquist, B. W., Brumer, S. E., Fairall, C. W., Huebert, B. J., Zappa, C. J., Brooks, I. M., . . . Pascal, R. W. (2017). Wind Speed and Sea State Dependencies of Air-Sea Gas Transfer: Results From the High Wind Speed Gas Exchange Study (HiWinGS). *Journal of Geophysical Research-Oceans*, *122*(10), 8034-8062. https://doi.org/10.1002/2017jc013181

Blomquist, B. W., Huebert, B. J., Fairall, C. W., Bariteau, L., Edson, J. B., Hare, J. E., & McGillis, W. R. (2014). Advances in Air-Sea Flux Measurement by Eddy Correlation. *Boundary-Layer Meteorology*, *152*(3), 245-276. https://doi.org/10.1007/s10546-014-9926-2

Blot, R., Clarke, A. D., Freitag, S., Kapustin, V., Howell, S. G., Jensen, J. B., . . . Brekhovskikh, V. (2013). Ultrafine sea spray aerosol over the southeastern Pacific: open-ocean contributions to marine boundary layer CCN. *Atmospheric Chemistry and Physics*, *13*(14), 7263-7278. https://doi.org/10.5194/acp-13-7263-2013

Bock, J., Michou, M., Nabat, P., Abe, M., Mulcahy, J. P., Olivie, D. J. L., . . . Seferian, R. (2021). Evaluation of ocean dimethylsulfide concentration and emission in CMIP6 models. *Biogeosciences*, *18*(12), 3823-3860. https://doi.org/10.5194/bg-18-3823-2021

Bondy, A. L., Kirpes, R. M., Merzel, R. L., Pratt, K. A., Holl, M. M. B., & Ault, A. P. (2017). Atomic Force Microscopy-Infrared Spectroscopy of Individual Atmospheric Aerosol Particles: Subdiffraction Limit Vibrational Spectroscopy and Morphological Analysis. *Analytical Chemistry*, *89*(17), 8594-8598. https://doi.org/10.1021/acs.analchem.7b02381

Bottenus, C. L. H., Massoli, P., Sueper, D., Canagaratna, M. R., VanderSchelden, G., Jobson, B. T., & VanReken, T. M. (2018). Identification of amines in wintertime ambient particulate material using high resolution aerosol mass spectrometry. *Atmospheric Environment*, *180*, 173-183. https://doi.org/10.1016/j.atmosenv.2018.01.044

Browse, J., Carslaw, K. S., Mann, G. W., Birch, C. E., Arnold, S. R., & Leck, C. (2014). The complex response of Arctic aerosol to sea-ice retreat. *Atmospheric Chemistry and Physics*, *14*(14), 7543-7557. https://doi.org/10.5194/acp-14-7543-2014

Brumer, S. E., Zappa, C. J., Brooks, I. M., Tamura, H., Brown, S. M., Blomquist, B. W., . . . Cifuentes-Lorenzen, A. (2017). Whitecap Coverage Dependence on Wind and Wave Statistics as Observed during SO GasEx and HiWinGS. *Journal of Physical Oceanography*, *47*(9), 2211-2235. https://doi.org/10.1175/jpo-d-17-0005.1

Burrows, S. M., Easter, R., Liu, X., Ma, P. L., Wang, H., Elliott, S. M., . . . Rasch, P. J. (2018). OCEANFILMS sea-spray organic aerosol emissions – Part 1: implementation and impacts on clouds. *Atmos. Chem. Phys. Discuss.*, *2018*, 1-27. https://doi.org/10.5194/acp-2018-70

Burrows, S. M., Easter, R. C., Liu, X. H., Ma, P. L., Wang, H. L., Elliott, S. M., . . . Rasch, P. J. (2022). OCEANFILMS (Organic Compounds from Ecosystems to Aerosols: Natural Films and Interfaces via Langmuir Molecular Surfactants) sea spray organic aerosol emissions - implementation in a global climate model and impacts on clouds. *Atmospheric Chemistry and Physics*, *22*(8), 5223-5251. https://doi.org/10.5194/acp-22-5223-2022

Burrows, S. M., Gobrogge, E., Fu, L., Link, K., Elliott, S. M., Wang, H. F., & Walker, R. (2016). OCEANFILMS-2: Representing coadsorption of saccharides in marine films and potential impacts on modeled marine aerosol chemistry. *Geophysical Research Letters*, *43*(15), 8306-8313. https://doi.org/10.1002/2016gl069070

Burrows, S. M., McCluskey, C. S., Cornwell, G., Steinke, I., Zhang, K., Zhao, B., . . . DeMott, P. J. (2022). Ice-Nucleating Particles That Impact Clouds and Climate: Observational and Modeling Research Needs. *Reviews of Geophysics*, *60*(2), Article e2021RG000745. https://doi.org/10.1029/2021rg000745

Burrows, S. M., Ogunro, O., Frossard, A. A., Russell, L. M., Rasch, P. J., & Elliott, S. M. (2014). A physically based framework for modeling the organic fractionation of sea spray aerosol from bubble film Langmuir equilibria. *Atmospheric Chemistry and Physics*, *14*(24), 13601-13629. https://doi.org/10.5194/acp-14-13601-2014

Callaghan, A. H., Deane, G. B., & Stokes, M. D. (2008). Observed physical and environmental causes of scatter in whitecap coverage values in a fetch-limited coastal zone. *Journal of*

Geophysical Research-Oceans, *113*(C5), Article C05022. https://doi.org/10.1029/2007jc004453
Carlson, C. A., & Hansell, D. A. (2015). DOM Sources, Sinks, Reactivity, and Budgets. *Biogeochemistry of Marine Dissolved Organic Matter, 2nd Edition*, 65-126. https://doi.org/10.1016/b978-0-12-405940-5.00003-0
Cavalli, F., Facchini, M. C., Decesari, S., Mircea, M., Emblico, L., Fuzzi, S., . . . Dell'Acqua, A. (2004). Advances in characterization of size-resolved organic matter in marine aerosol over the North Atlantic. *Journal of Geophysical Research-Atmospheres*, *109*(D24). https://doi.org/D24215
10.1029/2004jd005137
Ceburnis, D., O'Dowd, C. D., Jennings, G. S., Facchini, M. C., Emblico, L., Decesari, S., . . . Sakalys, J. (2008a). Marine aerosol chemistry gradients: Elucidating primary and secondary processes and fluxes. *Geophysical Research Letters*, *35*(7). https://doi.org/10.1029/2008gl033462
Ceburnis, D., O'Dowd, C. D., Jennings, G. S., Facchini, M. C., Emblico, L., Decesari, S., . . . Sakalys, J. (2008b). Marine aerosol chemistry gradients: Elucidating primary and secondary processes and fluxes. *Geophysical Research Letters*, *35*(7), -. https://doi.org/Artn L07804 Doi 10.1029/2008gl033462
Chamaillard, K., Kleefeld, C., Jennings, S. G., Ceburnis, D., & O'Dowd, C. D. (2006). Light scattering properties of sea-salt aerosol particles inferred from modeling studies and ground-based measurements. *Journal of Quantitative Spectroscopy & Radiative Transfer*, *101*(3), 498-511. https://doi.org/10.1016/j.jqsrt.2006.02.062
Chang, R. Y. W., Leck, C., Graus, M., Mueller, M., Paatero, J., Burkhart, J. F., . . . Abbatt, J. P. D. (2011). Aerosol composition and sources in the central Arctic Ocean during ASCOS. *Atmospheric Chemistry and Physics*, *11*(20), 10619-10636. https://doi.org/10.5194/acp-11-10619-2011
Charlson, R. J., Lovelock, J. E., Andreae, M. O., & Warren, S. G. (1987). OCEANIC PHYTOPLANKTON, ATMOSPHERIC SULFUR, CLOUD ALBEDO AND CLIMATE. *Nature*, *326*(6114), 655-661. https://doi.org/10.1038/326655a0
Charlson, R. J., Lovelock, J. E., Andreae, M. O., & Warren, S. G. (1987). Oceanic phytoplankton, atmospheric sulphur, cloud albedo and climate. *Nature*, *326*, 655. https://doi.org/10.1038/326655a0
Charlson, R. J., Schwartz, S. E., Hales, J. M., Cess, R. D., Coakley, J. A., Hansen, J. E., & Hofmann, D. J. (1992). Climate Forcing by Anthropogenic Aerosols. *Science*, *255*(5043), 423-430.
Chen, J., Wu, Z. J., Zhao, X., Wang, Y. J., Chen, J. C., Qiu, Y. T., . . . Li, S. M. (2021). Atmospheric Humic-Like Substances (HULIS) Act as Ice Active Entities. *Geophysical Research Letters*, *48*(14), Article e2021GL092443. https://doi.org/10.1029/2021gl092443
Claeys, M., Wang, W., Vermeylen, R., Kourtchev, I., Chi, X. G., Farhat, Y., . . . Maenhaut, W. (2010). Chemical characterisation of marine aerosol at Amsterdam Island during the austral summer of 2006-2007. *Journal of Aerosol Science*, *41*(1), 13-22. https://doi.org/10.1016/j.jaerosci.2009.08.003
Claflin, M. S., Liu, J., Russell, L. M., & Ziemann, P. J. (2021). Comparison of methods of functional group analysis using results from laboratory and field aerosol measurements. *Aerosol Science and Technology*, 1-21. https://doi.org/10.1080/02786826.2021.1918325
Clarke, A., Kapustin, V., Howell, S., Moore, K., Lienert, B., Masonis, S., . . . Covert, D. (2003). Sea-salt size distributions from breaking waves: Implications for marine aerosol production and optical extinction measurements during SEAS. *Journal of Atmospheric and Oceanic Technology*, *20*(10), 1362-1374. https://doi.org/10.1175/1520-0426(2003)020<1362:ssdfbw>2.0.co;2

Clarke, A. D., Ahlquist, N. C., & Covert, D. S. (1987). THE PACIFIC MARINE AEROSOL - EVIDENCE FOR NATURAL ACID SULFATES. *Journal of Geophysical Research-Atmospheres*, *92*(D4), 4179-4190. https://doi.org/10.1029/JD092iD04p04179
Clarke, A. D., Davis, D., Kapustin, V. N., Eisele, F., Chen, G., Paluch, I., . . . Albercook, C. (1998). Particle nucleation in the tropical boundary layer and its coupling to marine sulfur sources. *Science*, *282*(5386), 89-92. https://doi.org/10.1126/science.282.5386.89
Clarke, A. D., Eisele, F., Kapustin, V. N., Moore, K., Tanner, D., Mauldin, L., . . . Albercook, G. (1999). Nucleation in the equatorial free troposphere: Favorable environments during PEM-Tropics. *Journal of Geophysical Research-Atmospheres*, *104*(D5), 5735-5744. https://doi.org/10.1029/98jd02303
Clarke, A. D., Freitag, S., Simpson, R. M. C., Hudson, J. G., Howell, S. G., Brekhovskikh, V. L., . . . Zhou, J. (2013). Free troposphere as a major source of CCN for the equatorial pacific boundary layer: long-range transport and teleconnections. *Atmospheric Chemistry and Physics*, *13*(15), 7511-7529. https://doi.org/10.5194/acp-13-7511-2013
Clarke, A. D., & Kapustin, V. N. (2003). The Shoreline Environment Aerosol Study (SEAS): A context for marine aerosol measurements influenced by a coastal environment and long-range transport. *Journal of Atmospheric and Oceanic Technology*, *20*(10), 1351-1361. https://doi.org/10.1175/1520-0426(2003)020<1351:tseass>2.0.co;2
Clarke, A. D., Li, Z., & Litchy, M. (1996). Aerosol dynamics in the equatorial Pacific Marine boundary layer: Microphysics, diurnal cycles and entrainment. *Geophysical Research Letters*, *23*(7), 733-736. https://doi.org/10.1029/96gl00778
Clarke, A. D., Owens, S. R., & Zhou, J. C. (2006). An ultrafine sea-salt flux from breaking waves: Implications for cloud condensation nuclei in the remote marine atmosphere. *Journal of Geophysical Research-Atmospheres*, *111*(D6), Article D06202. https://doi.org/10.1029/2005jd006565
Cornwell, G. C., McCluskey, C. S., Levin, E. J. T., Suski, K. J., DeMott, P. J., Kreidenweis, S. M., & Prather, K. A. (2019). Direct Online Mass Spectrometry Measurements of Ice Nucleating Particles at a California Coastal Site. *Journal of Geophysical Research-Atmospheres*, *124*(22), 12157-12172. https://doi.org/10.1029/2019jd030466
Covert, D. S., Charlson, R. J., & Ahlquist, N. C. (1972). A Study of the Relationship of Chemical Composition and Humidity to Light Scattering by Aerosols. *Journal of Applied Meteorology*, *11*(6), 968-976. https://doi.org/10.1175/1520-0450(1972)011<0968:ASOTRO>2.0.CO;2
Covert, D. S., Kapustin, V. N., Quinn, P. K., & Bates, T. S. (1992). NEW PARTICLE FORMATION IN THE MARINE BOUNDARY-LAYER. *Journal of Geophysical Research-Atmospheres*, *97*(D18), 20581-20589. https://doi.org/10.1029/92jd02074
Crahan, K. K., Hegg, D. A., Covert, D. S., Jonsson, H., Reid, J. S., Khelif, D., & Brooks, B. J. (2004). Speciation of organic aerosols in the tropical mid-pacific and their relationship to light scattering. *Journal of the Atmospheric Sciences*, *61*(21), 2544-2558.
Crocker, D. R., Deane, G. B., Cao, R. C., Santander, M. V., Morris, C. K., Mitts, B. A., . . . Thiemens, M. H. (2022). Biologically Induced Changes in the Partitioning of Submicron Particulates Between Bulk Seawater and the Sea Surface Microlayer. *Geophysical Research Letters*, *49*(2), Article e2021GL094587. https://doi.org/10.1029/2021gl094587
Dasarathy, S., Kar, J., Tackett, J., Rodier, S. D., Lu, X., Vaughan, M., . . . Bowman, J. S. (2021). Multi-Year Seasonal Trends in Sea Ice, Chlorophyll Concentration, and Marine Aerosol Optical Depth in the Bellingshausen Sea. *Journal of Geophysical Research-Atmospheres*, *126*(21), Article e2021JD034737. https://doi.org/10.1029/2021jd034737
Dasarathy, S., Russell, L. M., Rodier, S. D., & Bowman, J. S. (2022 in review). Wind-driven and Seasonal Effects on marine aerosol production in the Bellingshausen Sea, Antarctica.
Davie-Martin, C. L., Giovannoni, S. J., Behrenfeld, M. J., Penta, W. B., & Halsey, K. H. (2020). Seasonal and Spatial Variability in the Biogenic Production and Consumption of Volatile

Organic Compounds (VOCs) by Marine Plankton in the North Atlantic Ocean. *Frontiers in Marine Science*, *7*, Article 611870. https://doi.org/10.3389/fmars.2020.611870
de Leeuw, G., Andreas, E. L., Anguelova, M. D., Fairall, C. W., Lewis, E. R., O'Dowd, C., . . . Schwartz, S. E. (2011). PRODUCTION FLUX OF SEA SPRAY AEROSOL. *Reviews of Geophysics*, *49*, Article Rg2001. https://doi.org/10.1029/2010rg000349
Deane, G. B., & Stokes, M. D. (2002). Scale dependence of bubble creation mechanisms in breaking waves. *Nature*, *418*(6900), 839-844. https://doi.org/10.1038/nature00967
Decesari, S., Finessi, E., Rinaldi, M., Paglione, M., Fuzzi, S., Stephanou, E. G., . . . Facchini, M. C. (2011). Primary and secondary marine organic aerosols over the North Atlantic Ocean during the MAP experiment. *Journal of Geophysical Research-Atmospheres*, *116*, Article D22210. https://doi.org/10.1029/2011jd016204
Dedrick, J. L., Saliba, G., Williams, A. S., Russell, L. M., & Lubin, D. (2022). Retrieval of the Sea Spray Aerosol Mode from Submicron Particle Size Distributions and Supermicron Scattering during LASIC. *Atmos. Meas. Tech. Discuss.*, *2022*, 1-43. https://doi.org/10.5194/amt-2022-46
Deike, L. (2022). Mass Transfer at the Ocean–Atmosphere Interface: The Role of Wave Breaking, Droplets, and Bubbles. *Annual Review of Fluid Mechanics*, *54*(1), 191-224. https://doi.org/10.1146/annurev-fluid-030121-014132
DeMott, P. J., Hill, T. C. J., McCluskey, C. S., Prather, K. A., Collins, D. B., Sullivan, R. C., . . . Franc, G. D. (2016). Sea spray aerosol as a unique source of ice nucleating particles. *Proceedings of the National Academy of Sciences of the United States of America*, *113*(21), 5797-5803. https://doi.org/10.1073/pnas.1514034112
Dror, T., Lehahn, Y., Altaratz, O., & Koren, I. (2018). Temporal-Scale Analysis of Environmental Controls on Sea Spray Aerosol Production Over the South Pacific Gyre. *Geophysical Research Letters*, *45*(16), 8637-8646. https://doi.org/10.1029/2018gl078707
Dziekan, P., Jensen, J. B., Grabowski, W. W., & Pawlowska, H. (2021). Impact of Giant Sea Salt Aerosol Particles on Precipitation in Marine Cumuli and Stratocumuli: Lagrangian Cloud Model Simulations. *Journal of the Atmospheric Sciences*, *78*(12), 4127-4142. https://doi.org/10.1175/jas-d-21-0041.1
Erinin, M. A., Neel, B., Ruth, D. J., Mazzatenta, M., Jaquette, R. D., Veron, F., & Deike, L. (2022). Speed and Acceleration of Droplets Generated by Breaking Wind-Forced Waves. *Geophysical Research Letters*, *49*(13), Article e2022GL098426. https://doi.org/10.1029/2022gl098426
Facchini, M. C., Decesari, S., Rinaldi, M., Carbone, C., Finessi, E., Mircea, M., . . . O'Dowd, C. D. (2008). Important source of marine secondary organic aerosol from biogenic amines. *Environmental Science & Technology*, *42*(24), 9116-9121. https://doi.org/10.1021/es8018385
Facchini, M. C., Decesari, S., Rinaldi, M., Finessi, E., Ceburnis, D., O'Dowd, C. D., & Stephanou, E. G. (2010). Marine SOA: Gas-to-particle conversion and oxidation of primary organic aerosol. *Geochimica Et Cosmochimica Acta*, *74*(12), A275-A275.
Facchini, M. C., Rinaldi, M., Decesari, S., Carbone, C., Finessi, E., Mircea, M., . . . O'Dowd, C. D. (2008). Primary submicron marine aerosol dominated by insoluble organic colloids and aggregates. *Geophysical Research Letters*, L17814 (17815 pp.). https://doi.org/10.1029/2008gl034210
Facchini, M. C., Rinaldi, M., Decesari, S., & Fuzzi, S. (2010). Marine organic aerosol and biological oceanic activity. *Chemical Engineering*, *22*.
Fairall, C. W., Banner, M. L., Peirson, W. L., Asher, W., & Morison, R. P. (2009). Investigation of the physical scaling of sea spray spume droplet production. *Journal of Geophysical Research-Oceans*, *114*, Article C10001. https://doi.org/10.1029/2008jc004918

Fan, J., Wang, Y., Rosenfeld, D., & Liu, X. (2016). Review of Aerosol–Cloud Interactions: Mechanisms, Significance, and Challenges. *Journal of the Atmospheric Sciences*. https://doi.org/10.1175/jas-d-16-0037.1

Feingold, G., Cotton, W. R., Kreidenweis, S. M., & Davis, J. T. (1999). The Impact of Giant Cloud Condensation Nuclei on Drizzle Formation in Stratocumulus: Implications for Cloud Radiative Properties. *Journal of the Atmospheric Sciences*, *56*(24), 4100-4117. https://doi.org/10.1175/1520-0469(1999)056<4100:TIOGCC>2.0.CO;2

Forestieri, S. D., & Moore, K. A. (2018). Temperature and Composition Dependence of Sea Spray Aerosol Production. *Geophysical Research Letters*. https://doi.org/10.1029/2018GL078193

Forestieri, S. D., Staudt, S. M., Kuborn, T. M., Faber, K., Ruehl, C. R., Bertram, T. H., & Cappa, C. D. (2018). Establishing the impact of model surfactants on cloud condensation nuclei activity of sea spray aerosol mimics. *Atmos. Chem. Phys.*, *18*(15), 10985-11005. https://doi.org/10.5194/acp-18-10985-2018

Frey, M. M., Norris, S. J., Brooks, I. M., Anderson, P. S., Nishimura, K., Yang, X., . . . Wolff, E. W. (2020). First direct observation of sea salt aerosol production from blowing snow above sea ice. *Atmospheric Chemistry and Physics*, *20*(4), 2549-2578. https://doi.org/10.5194/acp-20-2549-2020

Frossard, A. A., Russell, L. M., Burrows, S. M., Elliott, S. M., Bates, T. S., & Quinn, P. K. (2014). Sources and composition of submicron organic mass in marine aerosol particles. *Journal of Geophysical Research: Atmospheres*, *119*(22), 12,977-913,003. https://doi.org/10.1002/2014JD021913

Frossard, A. A., Russell, L. M., Massoli, P., Bates, T. S., & Quinn, P. K. (2014). Side-by-Side Comparison of Four Techniques Explains the Apparent Differences in the Organic Composition of Generated and Ambient Marine Aerosol Particles. *Aerosol Science and Technology*, *48*(3), V-X. https://doi.org/10.1080/02786826.2013.879979

Fu, P., Kawamura, K., Usukura, K., & Miura, K. (2013). Dicarboxylic acids, ketocarboxylic acids and glyoxal in the marine aerosols collected during a round-the-world cruise. *Marine Chemistry*, *148*, 22-32. https://doi.org/10.1016/j.marchem.2012.11.002

Fu, P. Q., Kawamura, K., Chen, J., Charriere, B., & Sempere, R. (2013). Organic molecular composition of marine aerosols over the Arctic Ocean in summer: contributions of primary emission and secondary aerosol formation. *Biogeosciences*, *10*(2), 653-667. https://doi.org/10.5194/bg-10-653-2013

Fu, P. Q., Kawamura, K., & Miura, K. (2011). Molecular characterization of marine organic aerosols collected during a round-the-world cruise. *Journal of Geophysical Research-Atmospheres*, *116*, Article D13302. https://doi.org/10.1029/2011jd015604

Fuentes, E., Coe, H., Green, D., de Leeuw, G., & McFiggans, G. (2010). On the impacts of phytoplankton-derived organic matter on the properties of the primary marine aerosol - Part 1: Source fluxes [Article]. *Atmospheric Chemistry and Physics*, *10*(19), 9295-9317. https://doi.org/10.5194/acp-10-9295-2010

Gagosian, R. B. (1983). REVIEW OF MARINE ORGANIC GEOCHEMISTRY. *Reviews of Geophysics*, *21*(5), 1245-1258. https://doi.org/10.1029/RG021i005p01245

Gali, M., Devred, E., Babin, M., & Levasseur, M. (2019). Decadal increase in Arctic dimethylsulfide emission. *Proceedings of the National Academy of Sciences of the United States of America*, *116*(39), 19311-19317. https://doi.org/10.1073/pnas.1904378116

Gali, M., Levasseur, M., Devred, E., Simo, R., & Babin, M. (2018). Sea-surface dimethylsulfide (DMS) concentration from satellite data at global and regional scales [Article]. *Biogeosciences*, *15*(11), 3497-3519. https://doi.org/10.5194/bg-15-3497-2018

Gantt, B., & Meskhidze, N. (2013). The physical and chemical characteristics of marine primary organic aerosol: a review. *Atmospheric Chemistry and Physics*, *13*(8), 3979-3996. https://doi.org/10.5194/acp-13-3979-2013
Gantt, B., Meskhidze, N., Facchini, M. C., Rinaldi, M., Ceburnis, D., & O'Dowd, C. D. (2011). Wind speed dependent size-resolved parameterization for the organic mass fraction of sea spray aerosol. *Atmospheric Chemistry and Physics*, *11*(16), 8777-8790. https://doi.org/10.5194/acp-11-8777-2011
Gantt, B., Meskhidze, N., & Kamykowski, D. (2009). A new physically-based quantification of marine isoprene and primary organic aerosol emissions. *Atmospheric Chemistry and Physics*, *9*(14), 4915-4927. https://doi.org/10.5194/acp-9-4915-2009
Gantt, B., Meskhidze, N., Zhang, Y., & Xu, J. (2010). The effect of marine isoprene emissions on secondary organic aerosol and ozone formation in the coastal United States. *Atmospheric Environment*, *44*(1), 115-121. https://doi.org/10.1016/j.atmosenv.2009.08.027
Gao, Q., Leck, C., Rauschenberg, C., & Matrai, P. A. (2012). On the chemical dynamics of extracellular polysaccharides in the high Arctic surface microlayer. *Ocean Science*, *8*(4), 401-418. https://doi.org/10.5194/os-8-401-2012
Garbe, C. S., Rutgersson, A., Boutin, J., de Leeuw, G., Delille, B., Fairall, C. W., . . . Zappa, C. J. (2014). Transfer Across the Air-Sea Interface. *Ocean-Atmosphere Interactions of Gases and Particles*, 55-112. https://doi.org/10.1007/978-3-642-25643-1_2
Gañán-Calvo, A. M. (2022). The complexity of aerosol production from bubble bursting. *Proceedings of the National Academy of Sciences*, *119*(34), e2208770119. https://doi.org/10.1073/pnas.2208770119
Geever, M., O'Dowd, C. D., van Ekeren, S., Flanagan, R., Nilsson, E. D., de Leeuw, G., & Rannik, U. (2005). Submicron sea spray fluxes. *Geophysical Research Letters*, *32*(15), Article L15810. https://doi.org/10.1029/2005gl023081
Gettelman, A., Lin, L., Medeiros, B., & Olson, J. (2016). Climate Feedback Variance and the Interaction of Aerosol Forcing and Feedbacks. *Journal of Climate*, *29*(18), 6659-6675. https://doi.org/10.1175/jcli-d-16-0151.1
Gettelman, A., & Sherwood, S. C. (2016). Processes Responsible for Cloud Feedback. *Current Climate Change Reports*, *2*(4), 179-189. https://doi.org/10.1007/s40641-016-0052-8
Gilardoni, S., Liu, S., Takahama, S., Russell, L. M., Allan, J. D., Steinbrecher, R., . . . Baumgardner, D. (2009). Characterization of organic ambient aerosol during MIRAGE 2006 on three platforms. *Atmospheric Chemistry and Physics*, *9*(15), 5417-5432.
Gilardoni, S., Massoli, P., Paglione, M., Giulianelli, L., Carbone, C., Rinaldi, M., . . . Facchini, M. C. (2016). Direct observation of aqueous secondary organic aerosol from biomass-burning emissions [Article]. *Proceedings of the National Academy of Sciences of the United States of America*, *113*(36), 10013-10018. https://doi.org/10.1073/pnas.1602212113
Gong, S. L. (2003). A parameterization of sea-salt aerosol source function for sub- and super-micron particles. *Global Biogeochemical Cycles*, *17*(4), Article 1097. https://doi.org/10.1029/2003gb002079
Grythe, H., Strom, J., Krejci, R., Quinn, P., & Stohl, A. (2014). A review of sea-spray aerosol source functions using a large global set of sea salt aerosol concentration measurements. In.
Hatton, A. D., & Wilson, S. T. (2007). Particulate dimethylsulphoxide and dimethylsulphoniopropionate in phytoplankton cultures and Scottish coastal waters. *Aquatic Sciences*, *69*(3), 330-340. https://doi.org/10.1007/s00027-007-0891-4
Hawkins, L. N., & Russell, L. M. (2010). Polysaccharides, Proteins, and Phytoplankton Fragments: Four Chemically Distinct Types of Marine Primary Organic Aerosol

Classified by Single Particle Spectromicroscopy. *Advances in Meteorology*, *2010*(Article ID 612132), 14. https://doi.org/10.1155/2010/612132
Hegg, D. A., Ferek, R. J., Hobbs, P. V., & Radke, L. F. (1991). DIMETHYL SULFIDE AND CLOUD CONDENSATION NUCLEUS CORRELATIONS IN THE NORTHEAST PACIFIC-OCEAN. *Journal of Geophysical Research-Atmospheres*, *96*(D7), 13189-13191. https://doi.org/10.1029/91jd01309
Hegg, D. A., Radke, L. F., & Hobbs, P. V. (1990). PARTICLE-PRODUCTION ASSOCIATED WITH MARINE CLOUDS. *Journal of Geophysical Research-Atmospheres*, *95*(D9), 13917-13926. https://doi.org/10.1029/JD095iD09p13917
Heslin-Rees, D., Burgos, M., Hansson, H. C., Krejci, R., Strom, J., Tunved, P., & Zieger, P. (2020). From a polar to a marine environment: has the changing Arctic led to a shift in aerosol light scattering properties? *Atmospheric Chemistry and Physics*, *20*(21), 13671-13686. https://doi.org/10.5194/acp-20-13671-2020
Holben, B. N., Tanre, D., Smirnov, A., Eck, T. F., Slutsker, I., Abuhassan, N., . . . Zibordi, G. (2001). An emerging ground-based aerosol climatology: Aerosol optical depth from AERONET. *Journal of Geophysical Research-Atmospheres*, *106*(D11), 12067-12097. https://doi.org/10.1029/2001jd900014
Holland, H. D. (1978). *The Chemistry of the Atmosphere and Oceans*. John Wiley.
Hoppel, W. A., Frick, G. M., & Fitzgerald, J. W. (2002). Surface source function for sea-salt aerosol and aerosol dry deposition to the ocean surface. *Journal of Geophysical Research-Atmospheres*, *107*(D19), Article 4382. https://doi.org/10.1029/2001jd002014
Ichoku, C., Kaufman, Y. J., Remer, L. A., & Levy, R. (2004). Global aerosol remote sensing from MODIS. *Trace Constituents in the Troposphere and Lower Stratosphere*, *34*(4), 820-827. https://doi.org/10.1016/j.asr.2003.07.071
Ickes, L., Porter, G. C. E., Wagner, R., Adams, M. P., Bierbauer, S., Bertram, A. K., . . . Salter, M. E. (2020). The ice-nucleating activity of Arctic sea surface microlayer samples and marine algal cultures. *Atmospheric Chemistry and Physics*, *20*(18), 11089-11117. https://doi.org/10.5194/acp-20-11089-2020
Irish, V. E., Elizondo, P., Chen, J., Chou, C., Charette, J., Lizotte, M., . . . Bertram, A. K. (2017). Ice-nucleating particles in Canadian Arctic sea-surface microlayer and bulk seawater. *Atmospheric Chemistry and Physics*, *17*(17), 10583-10595. https://doi.org/10.5194/acp-17-10583-2017
Irish, V. E., Hanna, S. J., Willis, M. D., China, S., Thomas, J. L., Wentzell, J. J. B., . . . Bertram, A. K. (2019). Ice nucleating particles in the marine boundary layer in the Canadian Arctic during summer 2014. *Atmospheric Chemistry and Physics*, *19*(2), 1027-1039. https://doi.org/10.5194/acp-19-1027-2019
Ito, A., & Kawamiya, M. (2010). Potential impact of ocean ecosystem changes due to global warming on marine organic carbon aerosols. *Global Biogeochemical Cycles*, *24*, Article Gb1012. https://doi.org/10.1029/2009gb003559
Jaegle, L., Quinn, P. K., Bates, T. S., Alexander, B., & Lin, J. T. (2011). Global distribution of sea salt aerosols: new constraints from in situ and remote sensing observations. *Atmospheric Chemistry and Physics*, *11*(7), 3137-3157. https://doi.org/10.5194/acp-11-3137-2011
Jensen, J. B., & Lee, S. H. (2008). Giant Sea-Salt Aerosols and Warm Rain Formation in Marine Stratocumulus. *Journal of the Atmospheric Sciences*, *65*(12), 3678-3694. https://doi.org/10.1175/2008jas2617.1
Jiang, X., Rotily, L., Villermaux, E., & Wang, X. (2022). Reply to Gañán-Calvo: Aerosol production from the bursting of submillimeter bubbles. *Proceedings of the National Academy of Sciences*, *119*(34), e2209370119. https://doi.org/10.1073/pnas.2209370119

Jiang, X. H., Rotily, L., Villermaux, E., & Wang, X. F. (2022). Submicron drops from flapping bursting bubbles. *Proceedings of the National Academy of Sciences of the United States of America*, *119*(1), Article e2112924119. https://doi.org/10.1073/pnas.2112924119
Jung, E., Albrecht, B. A., Jonsson, H. H., Chen, Y. C., Seinfeld, J. H., Sorooshian, A., . . . Russell, L. M. (2015). Precipitation effects of giant cloud condensation nuclei artificially introduced into stratocumulus clouds. *Atmospheric Chemistry and Physics*, *15*(10), 5645-5658. https://doi.org/10.5194/acp-15-5645-2015
Kasparian, J., Hassler, C., Ibelings, B., Berti, N., Bigorre, S., Djambazova, V., . . . Beniston, M. (2017). Assessing the Dynamics of Organic Aerosols over the North Atlantic Ocean. *Scientific Reports*, *7*, Article 45476. https://doi.org/10.1038/srep45476
Katoshevski, D., Nenes, A., & Seinfeld, J. H. (1999). A study of processes that govern the maintenance of aerosols in the marine boundary layer. *Journal of Aerosol Science*, *30*(4), 503-532. https://doi.org/10.1016/s0021-8502(98)00740-x
Kaufman, Y. J., Smirnov, A., Holben, B. N., & Dubovik, O. (2001). Baseline maritime aerosol: methodology to derive the optical thickness and scattering properties. *Geophysical Research Letters*, *28*(17), 3251-3254. https://doi.org/10.1029/2001gl013312
Kawamura, K., & Gagosian, R. B. (1987). Implications of omega-oxocarboxylic acids in the remote marine atmosphere for photooxidation of unsaturated fatty-acids. *Nature*, *325*(6102), 330-332. https://doi.org/10.1038/325330a0
Kazil, J., Lovejoy, E. R., Barth, M. C., & O'Brien, K. (2006). Aerosol nucleation over oceans and the role of galactic cosmic rays. *Atmospheric Chemistry and Physics*, *6*, 4905-4924. https://doi.org/10.5194/acp-6-4905-2006
Keene, W., Maring, H., Maben, J., Kieber, D., Pszenny, A., Dahl, E., . . . Sander, R. (2007). Chemical and physical characteristics of nascent aerosols produced by bursting bubbles at a model air-sea interface [Article]. *Journal of Geophysical Research-Atmospheres*, *112*(D21), Article ARTN D21202. https://doi.org/10.1029/2007JD008464
Keene, W. C., Long, M. S., Reid, J. S., Frossard, A. A., Kieber, D. J., Maben, J. R., . . . Bates, T. S. (2017). Factors That Modulate Properties of Primary Marine Aerosol Generated From Ambient Seawater on Ships at Sea. *Journal of Geophysical Research-Atmospheres*, *122*(21), 11961-11990. https://doi.org/10.1002/2017jd026872
Keene, W. C., Maring, H., Maben, J. R., Kieber, D. J., Pszenny, A. A. P., Dahl, E. E., . . . Sander, R. (2007). Chemical and physical characteristics of nascent aerosols produced by bursting bubbles at a model air-sea interface. *Journal of Geophysical Research-Atmospheres*, *112*(D21). https://doi.org/D21202 10.1029/2007jd008464
Kieber, D. J., Keene, W. C., Frossard, A. A., Long, M. S., Maben, J. R., Russell, L. M., . . . Bates, T. S. (2016). Coupled ocean-atmosphere loss of marine refractory dissolved organic carbon. *Geophysical Research Letters*, *43*(6), 2765-2772. https://doi.org/10.1002/2016gl068273
Kim, M. H., Omar, A. H., Tackett, J. L., Vaughan, M. A., Winker, D. M., Trepte, C. R., . . . Magill, B. E. (2018). The CALIPSO version 4 automated aerosol classification and lidar ratio selection algorithm. *Atmospheric Measurement Techniques*, *11*(11), 6107-6135. https://doi.org/10.5194/amt-11-6107-2018
Kleefeld, C., O'Dowd, C. D., O'Reilly, S., Jennings, S. G., Aalto, P., Becker, E., . . . de Leeuw, G. (2002). Relative contribution of submicron and supermicron particles to aerosol light scattering in the marine boundary layer. *Journal of Geophysical Research-Atmospheres*, *107*(D19), Article 8103. https://doi.org/10.1029/2000jd000262
Kleefeld, C., O'Reilly, S., Jennings, S. G., Kunz, G., de Leeuw, G., Aalto, P., . . . O'Dowd, C. (2000, Aug 06-11). Aerosol concentrations and scattering coefficient at Mace Head, Ireland.*Aip Conference Proceedings* [Nucleation and atmospheric aerosols 2000]. 15th International Conference on Nucleation and Atmospheric Aerosols (ICNAA), Univ Missouri Rolla, Rolla, Mo.

Kleidman, R. G., Smirnov, A., Levy, R. C., Mattoo, S., & Tanre, D. (2012). Evaluation and Wind Speed Dependence of MODIS Aerosol Retrievals Over Open Ocean. *Ieee Transactions on Geoscience and Remote Sensing*, *50*(2), 429-435. https://doi.org/10.1109/tgrs.2011.2162073

Knopf, D. A., Alpert, P. A., Wang, B., & Aller, J. Y. (2011). Stimulation of ice nucleation by marine diatoms. *Nature Geoscience*, *4*(2), 88-90. https://doi.org/10.1038/ngeo1037

Korhonen, H., Carslaw, K. S., Forster, P. M., Mikkonen, S., Gordon, N. D., & Kokkola, H. (2010). Aerosol climate feedback due to decadal increases in Southern Hemisphere wind speeds. *Geophysical Research Letters*, *37*, Article L02805. https://doi.org/10.1029/2009gl041320

Korhonen, H., Carslaw, K. S., Spracklen, D. V., Mann, G. W., & Woodhouse, M. T. (2008). Influence of oceanic dimethyl sulfide emissions on cloud condensation nuclei concentrations and seasonality over the remote Southern Hemisphere oceans: A global model study. *Journal of Geophysical Research-Atmospheres*, *113*(D15), Article D15204. https://doi.org/10.1029/2007jd009718

Kreidenweis, S. M., McInnes, L. M., & Brechtel, F. J. (1998). Observations of aerosol volatility and elemental composition at Macquarie Island during the First Aerosol Characterization Experiment (ACE 1). *Journal of Geophysical Research-Atmospheres*, *103*(D13), 16511-16524. https://doi.org/10.1029/98jd00800

Kuznetsova, M., Lee, C., & Aller, J. (2005). Characterization of the proteinaceous matter in marine aerosols. *Marine Chemistry*, *96*(3-4), 359-377. https://doi.org/10.1016/j.marchem.2005.03.007

Lana, A., Bell, T. G., Simo, R., Vallina, S. M., Ballabrera-Poy, J., Kettle, A. J., . . . Liss, P. S. (2011). An updated climatology of surface dimethlysulfide concentrations and emission fluxes in the global ocean. *Global Biogeochemical Cycles*, *25*, Article Gb1004. https://doi.org/10.1029/2010gb003850

Lawler, M. J., Lewis, S. L., Russell, L. M., Quinn, P. K., Bates, T. S., Coffman, D. J., . . . Saltzman, E. S. (2020). North Atlantic marine organic aerosol characterized by novel offline thermal desorption mass spectrometry: polysaccharides, recalcitrant material, and secondary organics. *Atmospheric Chemistry and Physics*, *20*(24), 16007-16022. https://doi.org/10.5194/acp-20-16007-2020

Leck, C., Gao, Q., Rad, F. M., & Nilsson, U. (2013). Size-resolved atmospheric particulate polysaccharides in the high summer Arctic. *Atmospheric Chemistry and Physics*, *13*(24), 12573-12588. https://doi.org/10.5194/acp-13-12573-2013

Lehahn, Y., Koren, I., Rudich, Y., Bidle, K. D., Trainic, M., Flores, J. M., . . . Vardi, A. (2014). Decoupling atmospheric and oceanic factors affecting aerosol loading over a cluster of mesoscale North Atlantic eddies. *Geophysical Research Letters*, *41*(11), 4075-4081. https://doi.org/10.1002/2014gl059738

Levasseur, M. (2013). Impact of Arctic meltdown on the microbial cycling of sulphur. *Nature Geoscience*, *6*(9), 691-700. https://doi.org/10.1038/ngeo1910

Levy, R. C., Mattoo, S., Munchak, L. A., Remer, L. A., Sayer, A. M., Patadia, F., & Hsu, N. C. (2013). The Collection 6 MODIS aerosol products over land and ocean. *Atmospheric Measurement Techniques*, *6*(11), 2989-3034. https://doi.org/10.5194/amt-6-2989-2013

Lewis, E. R., & Schwartz, S. E. (2004). Sea salt aerosol production: Mechanisms, methods, measurements and models—A critical review. https://doi.org/10.1029/152GM01

Lewis, S. L., Russell, L. M., Saliba, G., Quinn, P. K., Bates, T. S., Carlson, C. A., . . . Behrenfeld, M. J. (2022). Characterization of Sea Surface Microlayer and Marine Aerosol Organic Composition Using STXM-NEXAFS Microscopy and FTIR Spectroscopy. *ACS Earth and Space Chemistry*. https://doi.org/10.1021/acsearthspacechem.2c00119

Lewis, S. L., Saliba, G., Russell, L. M., Quinn, P. K., Bates, T. S., & Behrenfeld, M. J. (2021). Seasonal Differences in Submicron Marine Aerosol Particle Organic Composition in the North Atlantic. *Frontiers in Marine Science*, *8*, Article 720208. https://doi.org/10.3389/fmars.2021.720208

Lhuissier, H., & Villermaux, E. (2012). Bursting bubble aerosols. *Journal of Fluid Mechanics*, *696*, 5-44. https://doi.org/10.1017/jfm.2011.418

Liss, P. S., Malin, G., Turner, S. M., & Holligan, P. M. (1994). DIMETHYL SULFIDE AND PHAEOCYSTIS - A REVIEW. *Journal of Marine Systems*, *5*(1), 41-53. https://doi.org/10.1016/0924-7963(94)90015-9

Liss, P. S., & Slater, P. G. (1974). FLUX OF GASES ACROSS AIR-SEA INTERFACE. *Nature*, *247*(5438), 181-184. https://doi.org/10.1038/247181a0

Liss, P. S., Watson, A. J., Liddicoat, M. I., Malin, G., Nightingale, P. D., Turner, S. M., & Upstillgoddard, R. C. (1993). TRACE GASES AND AIR-SEA EXCHANGES. *Philosophical Transactions of the Royal Society of London Series a-Mathematical Physical and Engineering Sciences*, *343*(1669), 531-541. https://doi.org/10.1098/rsta.1993.0064

Liu, J., Dedrick, J., Russell, L. M., Senum, G. I., Uin, J., Kuang, C. G., . . . Lubin, D. (2018). High summertime aerosol organic functional group concentrations from marine and seabird sources at Ross Island, Antarctica, during AWARE. *Atmospheric Chemistry and Physics*, *18*(12), 8571-8587. https://doi.org/10.5194/acp-18-8571-2018

Liu, S., Liu, C. C., Froyd, K. D., Schill, G. P., Murphy, D. M., Bui, T. P., . . . Gao, R. S. (2021). Sea spray aerosol concentration modulated by sea surface temperature. *Proceedings of the National Academy of Sciences of the United States of America*, *118*(9), Article e2020583118. https://doi.org/10.1073/pnas.2020583118

Long, M. S., Keene, W. C., Kieber, D. J., Erickson, D. J., & Maring, H. (2011). A sea-state based source function for size- and composition-resolved marine aerosol production. *Atmospheric Chemistry and Physics*, *11*(3), 1203-1216. https://doi.org/10.5194/acp-11-1203-2011

Long, M. S., Keene, W. C., Kieber, D. J., Frossard, A. A., Russell, L. M., Maben, J. R., . . . Bates, T. S. (2014). Light-enhanced primary marine aerosol production from biologically productive seawater [Article]. *Geophysical Research Letters*, *41*(7), 2661-2670. https://doi.org/10.1002/2014gl059436

Longhurst, A. (1995). Seasonal cycles of pelagic production and consumption. *Progress in Oceanography*, *36*(2), 77-167. https://doi.org/10.1016/0079-6611(95)00015-1

Lubin, D., Zhang, D. M., Silber, I., Scott, R. C., Kalogeras, P., Battaglia, A., . . . Vogelmann, A. M. (2020). The Atmospheric Radiation Measurement (ARM) West Antarctic Radiation Experiment. *Bulletin of the American Meteorological Society*, *101*(7), E1069-E1091. https://doi.org/10.1175/bams-d-18-0278.1

Maria, S. F., Russell, L. M., Gilles, M. K., & Myneni, S. C. B. (2004). Organic aerosol growth mechanisms and their climate-forcing implications. *Science*, *306*(5703), 1921-1924. https://doi.org/10.1126/science.1103491

Markuszewski, P., Petelski, T., & Zielinski, T. (2018). MARINE AEROSOL FLUXES DETERMINED BY SIMULTANEOUS MEASUREMENTS OF EDDY COVARIANCE AND GRADIENT METHOD. *Environmental Engineering and Management Journal*, *17*(2), 261-265. https://doi.org/10.30638/eemj.2018.027

Martensson, E. M., Nilsson, E. D., de Leeuw, G., Cohen, L. H., & Hansson, H. C. (2003). Laboratory simulations and parameterization of the primary marine aerosol production. *Journal of Geophysical Research-Atmospheres*, *108*(D9), Article 4297. https://doi.org/10.1029/2002jd002263

Matsumoto, K., & Uematsu, M. (2005). Free amino acids in marine aerosols over the western North Pacific Ocean. *Atmospheric Environment*, *39*(11), 2163-2170. https://doi.org/10.1016/j.atmosenv.2004.12.022
McCluskey, C. S., Hill, T. C. J., Humphries, R. S., Rauker, A. M., Moreau, S., Strutton, P. G., . . . DeMott, P. J. (2018). Observations of Ice Nucleating Particles Over Southern Ocean Waters. *Geophysical Research Letters*, *45*(21), 11,989-911,997. https://doi.org/10.1029/2018GL079981
McCluskey, C. S., Ovadnevaite, J., Rinaldi, M., Atkinson, J., Belosi, F., Ceburnis, D., . . . DeMott, P. J. (2018). Marine and Terrestrial Organic Ice-Nucleating Particles in Pristine Marine to Continentally Influenced Northeast Atlantic Air Masses. *Journal of Geophysical Research-Atmospheres*, *123*(11), 6196-6212, Article D028033. https://doi.org/10.1029/2017jd028033
McCoy, D. T., Burrows, S. M., Wood, R., Grosvenor, D. P., Elliott, S. M., Ma, P. L., . . . Hartmann, D. L. (2015). Natural aerosols explain seasonal and spatial patterns of Southern Ocean cloud albedo. *Science Advances*, *1*(6), Article e1500157. https://doi.org/10.1126/sciadv.1500157
Medwin, H. (1977). INSITU ACOUSTIC MEASUREMENTS OF MICRO-BUBBLES AT SEA. *Journal of Geophysical Research-Oceans and Atmospheres*, *82*(6), 971-976. https://doi.org/10.1029/JC082i006p00971
Medwin, H., & Breitz, N. D. (1989). AMBIENT AND TRANSIENT BUBBLE SPECTRAL DENSITIES IN QUIESCENT SEAS AND UNDER SPILLING BREAKERS. *Journal of Geophysical Research-Oceans*, *94*(C9), 12751-12759. https://doi.org/10.1029/JC094iC09p12751
Merikanto, J., Spracklen, D. V., Mann, G. W., Pickering, S. J., & Carslaw, K. S. (2009). Impact of nucleation on global CCN. *Atmospheric Chemistry and Physics*, *9*(21), 8601-8616. https://doi.org/10.5194/acp-9-8601-2009
Merkulova, L., Freud, E., Martensson, E. M., Nilsson, E. D., & Glantz, P. (2018). Effect of Wind Speed on Moderate Resolution Imaging Spectroradiometer (MODIS) Aerosol Optical Depth over the North Pacific. *Atmosphere*, *9*(2), Article 60. https://doi.org/10.3390/atmos9020060
Meskhidze, N., & Nenes, A. (2006). Phytoplankton and cloudiness in the Southern Ocean. *Science*, *314*(5804), 1419-1423. https://doi.org/10.1126/science.1131779
Meskhidze, N., Petters, M. D., Tsigaridis, K., Bates, T., O'Dowd, C., Reid, J., . . . Zorn, S. R. (2013). Production mechanisms, number concentration, size distribution, chemical composition, and optical properties of sea spray aerosols. *Atmos. Sci. Lett.*, *14*, 207-213. https://doi.org/10.1002/asl2.441
Meskhidze, N., Xu, J., & Gantt, B. (2010). The impact of marine organic emissions on global climate. *Geochimica Et Cosmochimica Acta*, *74*(12), A702-A702.
Middlebrook, A. M., Murphy, D. M., & Thomson, D. S. (1998). Observations of organic material in individual marine particles at Cape Grim during the First Aerosol Characterization Experiment (ACE 1). *Journal of Geophysical Research-Atmospheres*, *103*(D13), 16475-16483. https://doi.org/10.1029/97jd03719
Miller, L. A., Fripiat, F., Else, B. G. T., Bowman, J. S., Brown, K. A., Collins, R. E., . . . Zhou, J. (2015). Methods for biogeochemical studies of sea ice: The state of the art, caveats, and recommendations. *Elementa-Science of the Anthropocene*, *3*, 000038-Article No.: 000038. https://doi.org/10.12952/journal.elementa.000038
Ming, Y., & Russell, L. M. (2001). Predicted hygroscopic growth of sea salt aerosol. *Journal of Geophysical Research-Atmospheres*, *106*(D22), 28259-28274. https://doi.org/10.1029/2001jd000454
Mitts, B. A., Wang, X. F., Lucero, D. D., Beall, C. M., Deane, G. B., DeMott, P. J., & Prather, K. A. (2021). Importance of Supermicron Ice Nucleating Particles in Nascent Sea Spray.

Geophysical Research Letters, *48*(3), Article e2020GL089633. https://doi.org/10.1029/2020gl089633
Mochida, M., Kitamori, Y., Kawamura, K., Nojiri, Y., & Suzuki, K. (2002). Fatty acids in the marine atmosphere: Factors governing their concentrations and evaluation of organic films on sea-salt particles [4325 10.1029/2001jd001278]. *Journal of Geophysical Research-Atmospheres*, *107*(D17).
Modini, R., Harris, B., & Ristovski, Z. (2010). The organic fraction of bubble-generated, accumulation mode Sea Spray Aerosol (SSA) [Article]. *Atmospheric Chemistry and Physics*, *10*(6), 2867-2877. https://doi.org/10.5194/acp-10-2867-2010
Modini, R. L., Frossard, A. A., Ahlm, L., Russell, L. M., Corrigan, C. E., Roberts, G. C., . . . Leaitch, W. R. (2015). Primary marine aerosol-cloud interactions off the coast of California. *Journal of Geophysical Research: Atmospheres*, *120*(9), 4282-4303. https://doi.org/doi:10.1002/2014JD022963
Modini, R. L., Russell, L. M., Deane, G. B., & Stokes, M. D. (2013). Effect of soluble surfactant on bubble persistence and bubble-produced aerosol particles. *Journal of Geophysical Research-Atmospheres*, *118*(3), 1388-1400. https://doi.org/10.1002/jgrd.50186
Monahan, E. C. (1968). SEA SPRAY AS A FUNCTION OF LOW ELEVATION WIND SPEED. *Journal of Geophysical Research*, *73*(4), 1127-+. https://doi.org/10.1029/JB073i004p01127
Monahan, E. C., Fairall, C. W., Davidson, K. L., & Boyle, P. J. (1983). OBSERVED INTERRELATIONS BETWEEN 10M WINDS, OCEAN WHITECAPS AND MARINE AEROSOLS. *Quarterly Journal of the Royal Meteorological Society*, *109*(460), 379-392. https://doi.org/10.1002/qj.49710946010
Monahan, E. C., Staniec, A., & Vlahos, P. (2017). Spume Drops: Their Potential Role in Air-Sea Gas Exchange. *Journal of Geophysical Research-Oceans*, *122*(12), 9500-9517. https://doi.org/10.1002/2017jc013293
Mulcahy, J. P., O'Dowd, C. D., Jennings, S. G., & Ceburnis, D. (2008). Significant enhancement of aerosol optical depth in marine air under high wind conditions. *Geophysical Research Letters*, *35*(16), Article L16810. https://doi.org/10.1029/2008gl034303
Mungall, E. L., Abbatt, J. P. D., Wentzell, J. J. B., Lee, A. K. Y., Thomas, J. L., Blais, M., . . . Liggio, J. (2017). Microlayer source of oxygenated volatile organic compounds in the summertime marine Arctic boundary layer. *Proceedings of the National Academy of Sciences of the United States of America*, *114*(24), 6203-6208. https://doi.org/10.1073/pnas.1620571114
Murphy, D. M., Anderson, J. R., Qulnn, P. K., Mclnnes, L. M., Brechtel, F. J., Kreidenwels, S. M., . . . Buseck, P. R. (1998). Influence of sea-salt on aerosol radiative properties in the Southern Ocean marine boundary layer. *Nature*. https://doi.org/10.1038/32138
Myriokefalitakis, S., Vignati, E., Tsigaridis, K., Papadimas, C., Sciare, J., Mihalopoulos, N., . . . Kanakidou, M. (2010). Global Modeling of the Oceanic Source of Organic Aerosols. *Advances in Meteorology*, *2010*, Article 939171. https://doi.org/10.1155/2010/939171
Neel, B., Erinin, M. A., & Deike, L. (2022). Role of Contamination in Optimal Droplet Production by Collective Bubble Bursting. *Geophysical Research Letters*, *49*(1), Article e2021GL096740. https://doi.org/10.1029/2021gl096740
Nilsson, E. D., Rannik, Ü., Kumala, M., Buzorius, G., & O'dowd, C. D. (2001). Effects of continental boundary layer evolution, convection, turbulence and entrainment, on aerosol formation. *Tellus B: Chemical and Physical Meteorology*, *53*(4), 441-461. https://doi.org/10.3402/tellusb.v53i4.16617
Norris, S. J., Brooks, I. M., de Leeuw, G., Smith, M. H., Moerman, M., & Lingard, J. J. N. (2008). Eddy covariance measurements of sea spray particles over the Atlantic Ocean. *Atmospheric Chemistry and Physics*, *8*(3), 555-563. https://doi.org/10.5194/acp-8-555-2008

Novak, G. A., & Bertram, T. H. (2020). Reactive VOC Production from Photochemical and Heterogeneous Reactions Occurring at the Air-Ocean Interface. *Accounts of Chemical Research*, *53*(5), 1014-1023. https://doi.org/10.1021/acs.accounts.0c00095

O'Dowd, C., Scannell, C., Mulcahy, J., & Jennings, S. (2010). Wind Speed Influences on Marine Aerosol Optical Depth [Article]. *Advances in Meteorology*, *2010*, Article ARTN 830846. https://doi.org/10.1155/2010/830846

O'Dowd, C. D., & De Leeuw, G. (2007). Marine aerosol production: A review of the current knowledge. https://doi.org/10.1098/rsta.2007.2043

O'Dowd, C. D., Facchini, M. C., Cavalli, F., Ceburnis, D., Mircea, M., Decesari, S., . . . Putaud, J.-P. (2004). Biogenically driven organic contribution to marine aerosol. *Nature*, *431*(7009), 676--680. https://doi.org/10.1038/nature02959

O'Dowd, C. D., Facchini, M. C., Cavalli, F., Ceburnis, D., Mircea, M., Decesari, S., . . . Putaud, J. P. (2004). Biogenically driven organic contribution to marine aerosol. *Nature*, *431*(7009), 676-680. https://doi.org/10.1038/nature02959

O'Dowd, C. D., Jimenez, J. L., Bahreini, R., Flagan, R. C., Seinfeld, J. H., Hameri, K., . . . Hoffmann, T. (2002). Marine aerosol formation from biogenic iodine emissions. *Nature*, *417*(6889), 632-636. https://doi.org/10.1038/nature00775

O'Dowd, C. D., Lowe, J. A., & Smith, M. H. (1999). Coupling sea-salt and sulphate interactions and its impact on cloud droplet concentration predictions. *Geophysical Research Letters*, *26*(9), 1311-1314.

O'Dowd, C. D., Lowe, J. A., Smith, M. H., & Kaye, A. D. (1999). The relative importance of non-sea-salt sulphate and sea-salt aerosol to the marine cloud condensation nuclei population: An improved multi-component aerosol-cloud droplet parametrization. *Quarterly Journal of the Royal Meteorological Society*, *125*(556), 1295-1313.

Odowd, C. D., & Smith, M. H. (1993). PHYSICOCHEMICAL PROPERTIES OF AEROSOLS OVER THE NORTHEAST ATLANTIC - EVIDENCE FOR WIND-SPEED-RELATED SUBMICRON SEA-SALT AEROSOL PRODUCTION. *Journal of Geophysical Research-Atmospheres*, *98*(D1), 1137-1149. https://doi.org/10.1029/92jd02302

Odowd, C. D., Smith, M. H., Consterdine, I. E., & Lowe, J. A. (1997). Marine aerosol, sea-salt, and the marine sulphur cycle: A short review. *Atmospheric Environment*, *31*(1), 73-80. https://doi.org/10.1016/s1352-2310(96)00106-9

Ovadnevaite, J., Ceburnis, D., Canagaratna, M., Berresheim, H., Bialek, J., Martucci, G., . . . O'Dowd, C. (2012). On the effect of wind speed on submicron sea salt mass concentrations and source fluxes. *Journal of Geophysical Research-Atmospheres*, *117*, Article D16201. https://doi.org/10.1029/2011jd017379

Ovadnevaite, J., O'Dowd, C., Dall'Osto, M., Ceburnis, D., Worsnop, D. R., & Berresheim, H. (2011). Detecting high contributions of primary organic matter to marine aerosol: A case study. *Geophysical Research Letters*, *38*, Article L02807. https://doi.org/10.1029/2010gl046083

Painemal, D., Chang, F. L., Ferrare, R., Burton, S., Li, Z. J., Smith, W. L., . . . Clayton, M. (2020). Reducing uncertainties in satellite estimates of aerosol-cloud interactions over the subtropical ocean by integrating vertically resolved aerosol observations. *Atmospheric Chemistry and Physics*, *20*(12), 7167-7177. https://doi.org/10.5194/acp-20-7167-2020

Painemal, D., Spangenberg, D., Smith, W. L., Minnis, P., Cairns, B., Moore, R. H., . . . Ziemba, L. (2021). Evaluation of satellite retrievals of liquid clouds from the GOES-13 imager and MODIS over the midlatitude North Atlantic during the NAAMES campaign. *Atmospheric Measurement Techniques*, *14*(10), 6633-6646. https://doi.org/10.5194/amt-14-6633-2021

Patnaude, R. J., Perkins, R. J., Kreidenweis, S. M., & DeMott, P. J. (2021). Is Ice Formation by Sea Spray Particles at Cirrus Temperatures Controlled by Crystalline Salts? *Acs Earth*

and Space Chemistry, *5*(9), 2196-2211. https://doi.org/10.1021/acsearthspacechem.1c00228
Perry, K. D., & Hobbs, P. V. (1994). FURTHER EVIDENCE FOR PARTICLE NUCLEATION IN CLEAR-AIR ADJACENT TO MARINE CUMULUS CLOUDS. *Journal of Geophysical Research-Atmospheres*, *99*(D11), 22803-22818. https://doi.org/10.1029/94jd01926
Petelski, T., & Piskozub, J. (2006). Vertical coarse aerosol fluxes in the atmospheric surface layer over the North Polar Waters of the Atlantic. *Journal of Geophysical Research-Oceans*, *111*(C6), Article C06039. https://doi.org/10.1029/2005jc003295
Pilinis, C., & Seinfeld, J. H. (1987). CONTINUED DEVELOPMENT OF A GENERAL EQUILIBRIUM-MODEL FOR INORGANIC MULTICOMPONENT ATMOSPHERIC AEROSOLS. *Atmospheric Environment*, *21*(11), 2453-2466. https://doi.org/10.1016/0004-6981(87)90380-5
Pirjola, L., O'Dowd, C. D., Brooks, I. M., & Kulmala, M. (2000). Can new particle formation occur in the clean marine boundary layer? *Journal of Geophysical Research-Atmospheres*, *105*(D21), 26531-26546. https://doi.org/10.1029/2000jd900310
Pitzer, K. S., & Mayorga, G. (1973). THERMODYNAMICS OF ELECTROLYTES .2. ACTIVITY AND OSMOTIC COEFFICIENTS FOR STRONG ELECTROLYTES WITH ONE OR BOTH IONS UNIVALENT. *Journal of Physical Chemistry*, *77*(19), 2300-2308. https://doi.org/10.1021/j100638a009
Porter, J. N., Lienert, B. R., Sharma, S. K., Lau, E., & Horton, K. (2003). Vertical and horizontal aerosol scattering fields over Bellows Beach, Oahu, during the SEAS experiment. *Journal of Atmospheric and Oceanic Technology*, *20*(10), 1375-1387. https://doi.org/10.1175/1520-0426(2003)020<1375:vahasf>2.0.co;2
Poulain, S., Villermaux, E., & Bourouiba, L. (2018). Ageing and burst of surface bubbles. *Journal of Fluid Mechanics*, *851*, 636-671. https://doi.org/10.1017/jfm.2018.471
Prather, K., Bertram, T., Grassian, V., Deane, G., Stokes, M., DeMott, P., . . . Zhao, D. (2013). Bringing the ocean into the laboratory to probe the chemical complexity of sea spray aerosol [Article]. *Proceedings of the National Academy of Sciences of the United States of America*, *110*(19), 7550-7555. https://doi.org/10.1073/pnas.1300262110
Prather, K. A., Bertram, T. H., Grassian, V. H., Deane, G. B., Stokes, M. D., DeMott, P. J., . . . Zhao, D. (2013). Bringing the ocean into the laboratory to probe the chemical complexity of sea spray aerosol. *Proceedings of the National Academy of Sciences of the United States of America*, *110*(19), 7550-7555. https://doi.org/10.1073/pnas.1300262110
Quinn, P., Coffman, D., Johnson, J., Upchurch, L., & Bates, T. (2017). Small fraction of marine cloud condensation nuclei made up of sea spray aerosol [Article]. *Nature Geoscience*, *10*(9), 674-+. https://doi.org/10.1038/NGEO3003
Quinn, P., Coffman, D., Kapustin, V., Bates, T., & Covert, D. (1998). Aerosol optical properties in the marine boundary layer during the First Aerosol Characterization Experiment (ACE 1) and the underlying chemical and physical aerosol properties [Article]. *Journal of Geophysical Research-Atmospheres*, *103*(D13), 16547-16563. https://doi.org/10.1029/97JD02345
Quinn, P. K., & Bates, T. S. (2011). The case against climate regulation via oceanic phytoplankton sulphur emissions. *Nature*, *480*(7375), 51-56. https://doi.org/10.1038/nature10580
Quinn, P. K., Bates, T. S., Coffman, D. J., Upchurch, L., Johnson, J. E., Moore, R., . . . Behrenfeld, M. J. (2019). Seasonal Variations in Western North Atlantic Remote Marine Aerosol Properties. *Journal of Geophysical Research-Atmospheres*, *124*(24), 14240-14261. https://doi.org/10.1029/2019jd031740
Quinn, P. K., Bates, T. S., Miller, T. L., Coffman, D. J., Johnson, J. E., Harris, J. M., . . . Rood, M. J. (2000). Surface submicron aerosol chemical composition: What fraction is not

sulfate? *Journal of Geophysical Research-Atmospheres*, *105*(D5), 6785-6805. https://doi.org/10.1029/1999jd901034
Quinn, P. K., Bates, T. S., Schulz, K. S., Coffman, D. J., Frossard, A. A., Russell, L. M., . . . Kieber, D. J. (2014). Contribution of sea surface carbon pool to organic matter enrichment in sea spray aerosol. *Nature Geoscience*, *7*, 228. https://doi.org/10.1038/ngeo2092 https://www.nature.com/articles/ngeo2092#supplementary-information
Quinn, P. K., Coffman, D. J., Bates, T. S., Welton, E. J., Covert, D. S., Miller, T. L., . . . Anderson, J. (2004). Aerosol optical properties measured on board the Ronald H. Brown during ACE-Asia as a function of aerosol chemical composition and source region. *Journal of Geophysical Research-Atmospheres*, *109*(D19), -. https://doi.org/10.1029/2003jd004010
Quinn, P. K., Coffman, D. J., Johnson, J. E., Upchurch, L. M., & Bates, T. S. (2017). Small fraction of marine cloud condensation nuclei made up of sea spray aerosol. *Nature Geoscience*, *10*(9), 674-+. https://doi.org/10.1038/ngeo3003
Quinn, P. K., Collins, D. B., Grassian, V. H., Prather, K. A., & Bates, T. S. (2015). Chemistry and Related Properties of Freshly Emitted Sea Spray Aerosol. *Chemical Reviews*, *115*(10), 4383-4399. https://doi.org/10.1021/cr500713g
Raes, F. (1995). ENTRAINMENT OF FREE TROPOSPHERIC AEROSOLS AS A REGULATING MECHANISM FOR CLOUD CONDENSATION NUCLEI IN THE REMOTE MARINE BOUNDARY-LAYER. *Journal of Geophysical Research-Atmospheres*, *100*(D2), 2893-2903. https://doi.org/10.1029/94jd02832
Raes, F., VanDingenen, R., Cuevas, E., VanVelthoven, P. F. J., & Prospero, J. M. (1997). Observations of aerosols in the free troposphere and marine boundary layer of the subtropical Northeast Atlantic: Discussion of processes determining their size distribution. *Journal of Geophysical Research-Atmospheres*, *102*(D17), 21315-21328. https://doi.org/10.1029/97jd01122
Reiche, C. H., & Lasher-Trapp, S. (2010). The minor importance of giant aerosol to precipitation development within small trade wind cumuli observed during RICO. *Atmospheric Research*, *95*(4), 386-399. https://doi.org/10.1016/j.atmosres.2009.11.002
Repeta, D. J., Quan, T. M., Aluwihare, L. I., & Accardi, A. M. (2002). Chemical characterization of high molecular weight dissolved organic matter in fresh and marine waters. *Geochimica Et Cosmochimica Acta*, *66*(6), 955-962, Article Pii s0016-7037(01)00830-4. https://doi.org/10.1016/s0016-7037(01)00830-4
Reus, M., Strom, J., Curtius, J., Pirjola, L., Vignati, E., Arnold, F., . . . Raes, F. (2000). Aerosol production and growth in the upper free troposphere. *Journal of Geophysical Research-Atmospheres*, *105*(D20), 24751-24762. https://doi.org/10.1029/2000jd900382
Rinaldi, M., Decesari, S., Finessi, E., Giulianelli, L., Carbone, C., Fuzzi, S., . . . Facchini, M. C. (2010). Primary and secondary organic marine aerosol and oceanic biological activity: recent results and new perspectives for future studies. *Advances in Meteorology*, *2010*(Arctic ID 310682), 10.
Rinaldi, M., Decesari, S., Finessi, E., Giulianelli, L., Carbone, C., Fuzzi, S., . . . Facchini, M. C. (2010). Primary and Secondary Organic Marine Aerosol and Oceanic Biological Activity: Recent Results and New Perspectives for Future Studies. *Advances in Meteorology*, *2010*, Article 310682. https://doi.org/10.1155/2010/310682
Rinaldi, M., Fuzzi, S., Decesari, S., Marullo, S., Santoleri, R., Provenzale, A., . . . Facchini, M. C. (2013). Is chlorophyll-a the best surrogate for organic matter enrichment in submicron primary marine aerosol? *Journal of Geophysical Research-Atmospheres*, *118*(10), 4964-4973. https://doi.org/10.1002/jgrd.50417
Russell, L. M., Hawkins, L. N., Frossard, A. A., Quinn, P. K., & Bates, T. S. (2010). Carbohydrate-like composition of submicron atmospheric particles and their production

from ocean bubble bursting. *Proceedings of the National Academy of Sciences of the United States of America*, *107*(15), 6652-6657. https://doi.org/10.1073/pnas.0908905107
Russell, L. M., Pandis, S. N., & Seinfeld, J. H. (1994). AEROSOL PRODUCTION AND GROWTH IN THE MARINE BOUNDARY-LAYER. *Journal of Geophysical Research-Atmospheres*, *99*(D10), 20989-21003. https://doi.org/10.1029/94jd01932
Russell, L. M., & Singh, E. G. (2006). Submicron salt particle production in bubble bursting. *Aerosol Science and Technology*, *40*(9), 664-671. https://doi.org/10.1080/02786820600793951
Saliba, G., Chen, C., Lewis, S., Russell, L., Rivellini, L., Lee, A., . . . Behrenfeld, M. (2019). Factors driving the seasonal and hourly variability of sea-spray aerosol number in the North Atlantic [Article]. *Proceedings of the National Academy of Sciences of the United States of America*, *116*(41), 20309-20314. https://doi.org/10.1073/pnas.1907574116
Saliba, G., Chen, C.-L., Lewis, S., Russell, L. M., Quinn, P. K., Bates, T. S., . . . Behrenfeld, M. J. (2020). Seasonal Differences and Variability of Concentrations, Chemical Composition, and Cloud Condensation Nuclei of Marine Aerosol Over the North Atlantic [https://doi.org/10.1029/2020JD033145]. *Journal of Geophysical Research: Atmospheres*, *125*(19), e2020JD033145. https://doi.org/https://doi.org/10.1029/2020JD033145
Salisbury, D. J., Anguelova, M. D., & Brooks, I. M. (2013). On the variability of whitecap fraction using satellite-based observations. *Journal of Geophysical Research-Oceans*, *118*(11), 6201-6222. https://doi.org/10.1002/2013jc008797
Salter, M. E., Zieger, P., Navarro, J. C. A., Grythe, H., Kirkevag, A., Rosati, B., . . . Nilsson, E. D. (2015). An empirically derived inorganic sea spray source function incorporating sea surface temperature. *Atmospheric Chemistry and Physics*, *15*(19), 11047-11066. https://doi.org/10.5194/acp-15-11047-2015
Sanchez, K., Roberts, G., Saliba, G., Russell, L., Twohy, C., Reeves, M., . . . McRobert, I. (2021). Measurement report: Cloud processes and the transport of biological emissions affect southern ocean particle and cloud condensation nuclei concentrations [Article]. *Atmospheric Chemistry and Physics*, *21*(5), 3427-3446. https://doi.org/10.5194/acp-21-3427-2021
Sanchez, K. J., Chen, C.-L., Russell, L. M., Betha, R., Liu, J., Price, D. J., . . . Behrenfeld, M. J. (2018). Substantial Seasonal Contribution of Observed Biogenic Sulfate Particles to Cloud Condensation Nuclei. *Scientific Reports*, *8*(1), 3235. https://doi.org/10.1038/s41598-018-21590-9
Sanchez, K. J., Roberts, G. C., Saliba, G., Russell, L. M., Twohy, C., Reeves, M. J., . . . McRobert, I. M. (2020). Measurement report: Cloud Processes and the Transport of Biological Emissions Regulate Southern Ocean Particle and Cloud Condensation Nuclei Concentrations. *Atmos. Chem. Phys. Discuss.*, *2020*, 1-36. https://doi.org/10.5194/acp-2020-731
Sanchez, K. J., Russell, L. M., Modini, R. L., Frossard, A. A., Ahlm, L., Corrigan, C. E., . . . Seinfeld, J. H. (2016). Meteorological and aerosol effects on marine cloud microphysical properties. *Journal of Geophysical Research-Atmospheres*, *121*(8), 4142-4161. https://doi.org/10.1002/2015jd024595
Sanchez, K. J., Zhang, B., Liu, H. Y., Saliba, G., Chen, C. L., Lewis, S. L., . . . Moore, R. H. (2021). Linking marine phytoplankton emissions, meteorological processes, and downwind particle properties with FLEXPART. *Atmospheric Chemistry and Physics*, *21*(2), 831-851. https://doi.org/10.5194/acp-21-831-2021
Sawamura, P., Moore, R. H., Burton, S. P., Chemyakin, E., Muller, D., Kolgotin, A., . . . Anderson, B. E. (2017). HSRL-2 aerosol optical measurements and microphysical retrievals vs. airborne in situ measurements during DISCOVER-AQ 2013: an

intercomparison study. *Atmospheric Chemistry and Physics*, *17*(11), 7229-7243. https://doi.org/10.5194/acp-17-7229-2017
Schmitt-Kopplin, P., Liger-Belair, G., Koch, B. P., Flerus, R., Kattner, G., Harir, M., . . . Gebefuegi, I. (2012). Dissolved organic matter in sea spray: a transfer study from marine surface water to aerosols. *Biogeosciences*, *9*(4). https://doi.org/10.5194/bg-9-1571-2012
Schmitt-Kopplin, P., Liger-Belair, G., Koch, B. P., Flerus, R., Kattner, G., Harir, M., . . . Gebefugi, I. (2012). Dissolved organic matter in sea spray: a transfer study from marine surface water to aerosols. *Biogeosciences*, *9*(4), 1571-1582. https://doi.org/10.5194/bg-9-1571-2012
Schutgens, N., Dubovik, O., Hasekamp, O., Torres, O., Jethva, H., Leonard, P. J. T., . . . Stier, P. (2021). AEROCOM and AEROSAT AAOD and SSA study - Part 1: Evaluation and intercomparison of satellite measurements. *Atmospheric Chemistry and Physics*, *21*(9), 6895-6917. https://doi.org/10.5194/acp-21-6895-2021
Sciare, J., Favez, O., Sarda-Esteve, R., Oikonomou, K., Cachier, H., & Kazan, V. (2009). Long-term observations of carbonaceous aerosols in the Austral Ocean atmosphere: Evidence of a biogenic marine organic source. *Journal of Geophysical Research-Atmospheres*, *114*, Article D15302. https://doi.org/10.1029/2009jd011998
Seinfeld, J. H., & Pandis, S. N. (2016). *Atmospheric chemistry and physics: from air pollution to climate change*. John Wiley & Sons.
Sellegri, K., O'Dowd, C. D., Yoon, Y. J., Jennings, S. G., & de Leeuw, G. (2006). Surfactants and submicron sea spray generation. *Journal of Geophysical Research-Atmospheres*, *111*(D22), Article D22215. https://doi.org/10.1029/2005jd006658
Sellegri, K., O'Dowd, C. D., Yoon, Y. J., Jennings, S. G., & DeLeeuw, G. (2006). Surfactants and submicron sea spray generation. *Journal of Geophysical Research Atmospheres*. https://doi.org/10.1029/2005JD006658
Shank, L. M., Howell, S., Clarke, A. D., Freitag, S., Brekhovskikh, V., Kapustin, V., . . . Wood, R. (2012). Organic matter and non-refractory aerosol over the remote Southeast Pacific: oceanic and combustion sources. *Atmospheric Chemistry and Physics*, *12*(1). https://doi.org/10.5194/acp-12-557-2012
Shaw, G. E. (1987). AEROSOLS AS CLIMATE REGULATORS - A CLIMATE BIOSPHERE LINKAGE. *Atmospheric Environment*, *21*(4), 985-986. https://doi.org/10.1016/0004-6981(87)90094-1
Shaw, P. M., Russell, L. M., Jefferson, A., & Quinn, P. K. (2010). Arctic organic aerosol measurements show particles from mixed combustion in spring haze and from frost flowers in winter. *Geophysical Research Letters*, *37*. https://doi.org/10.1029/2010gl042831
Shaw, S. L., Gantt, B., & Meskhidze, N. (2010). Production and Emissions of Marine Isoprene and Monoterpenes: A Review. *Advances in Meteorology*, *2010*, Article 408696. https://doi.org/10.1155/2010/408696
Sherwood, S. C., Bony, S., Boucher, O., Bretherton, C., Forster, P. M., Gregory, J. M., & Stevens, B. (2015). ADJUSTMENTS IN THE FORCING-FEEDBACK FRAMEWORK FOR UNDERSTANDING CLIMATE CHANGE. *Bulletin of the American Meteorological Society*, *96*(2), 217-228. https://doi.org/10.1175/bams-d-13-00167.1
Smirnov, A., Holben, B. N., Giles, D. M., Slutsker, I., O'Neill, N. T., Eck, T. F., . . . Diehl, T. L. (2011). Maritime aerosol network as a component of AERONET - first results and comparison with global aerosol models and satellite retrievals. *Atmospheric Measurement Techniques*, *4*(3), 583-597. https://doi.org/10.5194/amt-4-583-2011
Smirnov, A., Sayer, A. M., Holben, B. N., Hsu, N. C., Sakerin, S. M., Macke, A., . . . Radionov, V. F. (2012). Effect of wind speed on aerosol optical depth over remote oceans, based on data from the Maritime Aerosol Network. *Atmospheric Measurement Techniques*, *5*(2), 377-388. https://doi.org/10.5194/amt-5-377-2012

Song, C. B., Dall'Osto, M., Lupi, A., Mazzola, M., Traversi, R., Becagli, S., . . . Shi, Z. B. (2021). Differentiation of coarse-mode anthropogenic, marine and dust particles in the High Arctic islands of Svalbard. *Atmospheric Chemistry and Physics*, *21*(14), 11317-11335. https://doi.org/10.5194/acp-21-11317-2021

Spiel, D. E. (1998). On the births of film drops from bubbles bursting on seawater surfaces. *Journal of Geophysical Research-Oceans*, *103*(C11), 24907-24918. https://doi.org/10.1029/98jc02233

Spracklen, D. V., Arnold, S. R., Sciare, J., Carslaw, K. S., & Pio, C. (2008). Globally significant oceanic source of organic carbon aerosol. *Geophysical Research Letters*, *35*(12), Article L12811. https://doi.org/10.1029/2008gl033359

Stefels, J., Steinke, M., Turner, S., Malin, G., & Belviso, S. (2007). Environmental constraints on the production and removal of the climatically active gas dimethylsulphide (DMS) and implications for ecosystem modelling. *Biogeochemistry*, *83*(1-3), 245-275. https://doi.org/10.1007/s10533-007-9091-5

Steinke, I., DeMott, P. J., Deane, G. B., Hill, T. C. J., Maltrud, M., Raman, A., & Burrows, S. M. (2022). A numerical framework for simulating the atmospheric variability of supermicron marine biogenic ice nucleating particles. *Atmospheric Chemistry and Physics*, *22*(2), 847-859. https://doi.org/10.5194/acp-22-847-2022

Stokes, M. D., Deane, G., Collins, D. B., Cappa, C., Bertram, T., Dommer, A., . . . Survilo, M. (2016). A miniature Marine Aerosol Reference Tank (miniMART) as a compact breaking wave analogue. *Atmospheric Measurement Techniques*, *9*(9), 4257-4267. https://doi.org/10.5194/amt-9-4257-2016

Stokes, M. D., Deane, G. B., Prather, K., Bertram, T. H., Ruppel, M. J., Ryder, O. S., . . . Zhao, D. (2013). A Marine Aerosol Reference Tank system as a breaking wave analogue for the production of foam and sea-spray aerosols. *Atmospheric Measurement Techniques*, *6*(4), 1085-1094. https://doi.org/10.5194/amt-6-1085-2013

Struthers, H., Ekman, A. M. L., Glantz, P., Iversen, T., Kirkevg, A., Martensson, E. M., . . . Nilsson, E. D. (2011). The effect of sea ice loss on sea salt aerosol concentrations and the radiative balance in the Arctic. *Atmospheric Chemistry and Physics*. https://doi.org/10.5194/acp-11-3459-2011

Tan, I., Barahona, D., & Coopman, Q. (2022). Potential Link Between Ice Nucleation and Climate Model Spread in Arctic Amplification. *Geophysical Research Letters*, *49*(4), Article e2021GL097373. https://doi.org/10.1029/2021gl097373

Tan, I., & Storelvmo, T. (2016). Sensitivity Study on the Influence of Cloud Microphysical Parameters on Mixed-Phase Cloud Thermodynamic Phase Partitioning in CAM5. *Journal of the Atmospheric Sciences*, *73*(2), 709-728. https://doi.org/10.1175/jas-d-15-0152.1

Tan, I., Storelvmo, T., & Zelinka, M. D. (2016). Observational constraints on mixed-phase clouds imply higher climate sensitivity. *Science*, *352*(6282), 224-227. https://doi.org/10.1126/science.aad5300

Tang, I. N., Tridico, A. C., & Fung, K. H. (1997). Thermodynamic and optical properties of sea salt aerosols. *Journal of Geophysical Research-Atmospheres*, *102*(D19), 23269-23275. https://doi.org/10.1029/97jd01806

Tinel, L., Rossignol, S., Ciuraru, R., Dumas, S., & George, C. (2016). Photosensitized reactions initiated by 6-carboxypterin: singlet and triplet reactivity. *Physical Chemistry Chemical Physics*, *18*(25), 17105-17115. https://doi.org/10.1039/c6cp03119f

Trueblood, J. V., Nicosia, A., Engel, A., Zancker, B., Rinaldi, M., Freney, E., . . . Sellegri, K. (2021). A two-component parameterization of marine ice-nucleating particles based on seawater biology and sea spray aerosol measurements in the Mediterranean Sea. *Atmospheric Chemistry and Physics*, *21*(6), 4659-4676. https://doi.org/10.5194/acp-21-4659-2021

Tsigaridis, K., Koch, D., & Menon, S. (2013). Uncertainties and importance of sea spray composition on aerosol direct and indirect effects. *Journal of Geophysical Research-Atmospheres*, *118*(1), 220-235. https://doi.org/10.1029/2012jd018165
Turekian, V. C., Macko, S. A., & Keene, W. C. (2003). Concentrations, isotopic compositions, and sources of size-resolved, particulate organic carbon and oxalate in near-surface marine air at Bermuda during spring. *Journal of Geophysical Research-Atmospheres*, *108*(D5), Article 4157. https://doi.org/10.1029/2002jd002053
Twohy, C. H., DeMott, P. J., Russell, L. M., Toohey, D. W., Rainwater, B., Geiss, R., . . . McRobert, I. M. (2021). Cloud-Nucleating Particles Over the Southern Ocean in a Changing Climate. *Earths Future*, *9*(3), Article e2020EF001673. https://doi.org/10.1029/2020ef001673
Twomey, S. (1977). The Influence of Pollution on the Shortwave Albedo of Clouds. *Journal of the Atmospheric Sciences*, *34*(7), 1149--1152. https://doi.org/10.1175/1520-0469(1977)034<1149:TIOPOT>2.0.CO;2
Tyree, C. A., Hellion, V. M., Alexandrova, O. A., & Allen, J. O. (2007). Foam droplets generated from natural and artificial seawaters. *Journal of Geophysical Research-Atmospheres*, *112*(D12), Article D12204. https://doi.org/10.1029/2006jd007729
Vagle, S., & Farmer, D. M. (1998). A comparison of four methods for bubble size and void fraction measurements. *Ieee Journal of Oceanic Engineering*, *23*(3), 211-222. https://doi.org/10.1109/48.701193
Vergara-Temprado, J., Miltenberger, A. K., Furtado, K., Grosvenor, D. P., Shipway, B. J., Hill, A. A., . . . Carslaw, K. S. (2018). Strong control of Southern Ocean cloud reflectivity by ice-nucleating particles. *Proceedings of the National Academy of Sciences of the United States of America*, *115*(11), 2687-2692. https://doi.org/10.1073/pnas.1721627115
Vergara-Temprado, J., Murray, B. J., Wilson, T. W., O'Sullivan, D., Browse, J., Pringle, K. J., . . . Carslaw, K. S. (2017). Contribution of feldspar and marine organic aerosols to global ice nucleating particle concentrations. *Atmospheric Chemistry and Physics*, *17*(5), 3637-3658. https://doi.org/10.5194/acp-17-3637-2017
Veron, F. (2015). Ocean Spray. *Annual Review of Fluid Mechanics, Vol 47*, *47*, 507-538. https://doi.org/10.1146/annurev-fluid-010814-014651
Veron, F., Hopkins, C., Harrison, E. L., & Mueller, J. A. (2012). Sea spray spume droplet production in high wind speeds. *Geophysical Research Letters*, *39*, Article L16602. https://doi.org/10.1029/2012gl052603
Vignati, E., Facchini, M. C., Rinaldi, M., Scannell, C., Ceburnis, D., Sciare, J., . . . O'Dowd, C. D. (2010). Global scale emission and distribution of sea-spray aerosol: Sea-salt and organic enrichment. *Atmospheric Environment*, *44*(5), 670-677. https://doi.org/10.1016/j.atmosenv.2009.11.013
Virkkula, A., Grythe, H., Backman, J., Petaja, T., Busetto, M., Lanconelli, C., . . . Andrews, E. (2022). Aerosol optical properties calculated from size distributions, filter samples and absorption photometer data at Dome C, Antarctica, and their relationships with seasonal cycles of sources. *Atmospheric Chemistry and Physics*, *22*(7), 5033-5069. https://doi.org/10.5194/acp-22-5033-2022
Walls, P. L. L., & Bird, J. C. (2017). Enriching particles on a bubble through drainage: Measuring and modeling the concentration of microbial particles in a bubble film at rupture. *Elementa-Science of the Anthropocene*, *5*, Article 34. https://doi.org/10.1525/elementa.230
Wang, S. L., Maltrud, M., Elliott, S., Cameron-Smith, P., & Jonko, A. (2018). Influence of dimethyl sulfide on the carbon cycle and biological production. *Biogeochemistry*, *138*(1), 49-68. https://doi.org/10.1007/s10533-018-0430-5
Wang, X. F., Deane, G. B., Moore, K. A., Ryder, O. S., Stokes, M. D., Beall, C. M., . . . Prather, K. A. (2017). The role of jet and film drops in controlling the mixing state of submicron

sea spray aerosol particles. *Proceedings of the National Academy of Sciences of the United States of America*, *114*(27), 6978-6983. https://doi.org/10.1073/pnas.1702420114
Warren, D. R., & Seinfeld, J. H. (1985). PREDICTION OF AEROSOL CONCENTRATIONS RESULTING FROM A BURST OF NUCLEATION. *Journal of Colloid and Interface Science*, *105*(1), 136-142. https://doi.org/10.1016/0021-9797(85)90356-x
Westervelt, D. M., Moore, R. H., Nenes, A., & Adams, P. J. (2012). Effect of primary organic sea spray emissions on cloud condensation nuclei concentrations. *Atmospheric Chemistry and Physics*, *12*(1), 89-101. https://doi.org/10.5194/acp-12-89-2012
Wex, H., Huang, L., Zhang, W., Hung, H., Traversi, R., Becagli, S., . . . Stratmann, F. (2019). Annual variability of ice-nucleating particle concentrations at different Arctic locations. *Atmospheric Chemistry and Physics*, *19*(7), 5293-5311. https://doi.org/10.5194/acp-19-5293-2019
Wilson, T. W., Ladino, L. A., Alpert, P. A., Breckels, M. N., Brooks, I. M., Browse, J., . . . Murray, B. J. (2015). A marine biogenic source of atmospheric ice-nucleating particles. *Nature*, *525*(7568), 234-+. https://doi.org/10.1038/nature14986
Wilson, T. W., Ladino, L. A., Alpert, P. A., Breckels, M. N., Brooks, I. M., Browse, J., . . . Murray, B. J. (2015). A marine biogenic source of atmospheric ice-nucleating particles. *Nature*, *525*, 234. https://doi.org/10.1038/nature14986
Wolf, M. J., Coe, A., Dove, L. A., Zawadowicz, M. A., Dooley, K., Biller, S. J., . . . Cziczo, D. J. (2019). Investigating the Heterogeneous Ice Nucleation of Sea Spray Aerosols Using Prochlorococcus as a Model Source of Marine Organic Matter. *Environmental Science & Technology*, *53*(3), 1139-1149. https://doi.org/10.1021/acs.est.8b05150
Woolf, D. K., Bowyer, P. A., & Monahan, E. C. (1987). DISCRIMINATING BETWEEN THE FILM DROPS AND JET DROPS PRODUCED BY A SIMULATED WHITECAP. *Journal of Geophysical Research-Oceans*, *92*(C5), 5142-5150. https://doi.org/10.1029/JC092iC05p05142
Wu, J. (1993). PRODUCTION OF SPUME DROPS BY THE WIND TEARING OF WAVE CRESTS - THE SEARCH FOR QUANTIFICATION. *Journal of Geophysical Research-Oceans*, *98*(C10), 18221-18227. https://doi.org/10.1029/93jc01834
Wu, J. (2002). Jet drops produced by bubbles bursting at the surface of seawater. *Journal of Physical Oceanography*, *32*(11), 3286-3290. https://doi.org/10.1175/1520-0485(2002)032<3286:jdpbbb>2.0.co;2
Xu, W., Ovadnevaite, J., Fossum, K. N., Lin, C. S., Huang, R. J., Ceburnis, D., & O'Dowd, C. (2022). Sea spray as an obscured source for marine cloud nuclei. *Nature Geoscience*, *15*(4), 282-+. https://doi.org/10.1038/s41561-022-00917-2
Xu, W., Ovadnevaite, J., Fossum, K. N., Lin, C. S., Huang, R. J., O'Dowd, C., & Ceburnis, D. (2021). Seasonal Trends of Aerosol Hygroscopicity and Mixing State in Clean Marine and Polluted Continental Air Masses Over the Northeast Atlantic. *Journal of Geophysical Research-Atmospheres*, *126*(11), Article e2020JD033851. https://doi.org/10.1029/2020jd033851
Yoon, Y. J., Ceburnis, D., Cavalli, F., Jourdan, O., Putaud, J. P., Facchini, M. C., . . . O'Dowd, C. D. (2007). Seasonal characteristics of the physicochemical properties of North Atlantic marine atmospheric aerosols. *Journal of Geophysical Research-Atmospheres*, *112*(D4). https://doi.org/D04206
10.1029/2005jd007044
Yu, L. S. (2019). Global Air-Sea Fluxes of Heat, Fresh Water, and Momentum: Energy Budget Closure and Unanswered Questions. *Annual Review of Marine Science, Vol 11*, *11*, 227-248. https://doi.org/10.1146/annurev-marine-010816-060704
Zabori, J., Krejci, R., Ekman, A. M. L., Martensson, E. M., Strom, J., de Leeuw, G., & Nilsson, E. D. (2012). Wintertime Arctic Ocean sea water properties and primary marine aerosol

concentrations. *Atmospheric Chemistry and Physics*, *12*(21), 10405-10421. https://doi.org/10.5194/acp-12-10405-2012

Zabori, J., Matisans, M., Krejci, R., Nilsson, E., & Strom, J. (2012). Artificial primary marine aerosol production: a laboratory study with varying water temperature, salinity, and succinic acid concentration [Article]. *Atmospheric Chemistry and Physics*, *12*(22), 10709-10724. https://doi.org/10.5194/acp-12-10709-2012

Zavarsky, A., & Marandino, C. A. (2019). The influence of transformed Reynolds number suppression on gas transfer parameterizations and global DMS and CO2 fluxes. *Atmospheric Chemistry and Physics*, *19*(3), 1819-1834. https://doi.org/10.5194/acp-19-1819-2019

Zheng, G. J., Wang, Y., Aiken, A. C., Gallo, F., Jensen, M. P., Kollias, P., . . . Wang, J. (2018). Marine boundary layer aerosol in the eastern North Atlantic: seasonal variations and key controlling processes. *Atmospheric Chemistry and Physics*, *18*(23), 17615-17635. https://doi.org/10.5194/acp-18-17615-2018

Zheng, G. J., Wang, Y., Wood, R., Jensen, M. P., Kuang, C. A., McCoy, I. L., . . . Wang, J. (2021). New particle formation in the remote marine boundary layer. *Nature Communications*, *12*(1), Article 527. https://doi.org/10.1038/s41467-020-20773-1

Zieger, P., Vaisanen, O., Corbin, J. C., Partridge, D. G., Bastelberger, S., Mousavi-Fard, M., . . . Salter, M. E. (2017). Revising the hygroscopicity of inorganic sea salt particles. *Nature Communications*, *8*, Article 15883. https://doi.org/10.1038/ncomms15883

Ziemann, P. J., & Atkinson, R. (2012). Kinetics, products, and mechanisms of secondary organic aerosol formation. *Chem. Soc. Rev.*, *41*(19), 6582-6605. https://doi.org/10.1039/C2CS35122F